



U.S. DEPARTMENT OF
ENERGY

Office of
Science



Brookhaven[™]
National Laboratory

COLLECTIVE FLOW IN SMALL SYSTEMS

BJÖRN SCHENKE, BROOKHAVEN NATIONAL LABORATORY

**OCTOBER 19 2021
RHIC-BES SEMINAR**

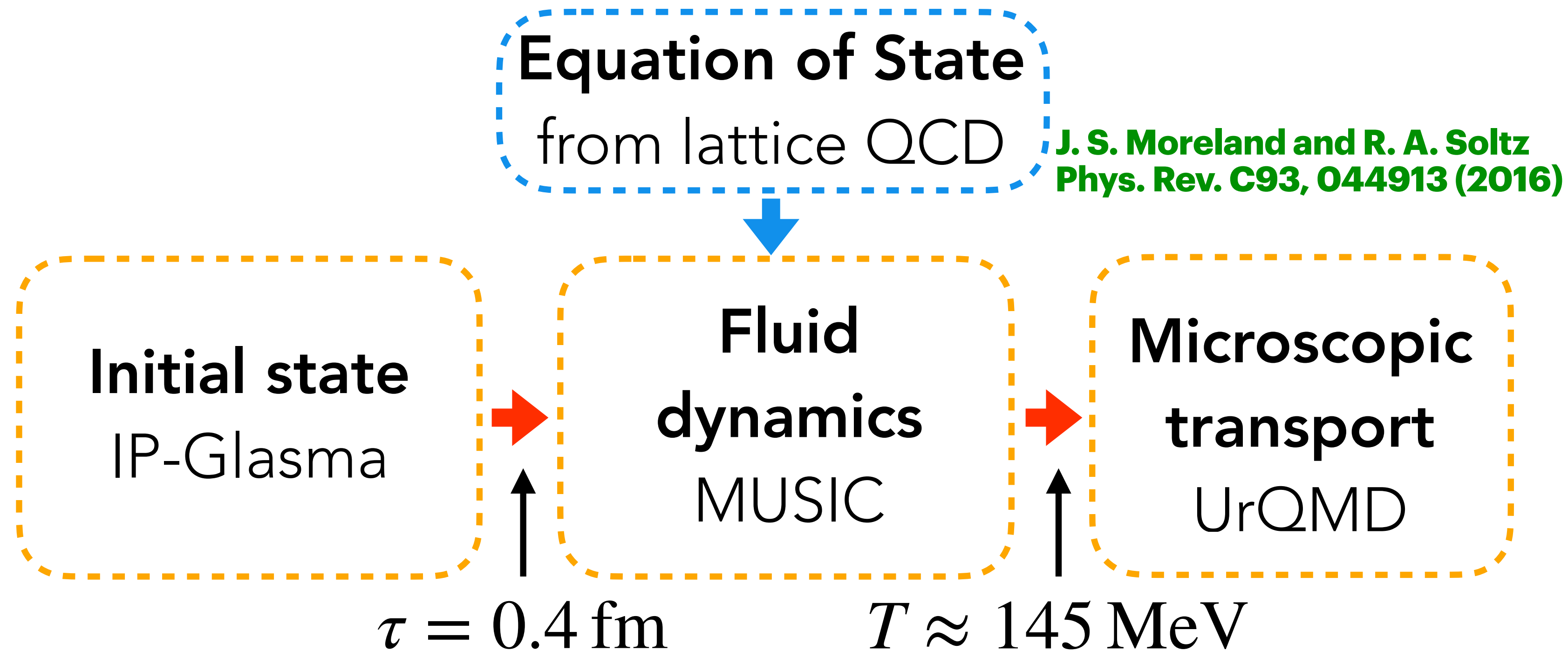
BULK DYNAMICS OF HEAVY ION AND SMALL SYSTEM COLLISIONS WITHIN A FRAMEWORK BUILT AROUND FLUID DYNAMICS

- **PART I: Very High Energy: Boost invariant calculations**
- **PART II: Corrections to the boost invariant framework**
- **PART III: Fully 3+1D calculations, suitable for the BES**

PART I: VERY HIGH ENERGY

- **Use the CGC to compute the initial energy momentum tensor**
- **Assume boost invariance and do 2+1D hydrodynamics**

THE HYBRID FRAMEWORK



Described in detail in

B. Schenke, C. Shen, P. Tribedy, Phys. Rev. C 102 (2020) 4, 044905
"Running the gamut of high energy nuclear collisions"

The term gamut was adopted from the field of **music**, where in middle age Latin "gamut" meant the entire range of musical notes of which musical melodies are composed

- **Exactly match $T^{\mu\nu}$ when switching from one part to the next**

B. Schenke, P. Tribedy, and R. Venugopalan, Phys. Rev. Lett. 108, 252301 (2012)

B. Schenke, S. Jeon, and C. Gale, Phys. Rev. Lett. 106, 042301 (2011)

S. A. Bass et al., Prog. Part. Nucl. Phys. 41, 255 (1998); M. Bleicher et al., J. Phys. G25, 1859 (1999)

INITIAL STATE GEOMETRY

Nucleus:

Sample nucleons from Woods Saxon distribution

Nucleon:

- consider substructure
- constrain parameters with HERA data

**Exclusive diffractive J/ψ production in $e+p$:
Incoherent x-sec sensitive to fluctuations**

H. Mäntysaari, B. Schenke, *Phys. Rev. Lett.* **117** (2016) 052301

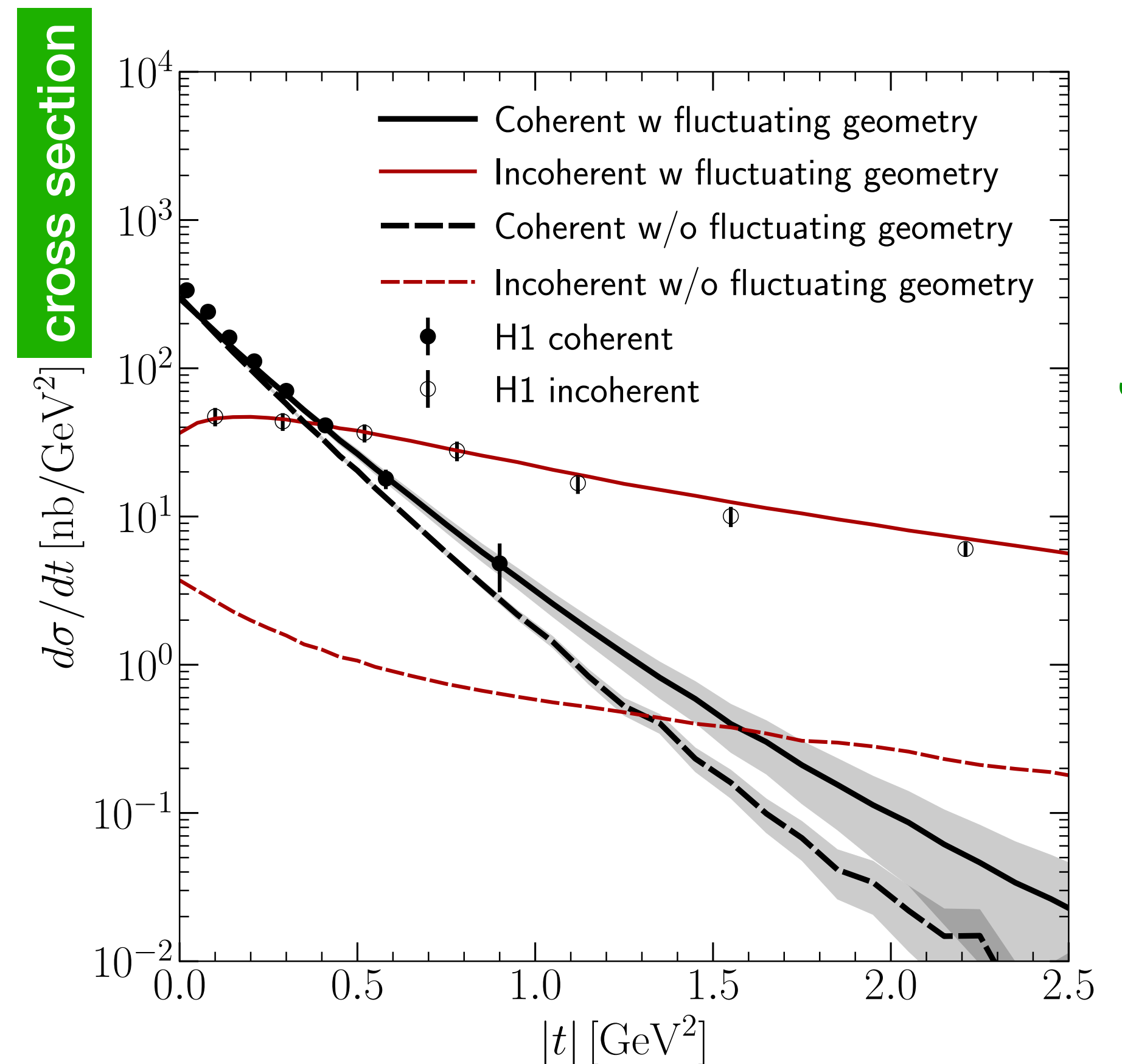
Phys.Rev. D **94** (2016) 034042

also see:

S. Schlichting, B. Schenke, *Phys.Lett.* **B739** (2014) 313-319

H. Mäntysaari, *Rep. Prog. Phys.* **83** 082201 (2020)

B. Schenke, *Rep. Prog. Phys.* **84** 082301 (2021)



(transverse momentum transfer)²

INITIAL STATE GEOMETRY

Nucleus:

Sample nucleons from Woods Saxon distribution

Nucleon:

- consider substructure
- constrain parameters with HERA data

**Exclusive diffractive J/Ψ production in $e+p$:
Incoherent x-sec sensitive to fluctuations**

H. Mäntysaari, B. Schenke, *Phys. Rev. Lett.* **117** (2016) 052301

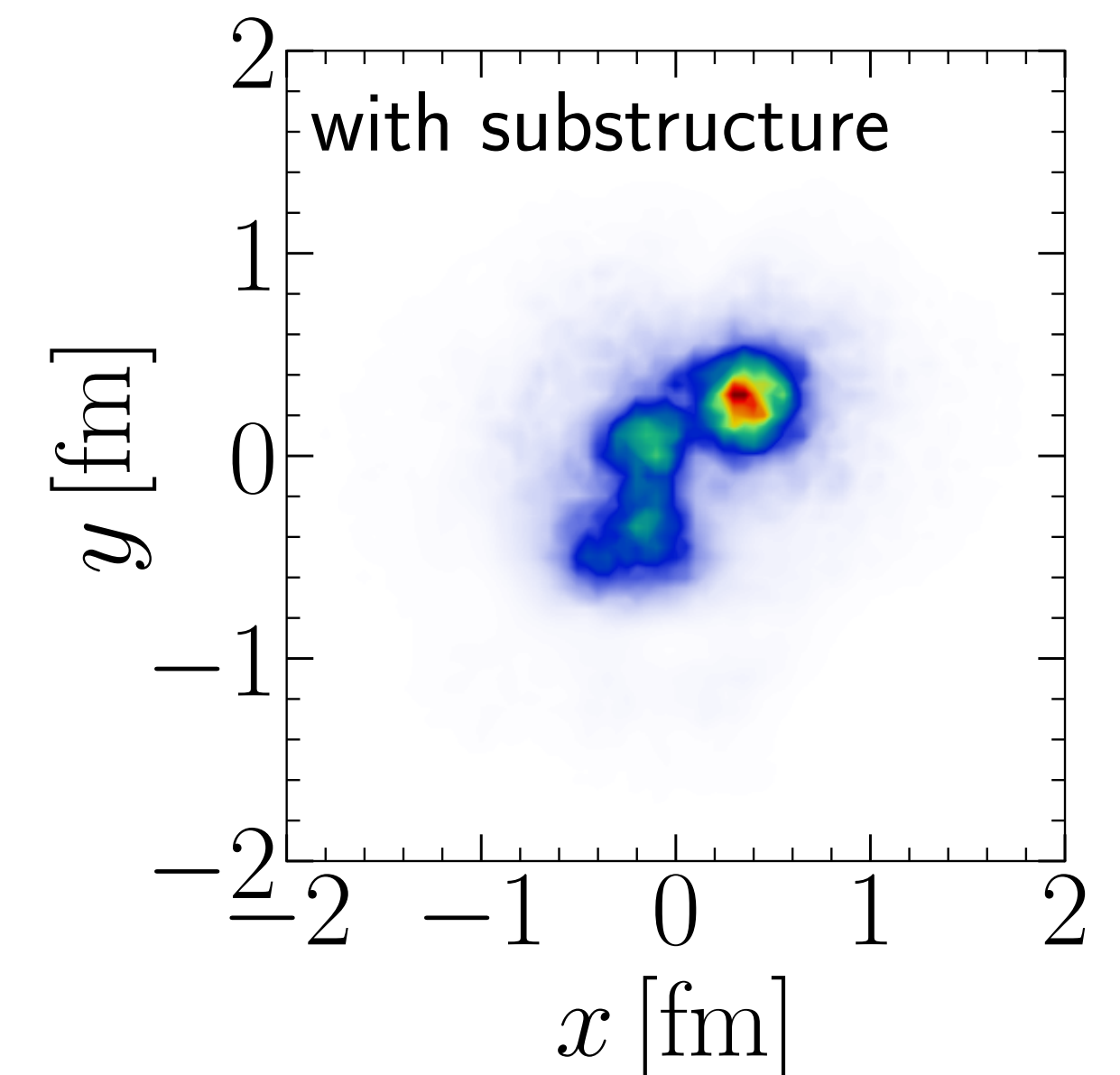
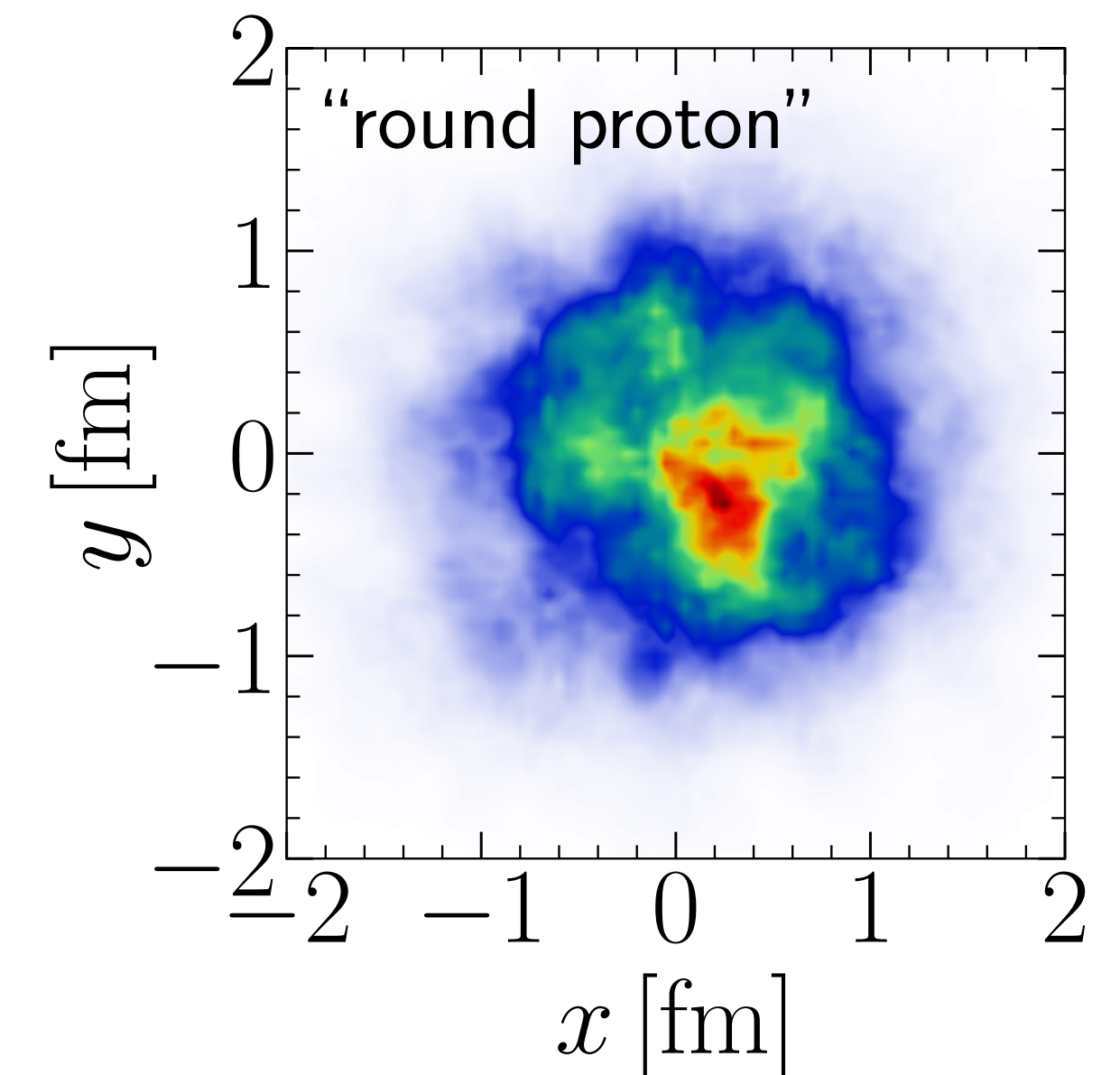
Phys.Rev. D **94** (2016) 034042

also see:

S. Schlichting, B. Schenke, *Phys.Lett.* **B739** (2014) 313-319

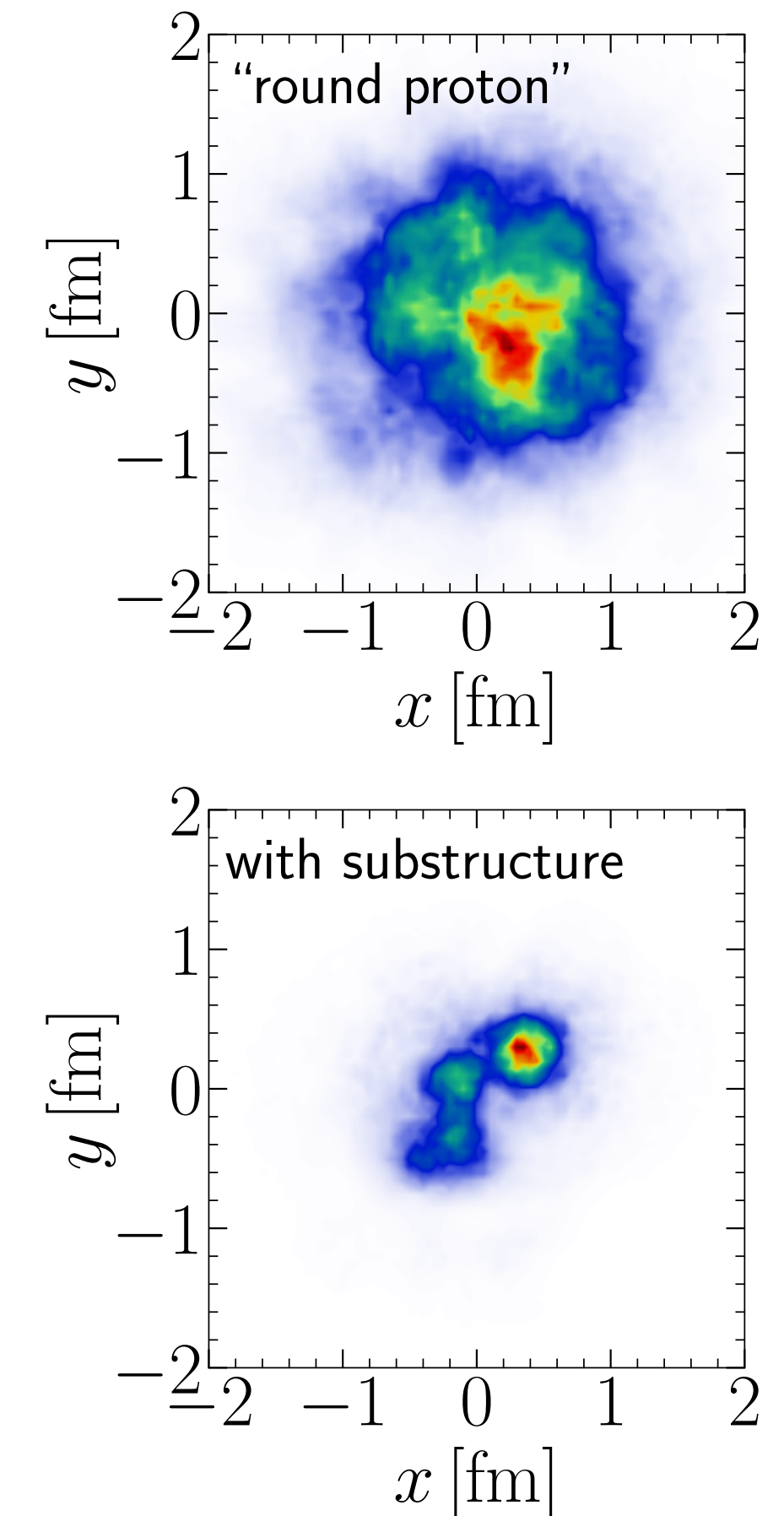
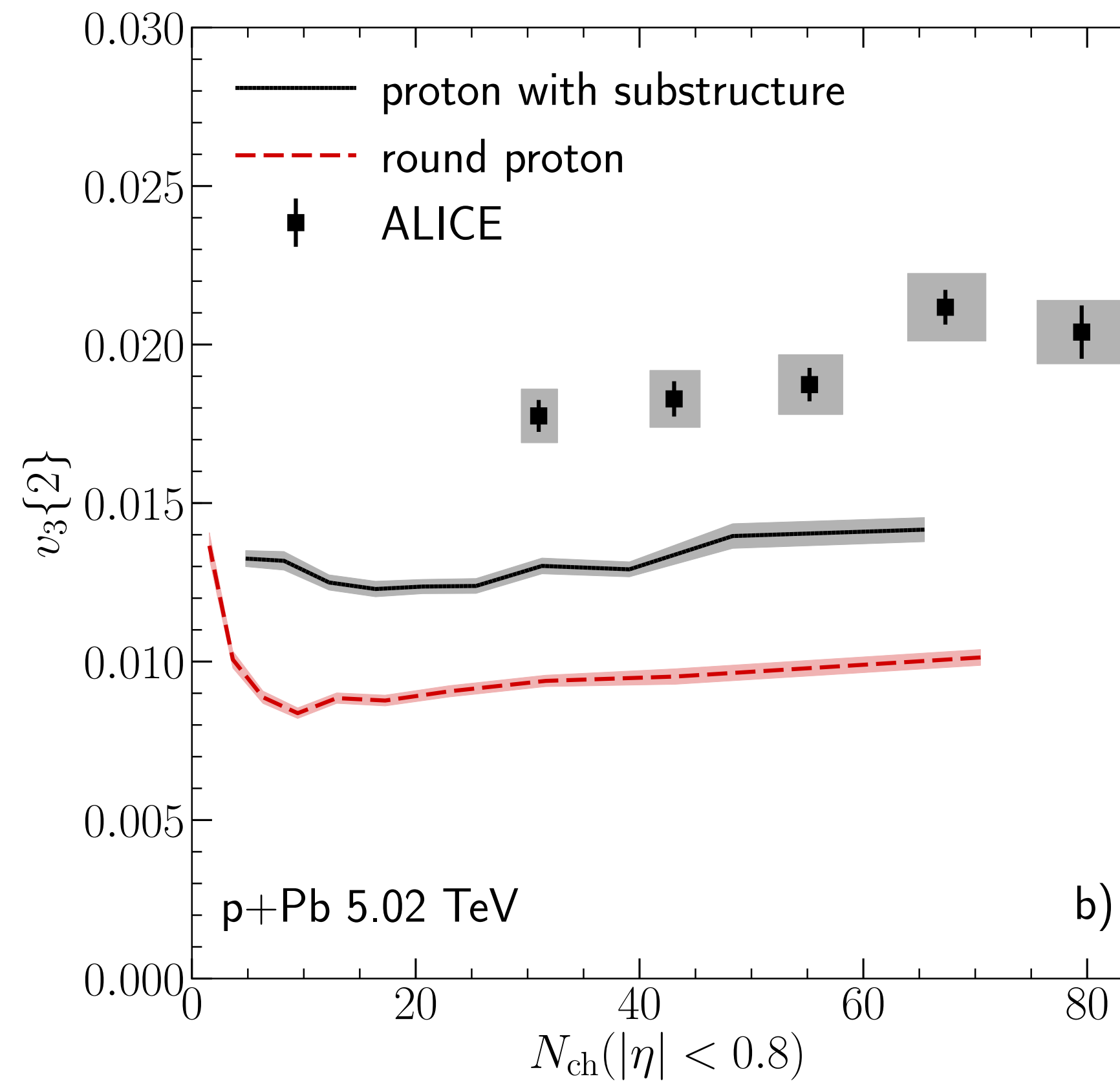
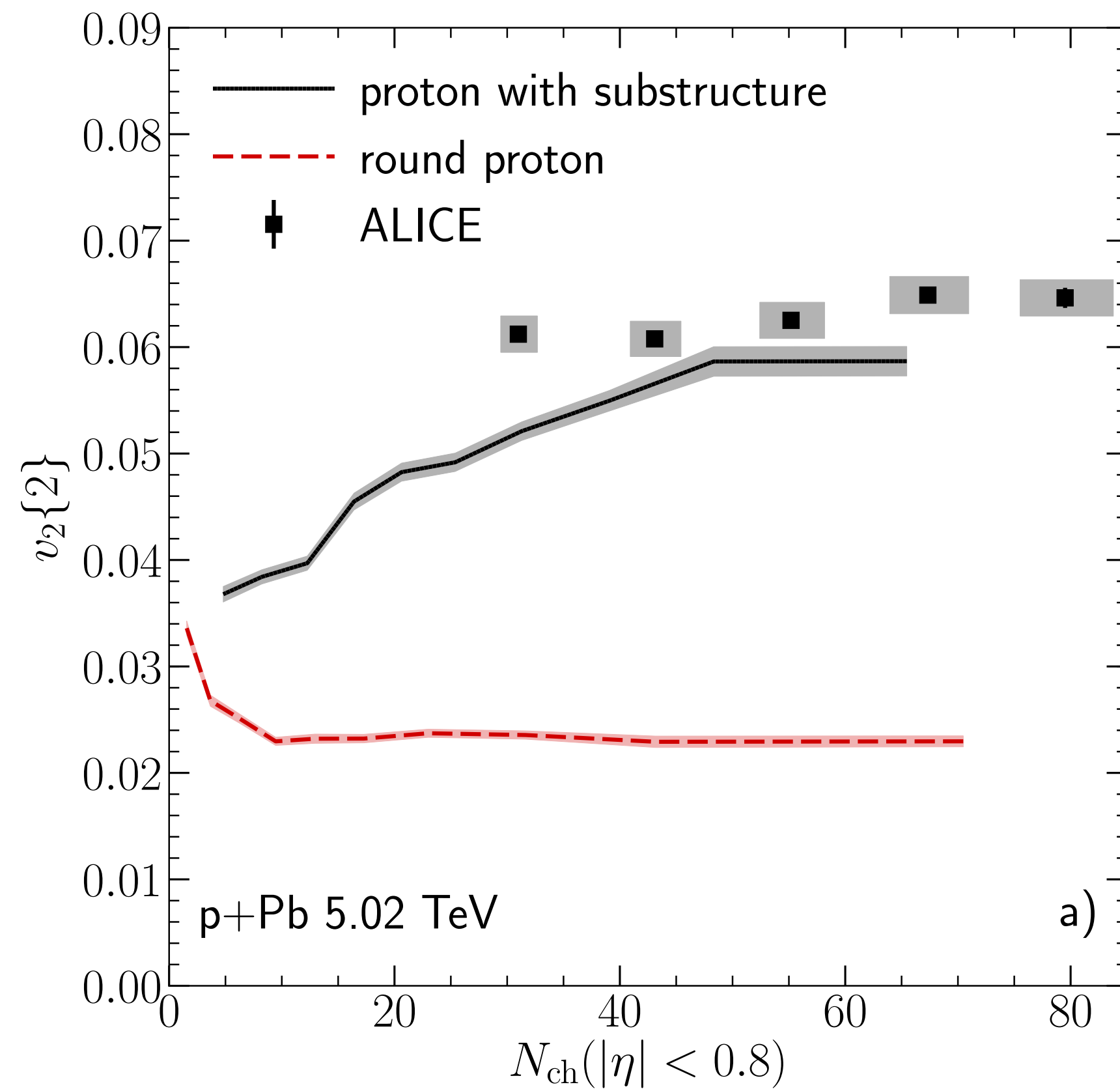
H. Mäntysaari, *Rep. Prog. Phys.* **83** 082201 (2020)

B. Schenke, *Rep. Prog. Phys.* **84** 082301 (2021)



NUCLEON SUBSTRUCTURE

Substructure is also needed to describe the anisotropic flow in p+A collisions with IP-Glasma



B. Schenke, Rep. Prog. Phys. 84 082301 (2021)

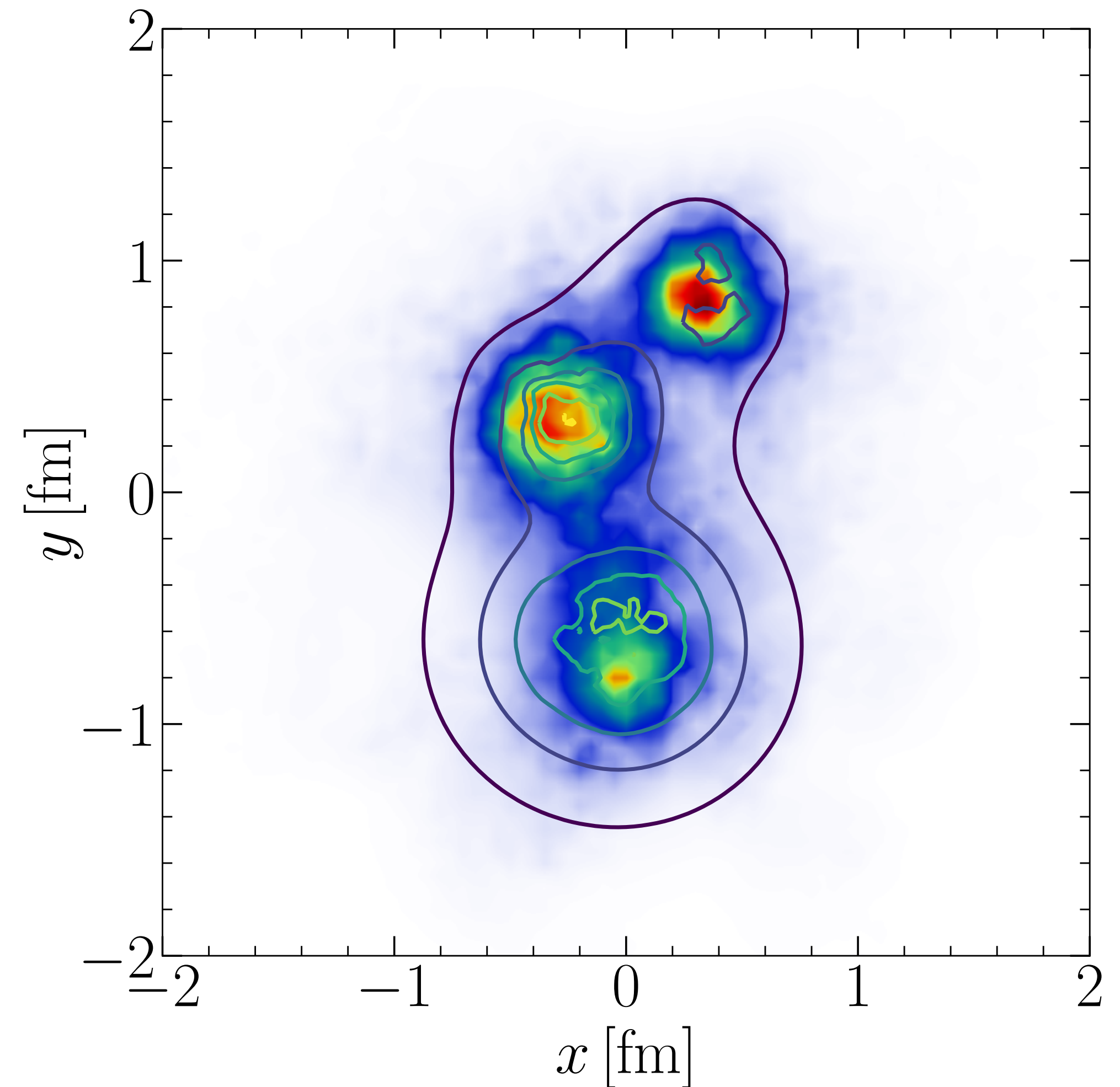
FIREBALL SHAPE ~ PROTON SHAPE

The shape of the overlap region in p+A collisions resembles the proton's shape

Color map: Energy density distribution (arbitrary units)

Contour lines: Shape of the projectile proton (quantified using a measure of the gluon density in the proton)

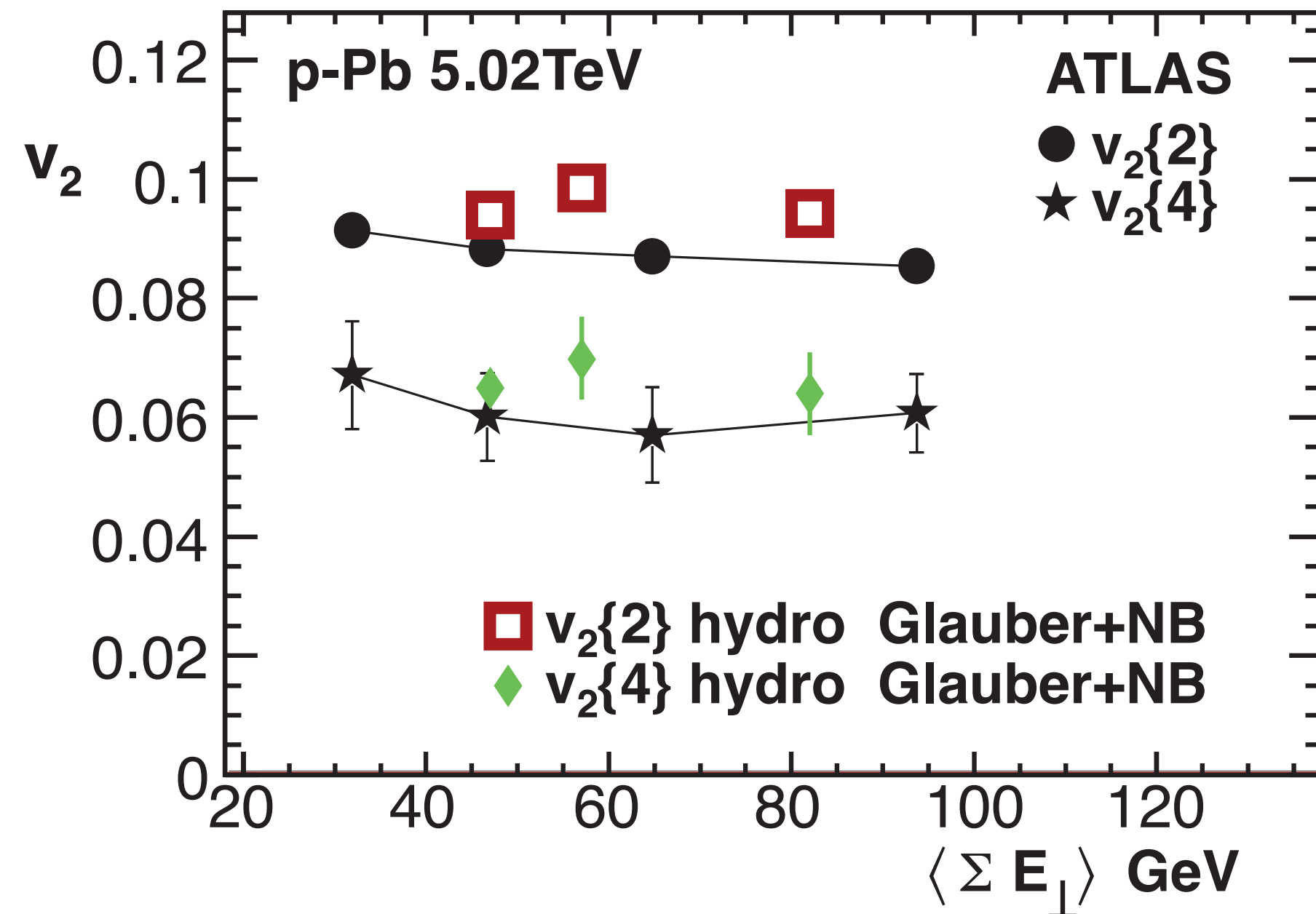
B. Schenke, Rep. Prog. Phys. 84 082301 (2021)



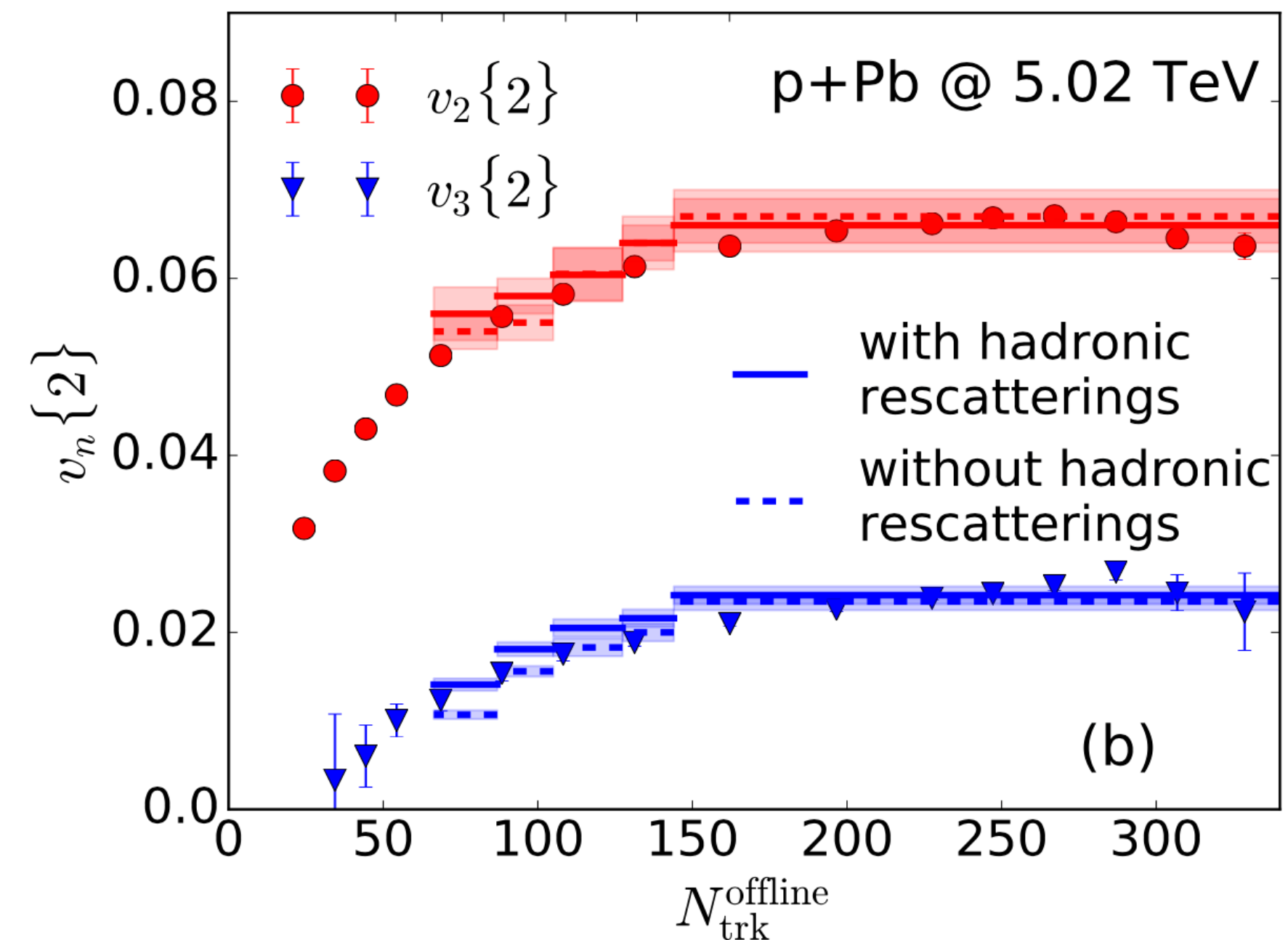
NUCLEON SUBSTRUCTURE

What about MC-Glauber (-like) models? They seem to get it right with just nucleons

ATLAS Coll. PLB725 (2013) 60-78



CMS Coll. PLB724, 213-240 (2013)



Bozek, Broniowski, PRC88 (2013) 014903

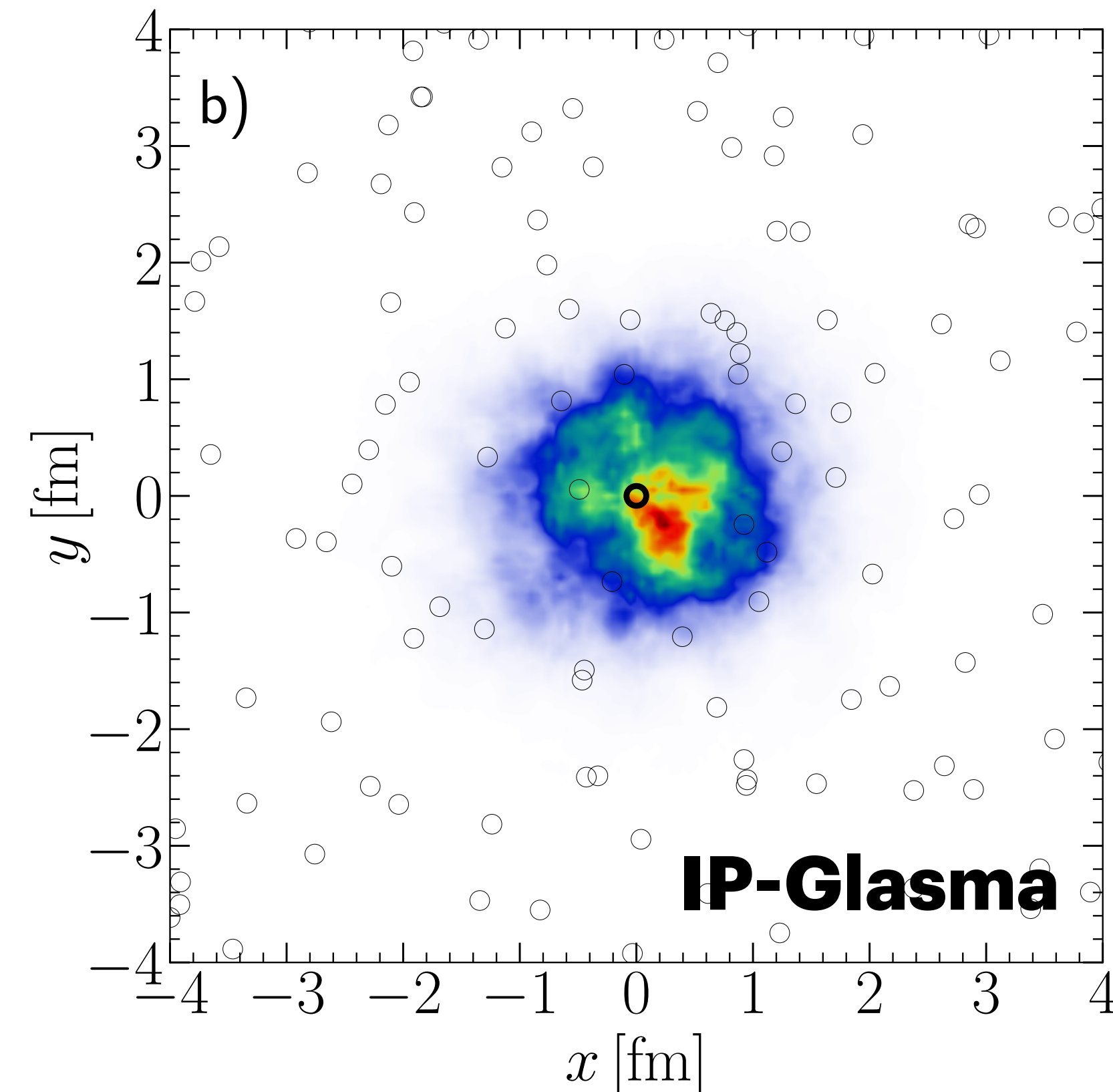
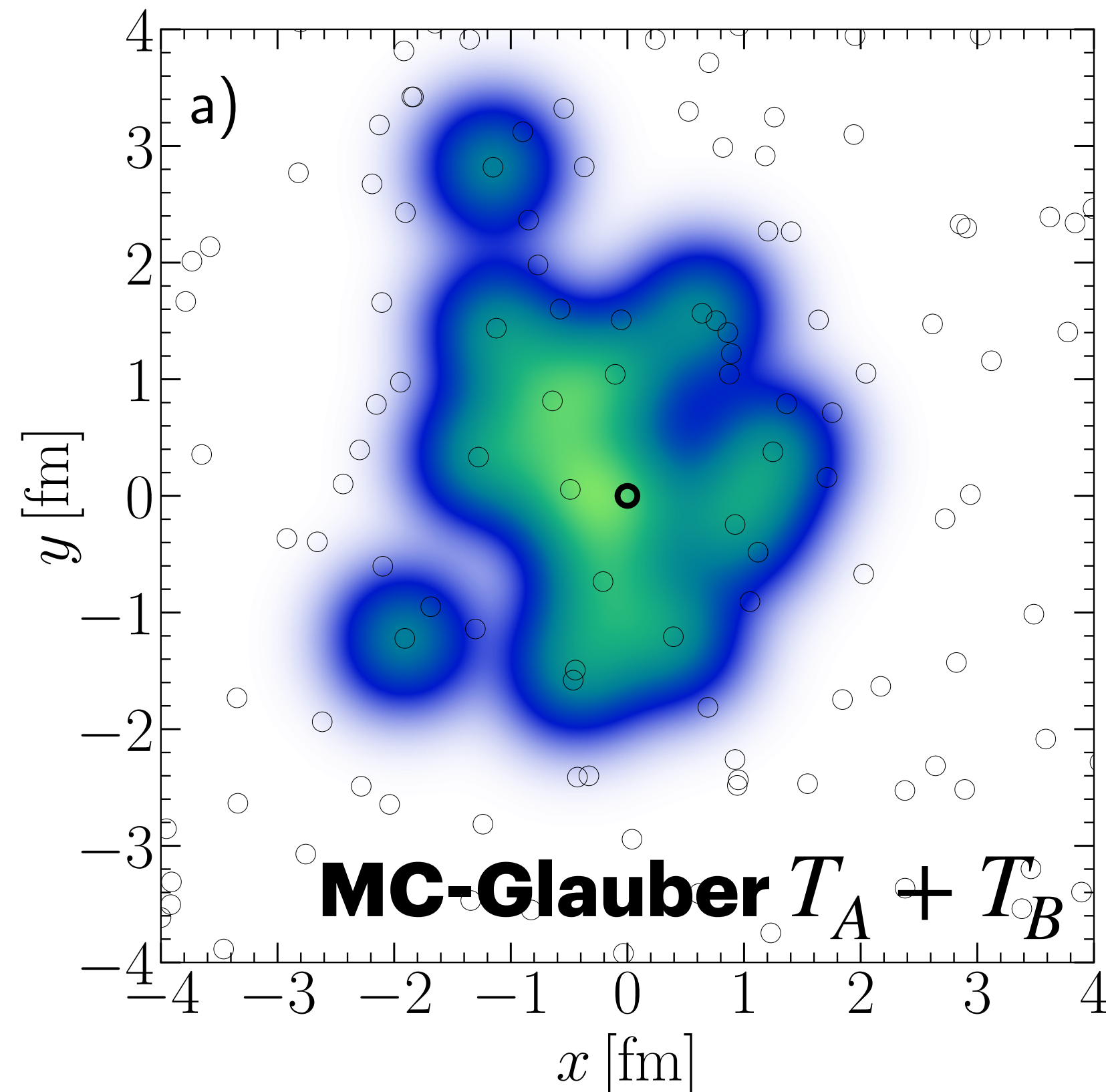
Shen, Paquet, Denicol, Jeon, Gale, PRC95 (2017) 014906

Also see: Kozlov, Luzum, Denicol, Jeon, Gale; Werner, Beicher, Guiot, Karpenko, Pierog; Romatschke; Kalaydzhyan, Shuryak, Zahed; Ghosh, Muhuri, Nayak, Varma; Qin, Mueller; Bozek, Broniowski, Torrieri; Habich, Miller, Romatschke, Xiang; T. Hirano, K. Kawaguchi, K. Murase; ...

MC-GLAUBER VS. IP-GLASMA

Proton position: thick circle; Nucleon positions in Pb: thin circles

Same configurations: Compare MC-Glauber $T_A + T_B$ to IP-Glasma with round nucleon
B. Schenke, Rep. Prog. Phys. 84 082301 (2021)



HOW SHOULD THE ENERGY DEPOSITION GO?

Energy (or entropy) deposition $\sim (T_A T_B)^q$ is preferred:

- **Bayesian analysis: Trento model prefers initial transverse entropy density to behave as $\sim \sqrt{T_A T_B}$ and also prefers a nucleon substructure**

J.S. Moreland, J.E. Bernhard, and S.A. Bass, *Phys. Rev. C* 92 (2015) 011901

G. Nijs, W. van der Schee, U. Gürsoy, R. Snellings, *Phys.Rev.Lett.* 126 (2021), *Phys.Rev.C* 103 (2021) 5, 054909

JETSCAPE Collaboration, *Phys.Rev.C* 103 (2021) 5, 054904

- **AdS/CFT based calculations also result in such a relation**

P. Romatschke, J.D. Hogg, *JHEP* 04 (2013) 048

- **IP-Glasma results in the initial energy density $\sim T_A T_B$**

- **$T_A + T_B$ disfavored by centrality dependence of v_2 in A+A** G. Giacalone, J. Noronha-Hostler, J.-Y. Ollitrault, *Phys. Rev. C* 95, 054910 (2017)

So, $T_A + T_B$ prescription with nucleons, that works for v_n in p+A, is generally disfavored

$\sim T_A T_B$ for round proton leads to too small fluctuations (eccentricities)

→ subnucleon fluctuations required

TRANSPORT COEFFICIENTS

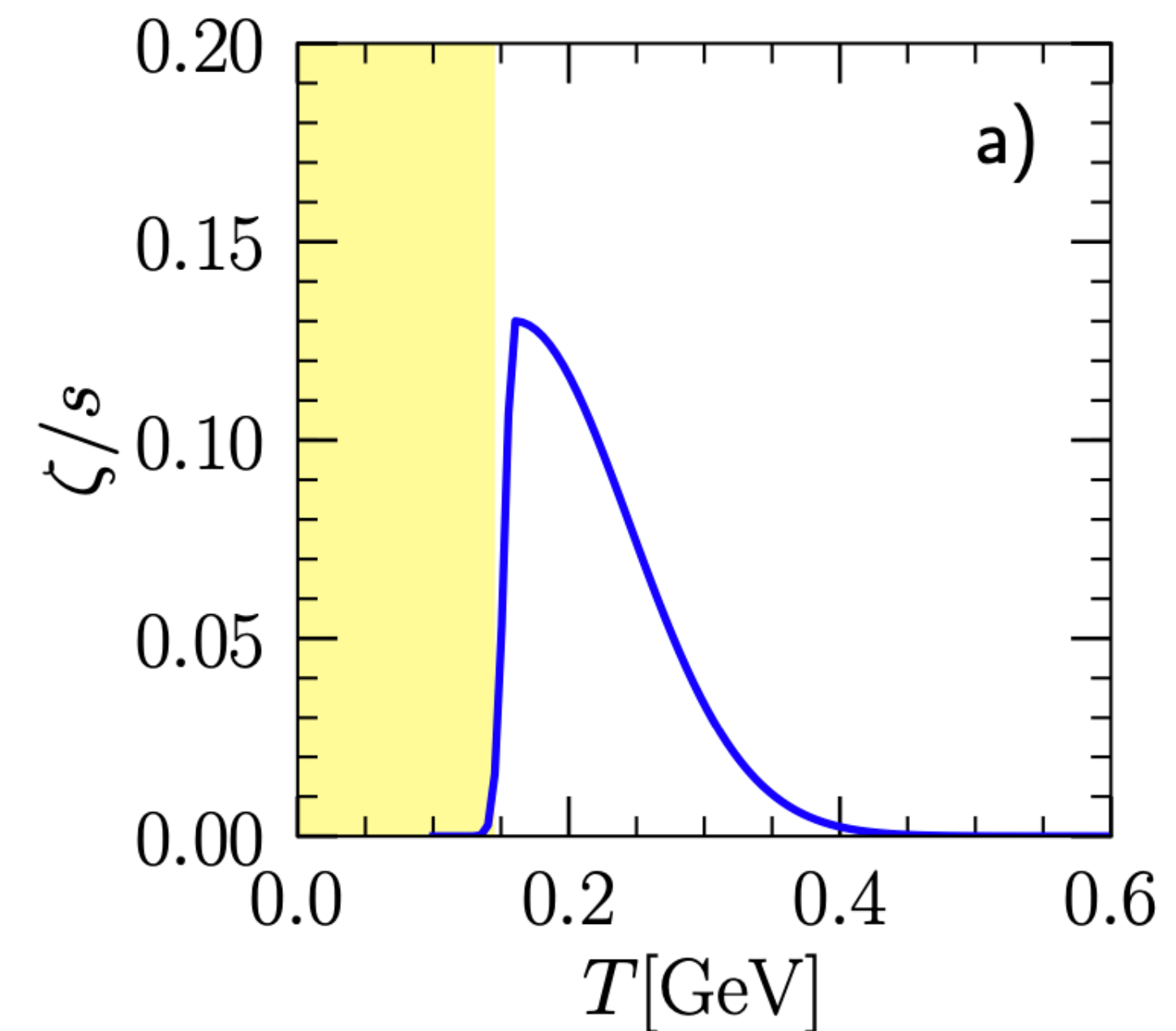
B. Schenke, C. Shen, P. Tribedy, Phys. Rev. C 102 (2020) 4, 044905

Transport coefficients:

Shear viscosity:

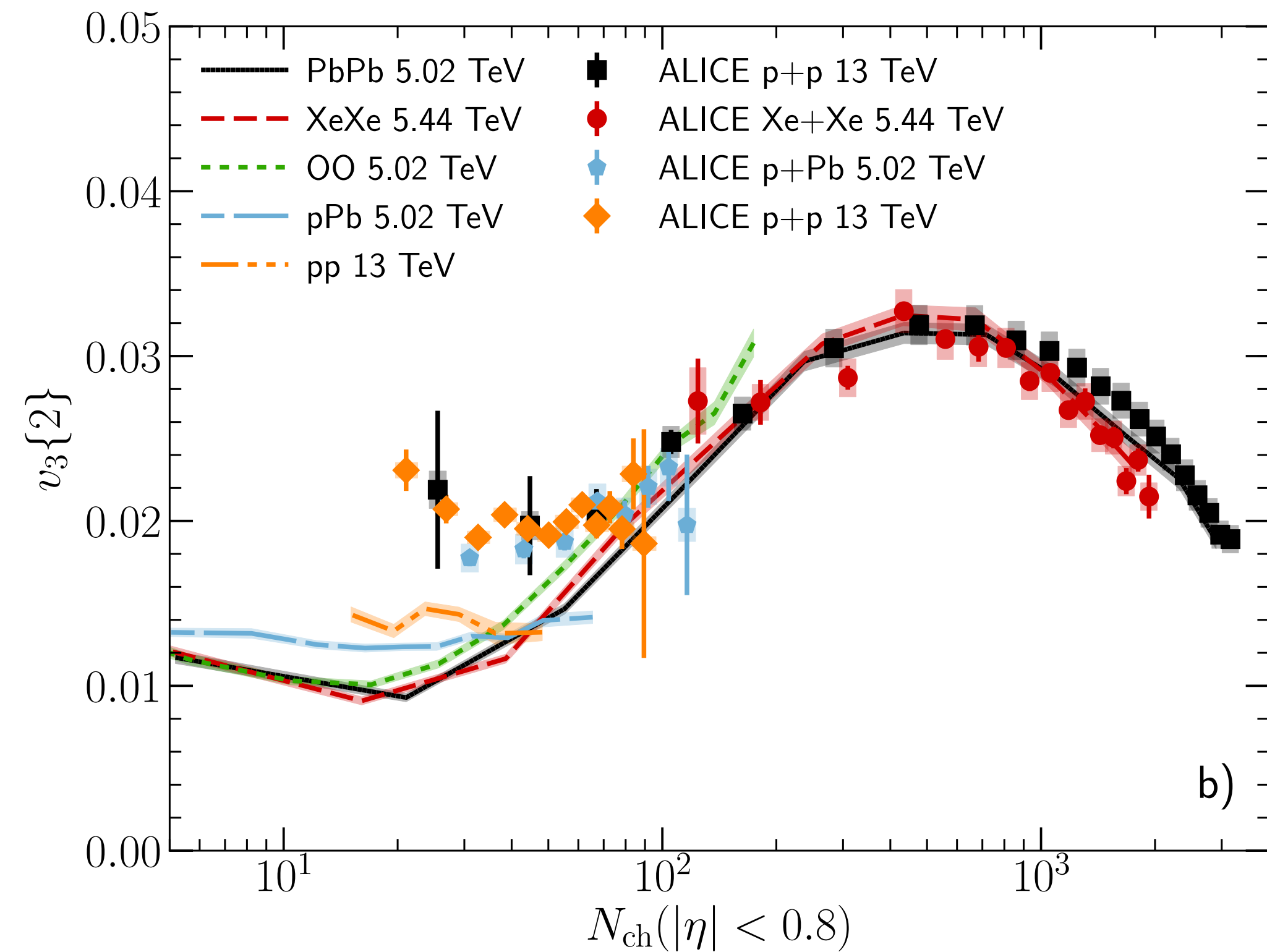
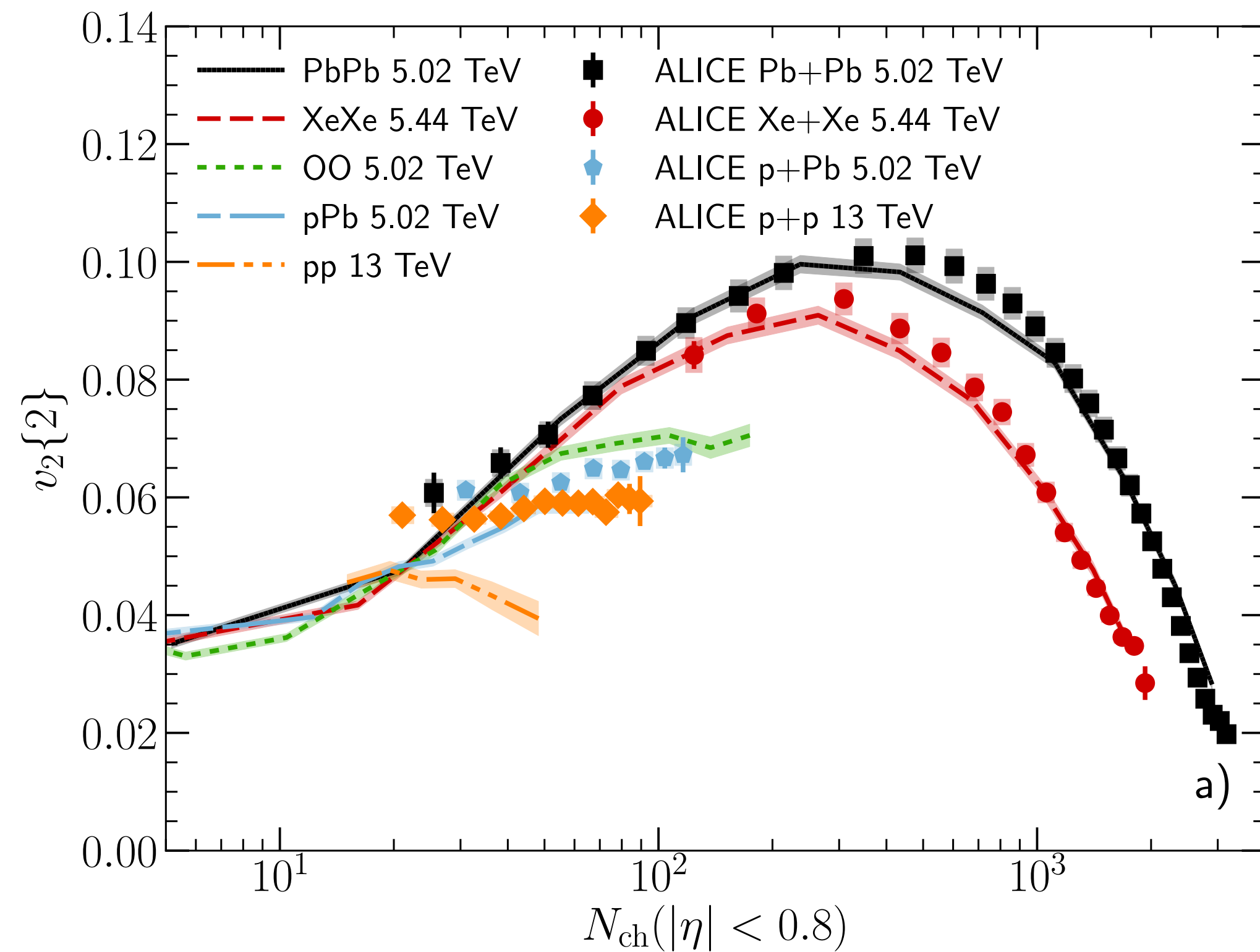
$$\eta/s = 0.12$$

Bulk viscosity:



SOME HYBRID MODEL RESULTS

B. Schenke, C. Shen, P. Tribedy, *Phys. Rev. C* 102 (2020) 4, 044905

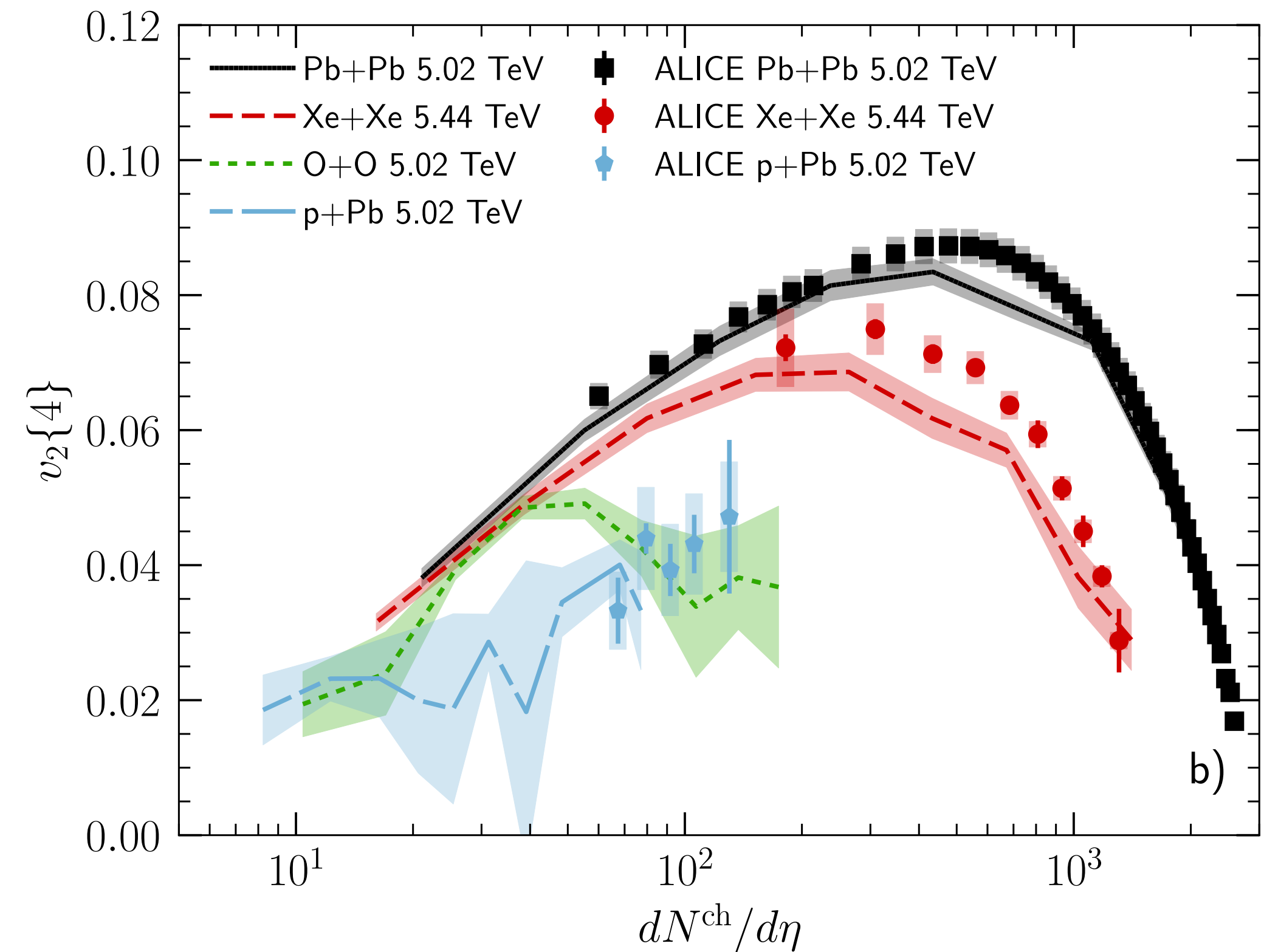
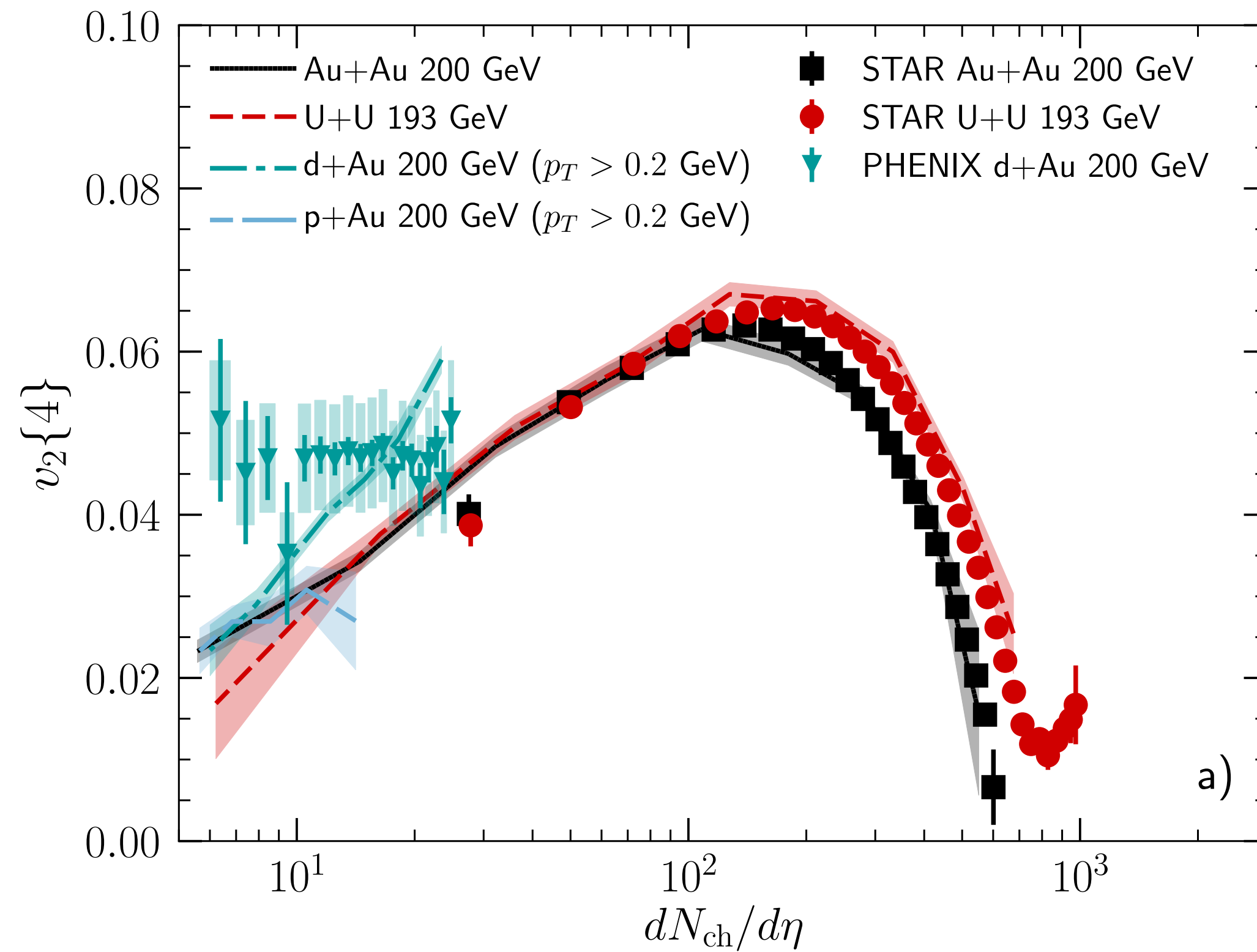


Parameters constrained only by HERA data (proton shape) and Au+Au data at RHIC

Underestimate v_n in p+p and v_3 in p+Pb

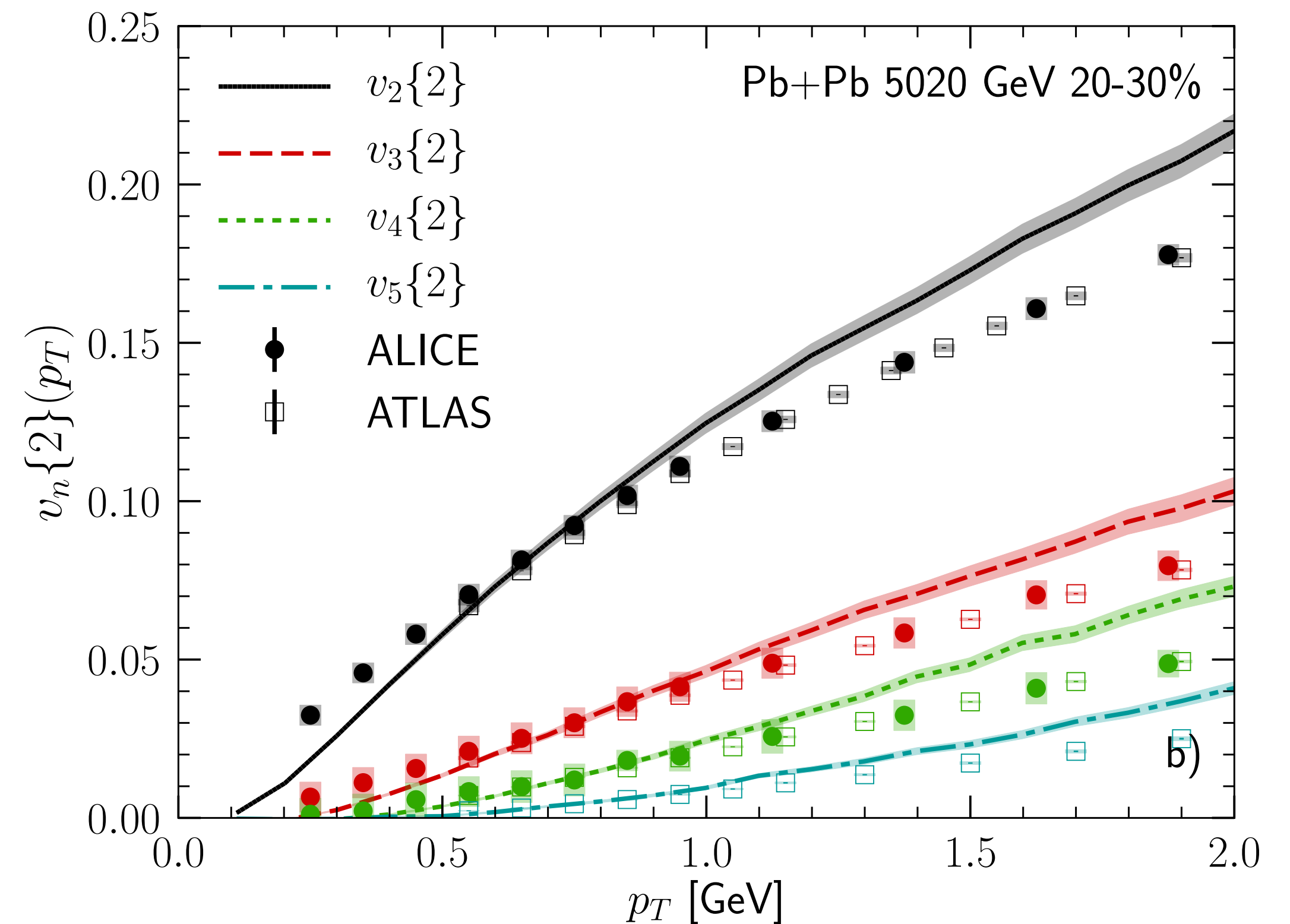
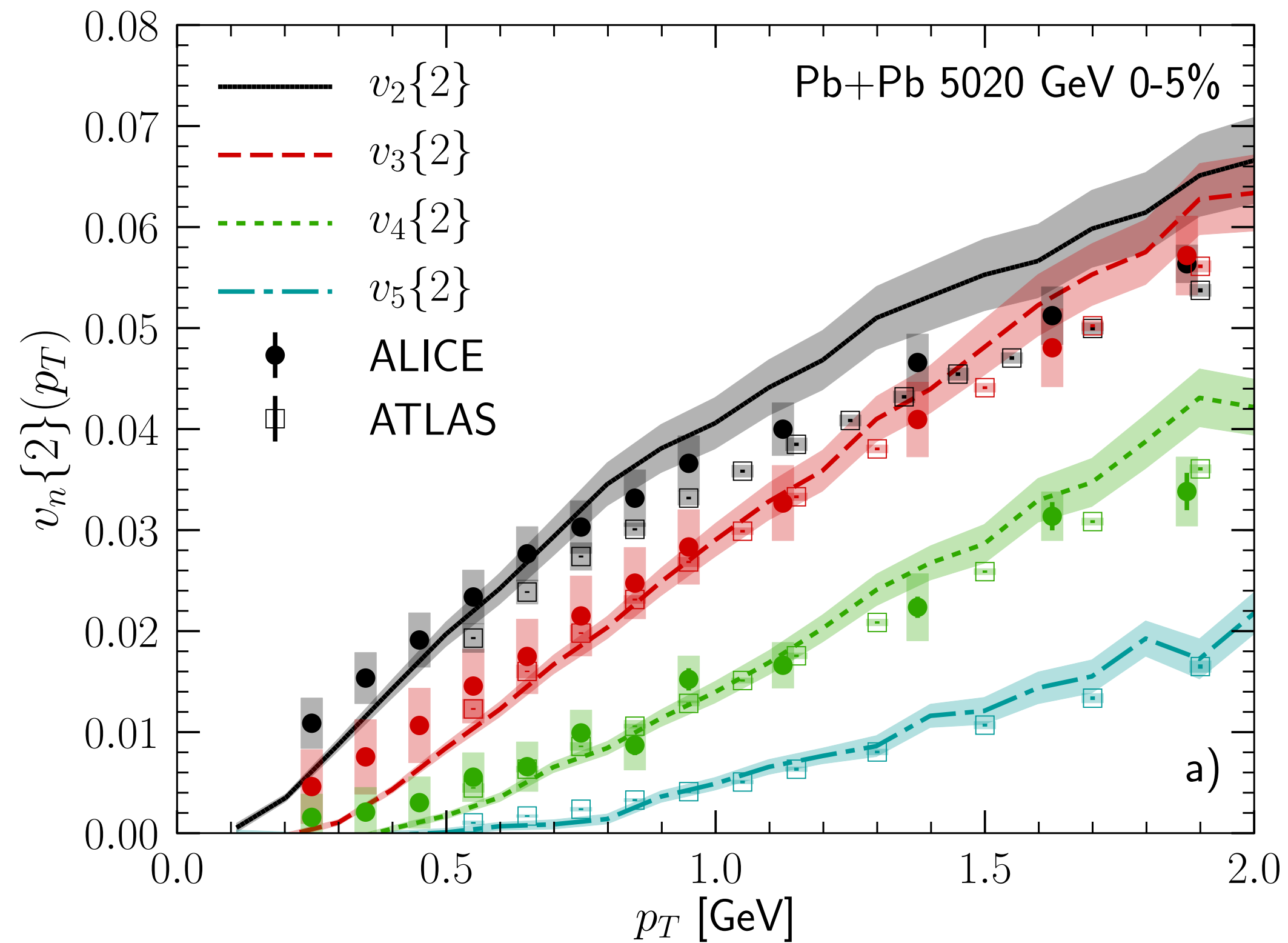
4-PARTICLE CUMULANTS

B. Schenke, C. Shen, P. Tribedy, Phys. Rev. C 102 (2020) 4, 044905



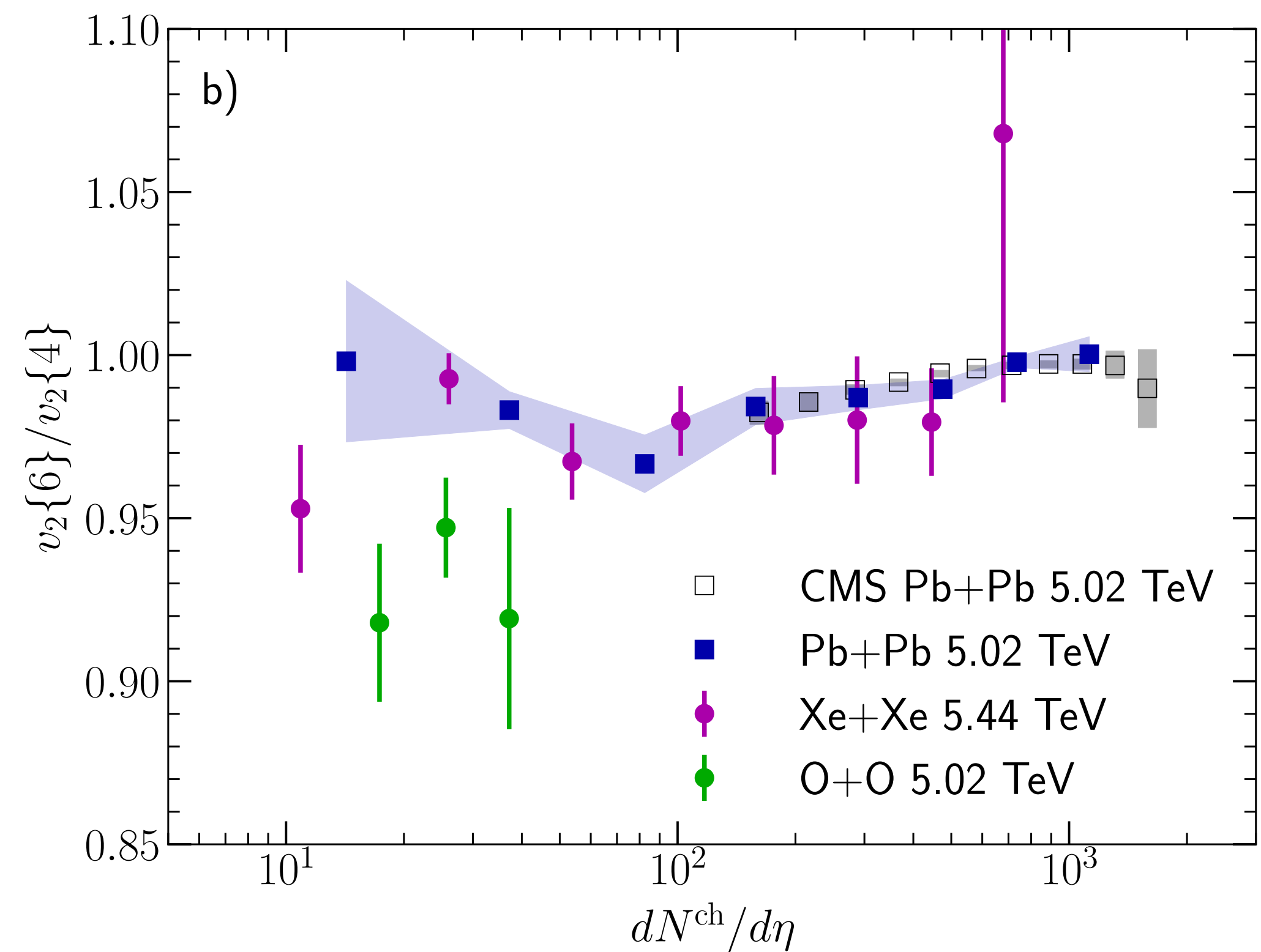
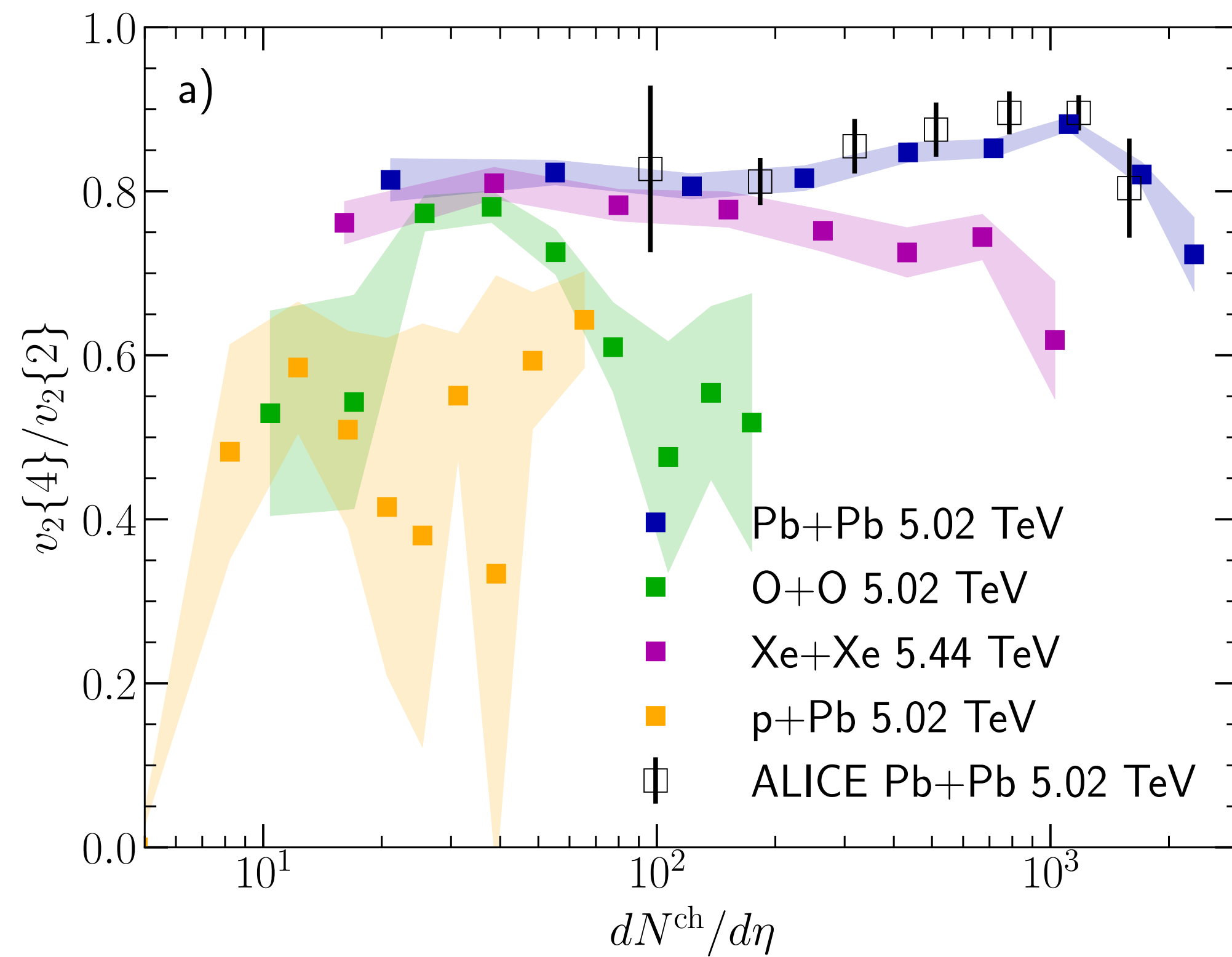
TRANSVERSE MOMENTUM DEPENDENCE

B. Schenke, C. Shen, P. Tribedy, Phys. Rev. C 102 (2020) 4, 044905



CUMULANT RATIOS

B. Schenke, C. Shen, P. Tribedy, Phys. Rev. C 102 (2020) 4, 044905

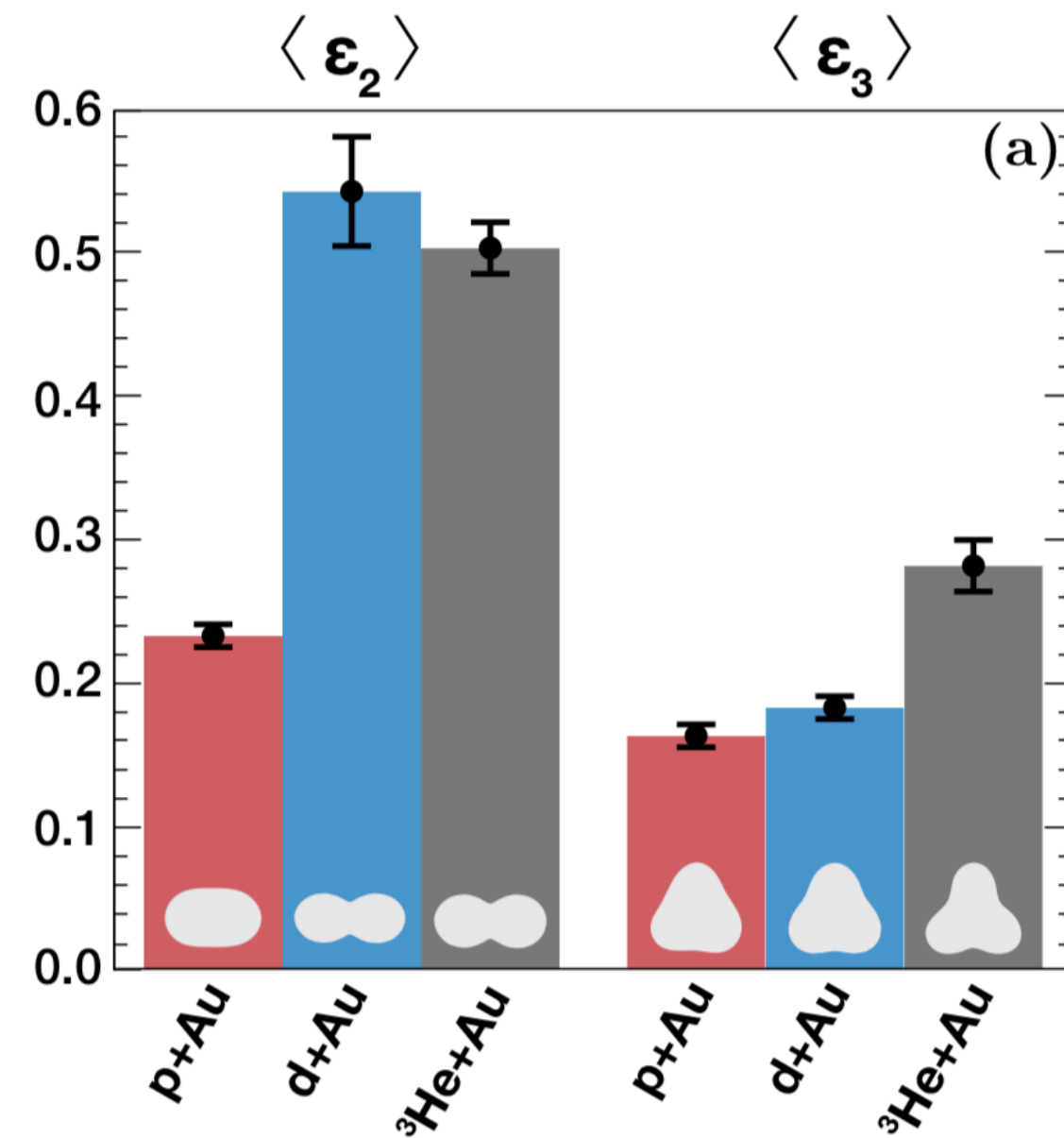


RHIC SYSTEM SCAN

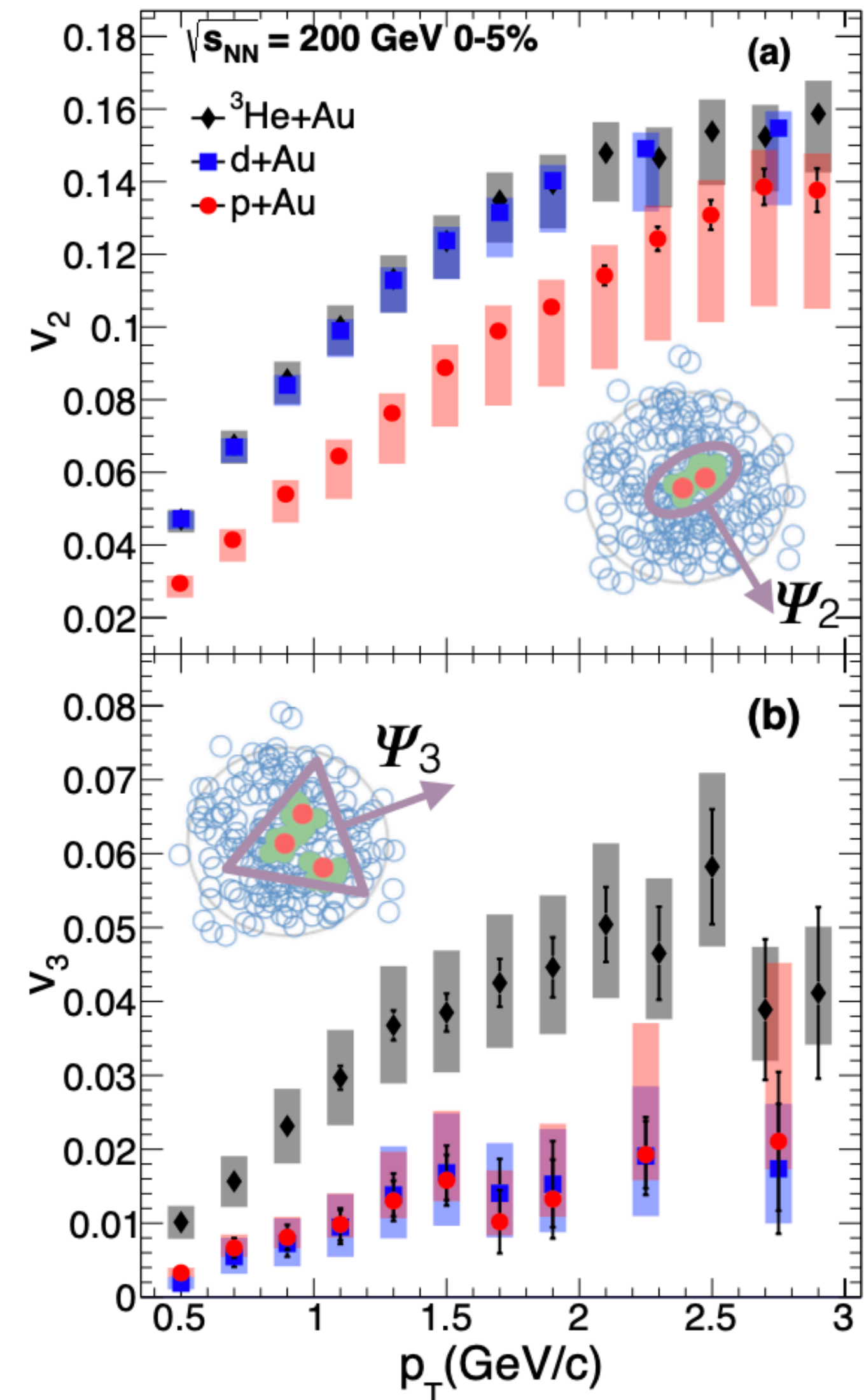
PHENIX Collaboration, *Nature Phys.* 15 (2019) no.3, 214-220

Idea: Engineer the geometry using different projectiles: p, d, ^3He

Simple model expectation: (using nucleon degrees of freedom)



Results confirmed expectation:

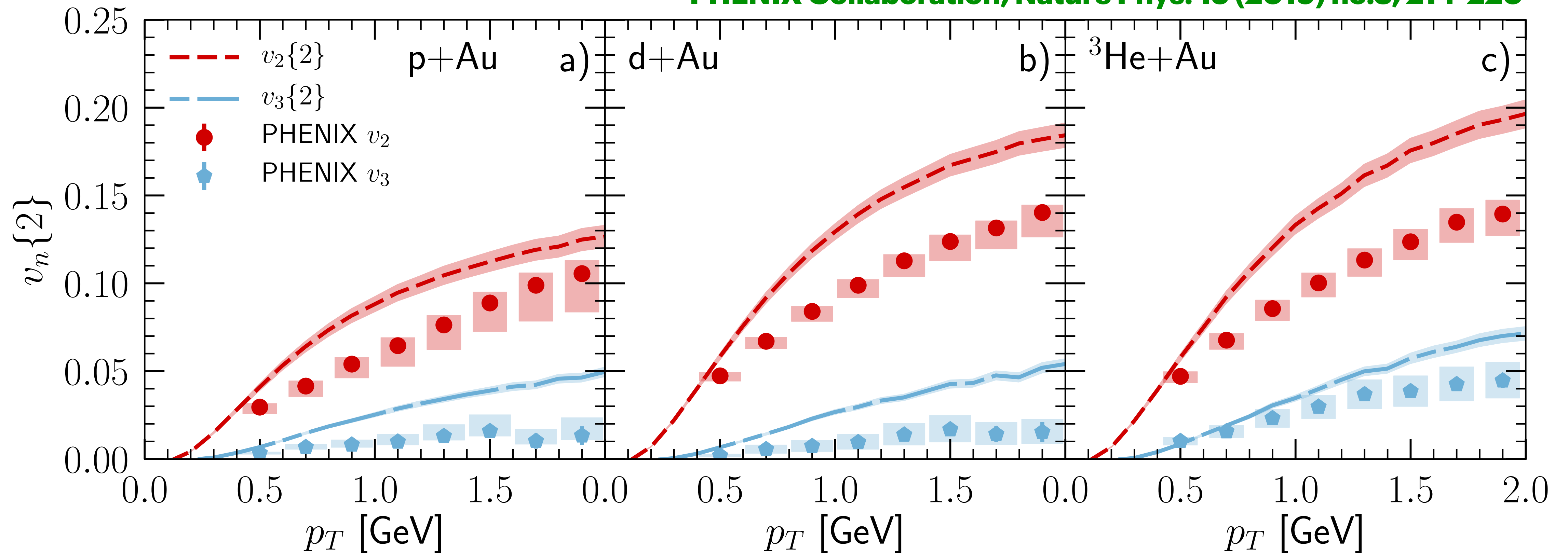


RHIC SYSTEM SCAN

B. Schenke, C. Shen, P. Tribedy, *Phys. Rev. C* 102 (2020) 4, 044905

Model results. Again, no fine tuning after fitting Au+Au data

PHENIX Collaboration, *Nature Phys.* 15 (2019) no.3, 214-220



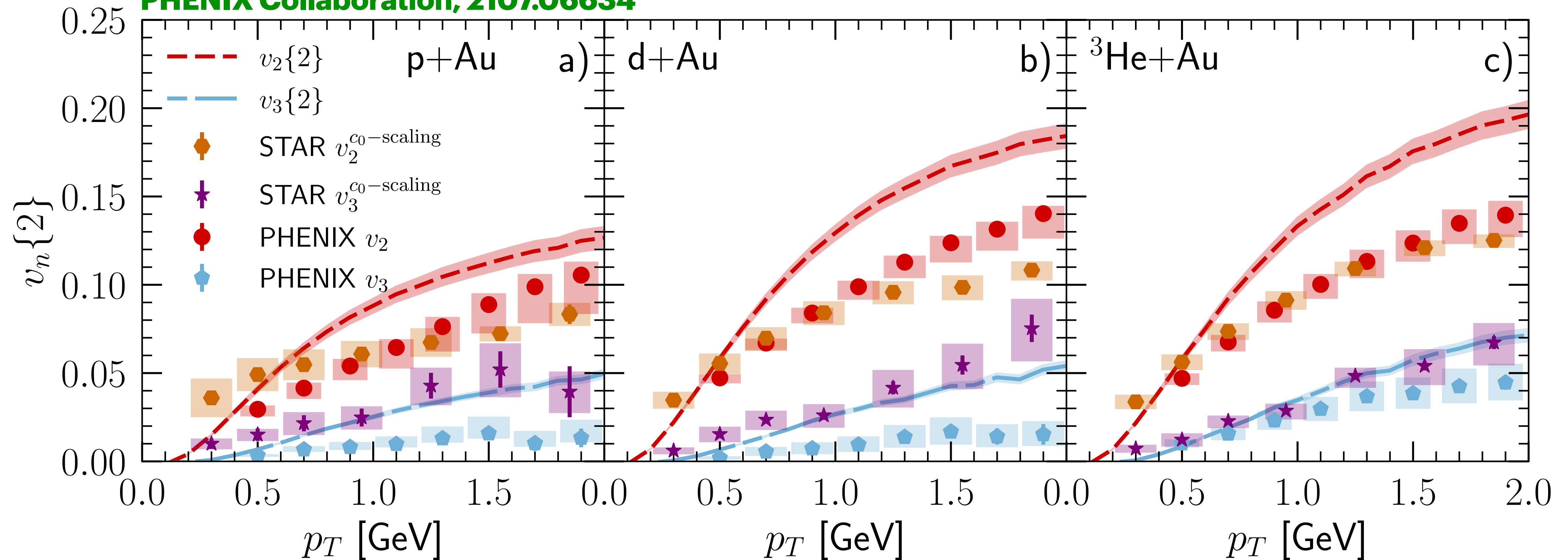
PHENIX VS. STAR

- Task force issued a report on the origin of the differences

https://indico.bnl.gov/event/11308/contributions/47820/attachments/35369/57704/Dunlop_PAC_2021.pdf

- PHENIX sees large changes in v_3 when changing η

PHENIX Collaboration, 2107.06634



PHENIX Collaboration, Nature Phys. 15 (2019) no.3, 214-220,
STAR data: New at QM2019, Shengli Huang IS 2021

STAR vs. PHENIX: Slide from P. Tribedy

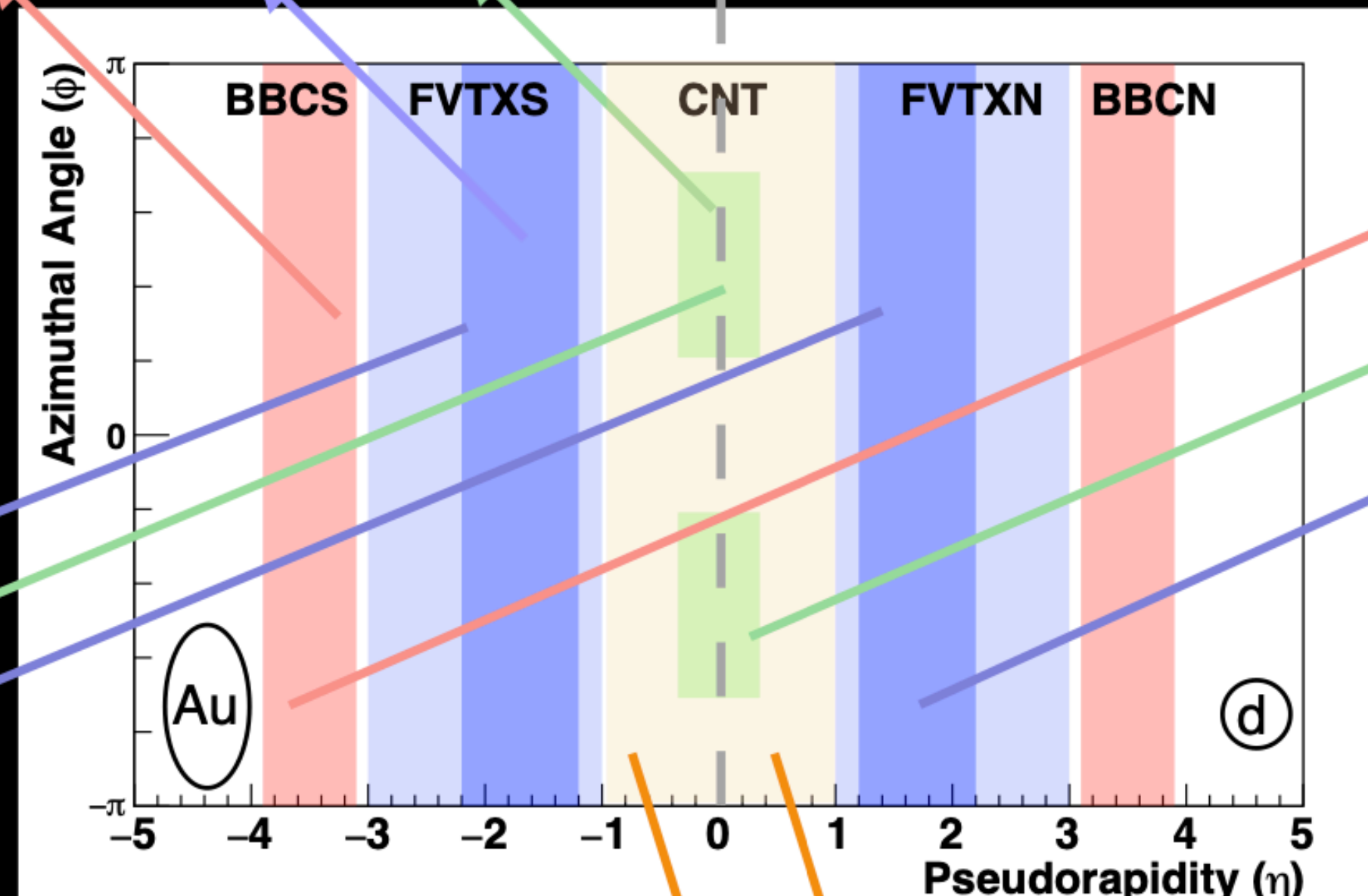
Strong acceptance dependence of (raw) harmonic coefficients

PHENIX (3x2PC,EP)
 $v_2(^3\text{He}+\text{Au}) \sim v_2(\text{d}+\text{Au}) > v_2(\text{p}+\text{Au})$ 😊
 $v_3(^3\text{He}+\text{Au}) > v_3(\text{d}+\text{Au}) \sim v_3(\text{p}+\text{Au})$ 😊

CGC+Hydro (Boost invariant)
 $v_2(^3\text{He}+\text{Au}) \sim v_2(\text{d}+\text{Au}) > v_2(\text{p}+\text{Au})$ 😊
 $v_3(^3\text{He}+\text{Au}) \sim v_3(\text{d}+\text{Au}) \sim v_3(\text{p}+\text{Au})$ 😞

Schenke, Shen, PT,
 Phys.Lett.B 803 (2020)
 135322

PHENIX collab, Nature Phys. 15, 214–220 (2019)



PHENIX (3x2PC)
 $v_2(\text{p}+\text{Au}) \geq v_2(\text{d}+\text{Au}) \geq v_2(^3\text{He}+\text{Au})$ 😞
 $v_3(^3\text{He}+\text{Au}) > 0$
 $v_3(\text{d}+\text{Au}) = ?$
 $v_3(\text{p}+\text{Au}) = ?$ 😞

PHENIX (3x2PC)
 $v_2(\text{p}+\text{Au}) \geq v_2(\text{d}+\text{Au}) \geq v_2(^3\text{He}+\text{Au})$ 😞
 $v_3(^3\text{He}+\text{Au}) > 0$
 $v_3(\text{d}+\text{Au}) = ?$
 $v_3(\text{p}+\text{Au}) = ?$ 😞

PHENIX collab., arXiv: 2107.06634v1,
 Nagle et. al, arXiv:2107.07287

PHENIX collab., arXiv: 2107.06634v1
 Nagle et. al, arXiv:2107.07287

STAR TPC (2PC)
 $v_2(^3\text{He}+\text{Au}) \sim v_2(\text{d}+\text{Au}) > v_2(\text{p}+\text{Au})$ 😊
 $v_3(^3\text{He}+\text{Au}) \sim v_3(\text{d}+\text{Au}) \sim v_3(\text{p}+\text{Au})$ 😞

😊 Shape engineering works

😞 Doesn't work (or can't be checked)

Shengli Huang, IS 2021

Collectivity, P. Tribedy, vConf21 26

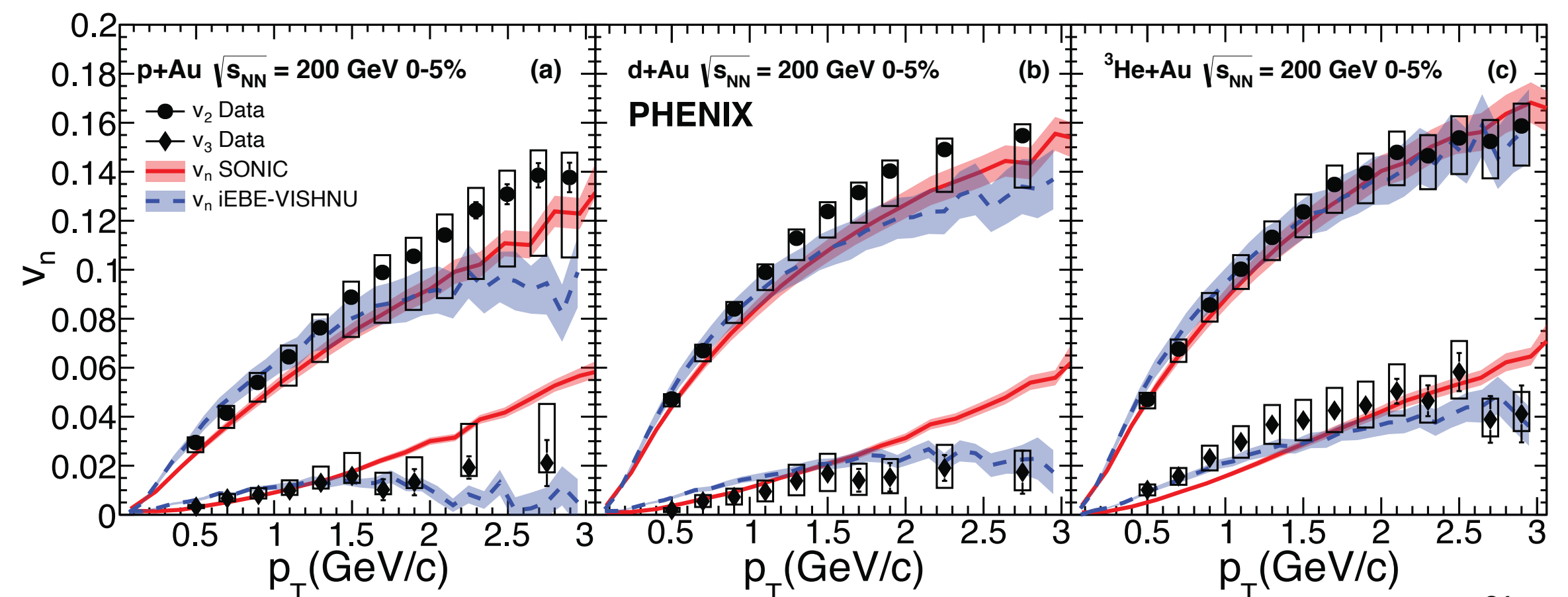
Björn Schenke, BNL

RAPIDITY DEPENDENCE

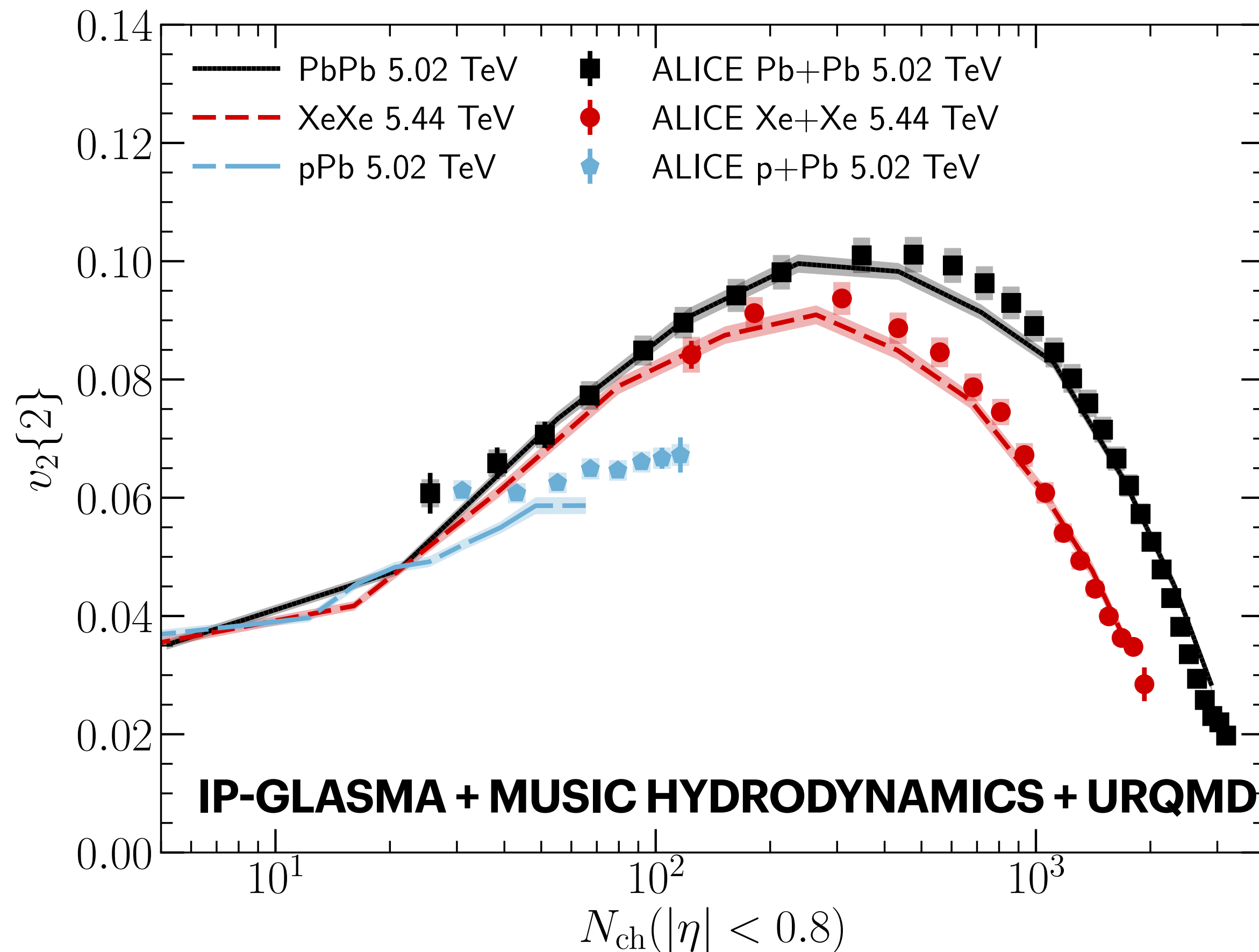
- Task force issued a report on the origin of the differences
https://indico.bnl.gov/event/11308/contributions/47820/attachments/35369/57704/Dunlop_PAC_2021.pdf
- PHENIX sees large changes in v_3 when changing η
- Strong indication that boost invariant calculations **cannot** be compared to the PHENIX data **PHENIX Collaboration, Nature Phys. 15 (2019) no.3, 214-220,**
- That includes ours **B. Schenke, C. Shen, P. Tribedy, Phys. Rev. C 102 (2020) 4, 044905**
B. Schenke, C. Shen, P. Tribedy, Phys.Lett.B 803 (2020) 135322
- But also SONIC
and iEbE-VISHNU results

M. Habich, J.L. Nagle, P. Romatschke
Eur. Phys. J. C 75, 15 (2015)

C. Shen, J.-F. Paquet, G. S. Denicol, S. Jeon, S., C. Gale
Phys. Rev. C 95, 014906 (2017).



ORIGINS OF MOMENTUM ANISOTROPHY



Anisotropic flow in heavy ion and high multiplicity small system collisions is driven by final state response to the initial geometry

**B. Schenke, C. Shen, P. Tribedy, Phys.Rev.C 102 (2020) 044905
ALICE Collaboration, Phys.Rev.Lett. 123 (2019) 142301**

ORIGINS OF MOMENTUM ANISOTROPY

The initial momentum distribution is already anisotropic

The Color Glass Condensate predicts anisotropic particle production because of

- 1. Local anisotropies in the color fields**
- 2. Local density gradients**
- 3. Quantum interference effects**

Gelis, Lappi Venugopalan PRD 78 054020 (2008), PRD 79 094017 (2009)

Dumitru, Gelis, McLerran, Venugopalan NPA810, 91 (2008)

Dumitru, Jalilian-Marian PRD 81 094015 (2010)

Dusling, Venugopalan PRD 87 (2013)

A. Dumitru, A.V. Giannini, Nucl.Phys.A933 (2014) 212

V. Skokov. Phys.Rev.D91 (2015) 054014

T. Lappi, B. Schenke, S. Schlichting, R. Venugopalan, JHEP 1601 (2016) 061

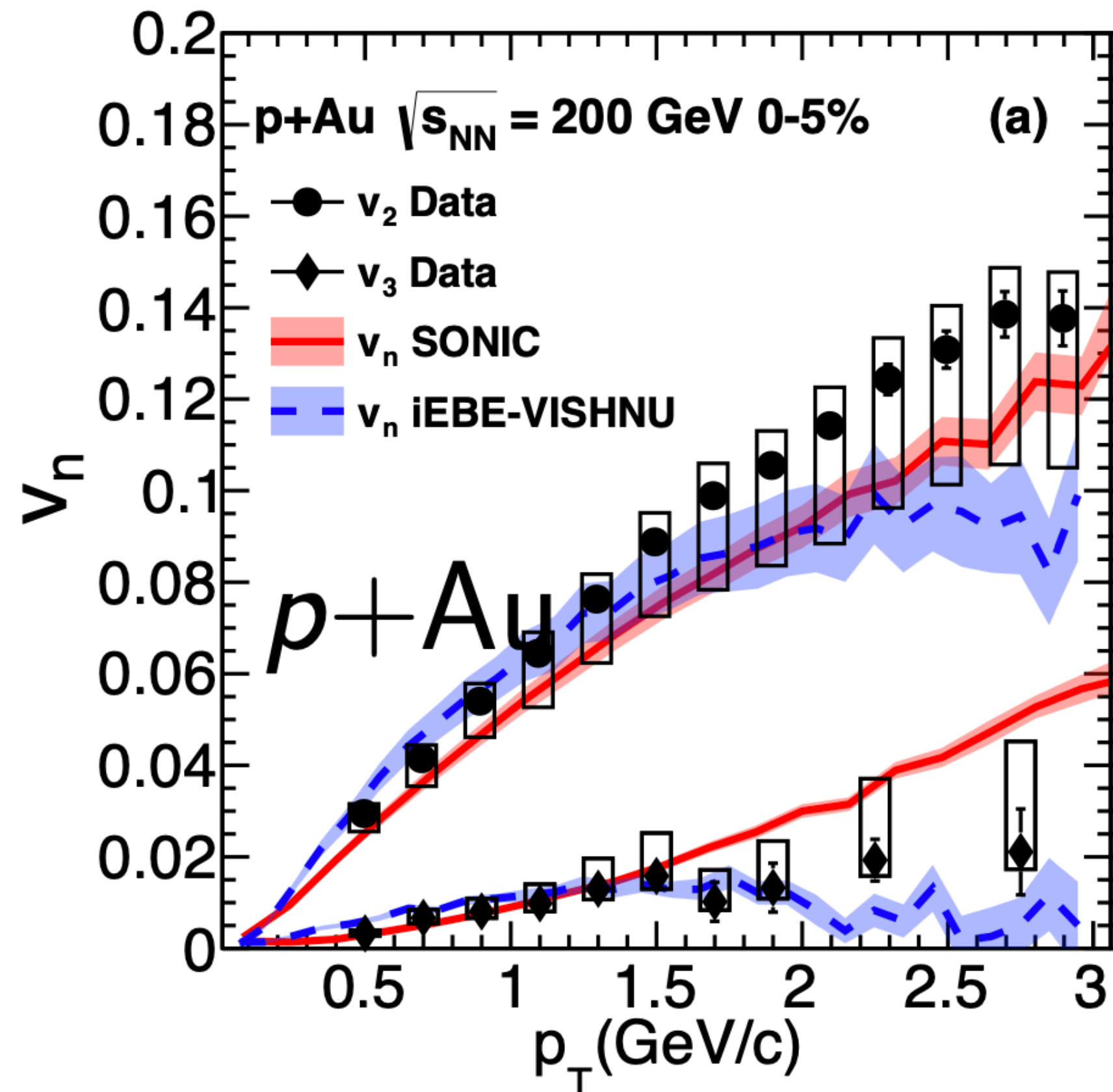
Kovner, Skokov, Phys.Rev. D98 (2018) no.1, 014004

...

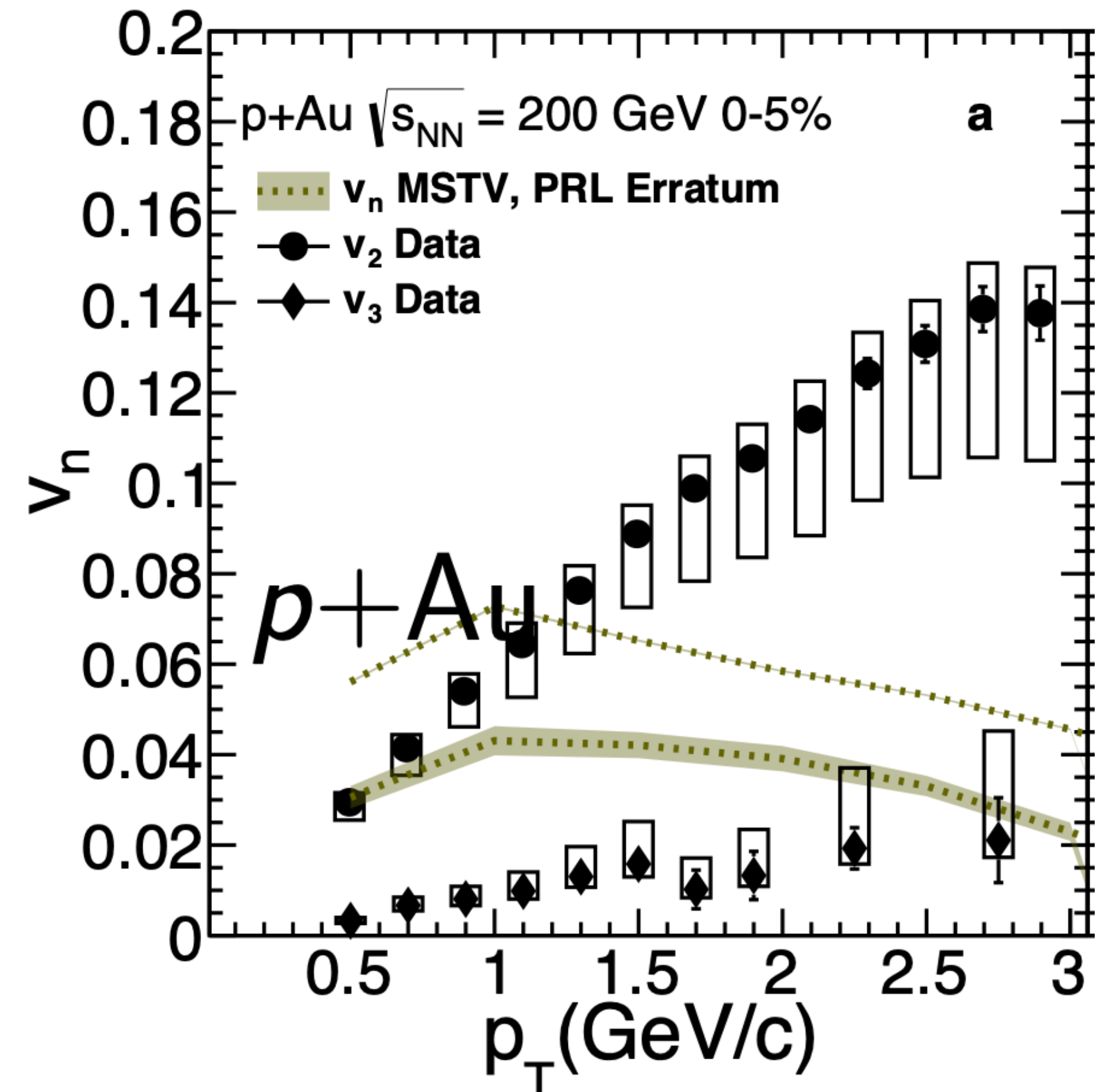
FINAL STATE EFFECTS ARE NEEDED

Qualitative features of the data are not well described by initial state anisotropy *alone*

GEOMETRY RESPONSE ONLY



INITIAL MOMENTUM ANISOTROPY ONLY



R. Belmont at the 2020 RHIC & AGS Users' Meeting

BUT INITIAL STATE EFFECTS ARE THERE

Our calculation using the IP-Glasma initial state and hydrodynamics includes both effects

Initial state anisotropies are significant and can affect the final result at low multiplicity

$$Q_\varepsilon = \frac{\text{Re}\langle \mathcal{E} V_2^* \rangle}{\sqrt{\langle |\mathcal{E}|^2 \rangle \langle |V_2|^2 \rangle}}$$

CORRELATION OF THE FINAL ELLIPTIC FLOW V_2

WITH

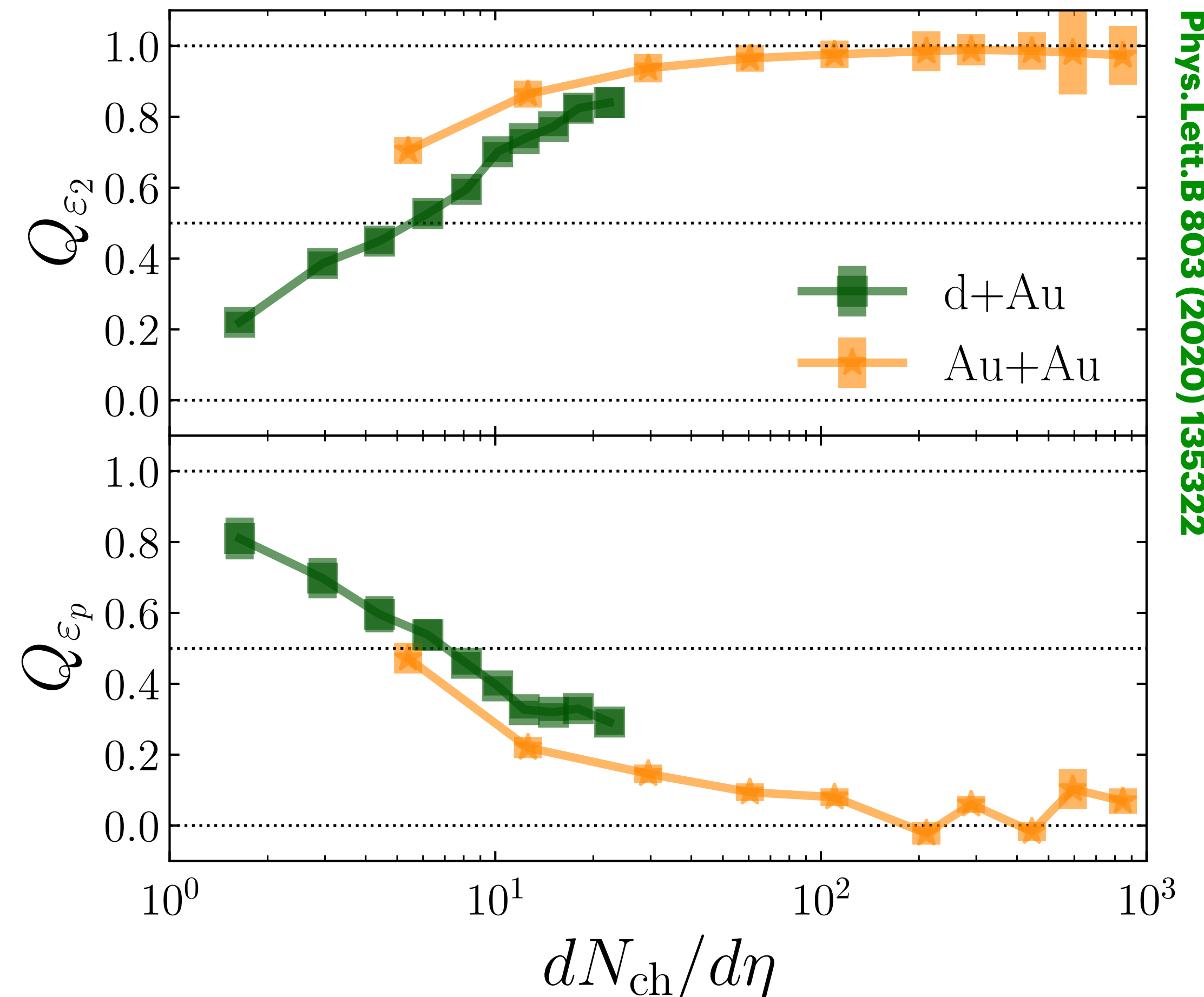
THE GEOMETRIC ELLIPTICITY

$$\mathcal{E}_2 = \varepsilon_2 e^{i2\psi_2} = \frac{\langle x^2 - y^2 \rangle + i\langle 2xy \rangle}{\langle x^2 + y^2 \rangle}$$

AND

THE INITIAL MOMENTUM ANISOTROPY

$$\mathcal{E}_p = \varepsilon_p e^{i2\psi_2^p} = \frac{\langle T^{xx} - T^{yy} \rangle + i\langle 2T^{xy} \rangle}{\langle T^{xx} + T^{yy} \rangle}$$



B. Schenke, C. Shen, P. Tribedy
Phys.Lett.B 803 (2020) 135322

HOW TO DISTINGUISH THE SOURCE OF ANISOTROPY

P. Bozek, Phys. Rev. C 93, 044908 (2016); B. Schenke, C. Shen, D. Teaney, Phys. Rev. C 102, 034905 (2020)

G. Giacalone, B. Schenke, C. Shen, Phys. Rev. Lett. 125 (2020) 19, 192301

Use the correlation of mean transverse momentum $[p_T]$ and v_2^2 at fixed multiplicity:

$$\hat{\rho}(v_n^2, [p_T]) = \frac{\langle \hat{\delta}v_n^2 \hat{\delta}[p_T] \rangle}{\langle (\hat{\delta}v_n^2)^2 \rangle \langle (\hat{\delta}[p_T])^2 \rangle}$$

$$\hat{\delta}O \equiv \delta O - \frac{\langle \delta O \delta N \rangle}{\sigma_N^2} \delta N$$

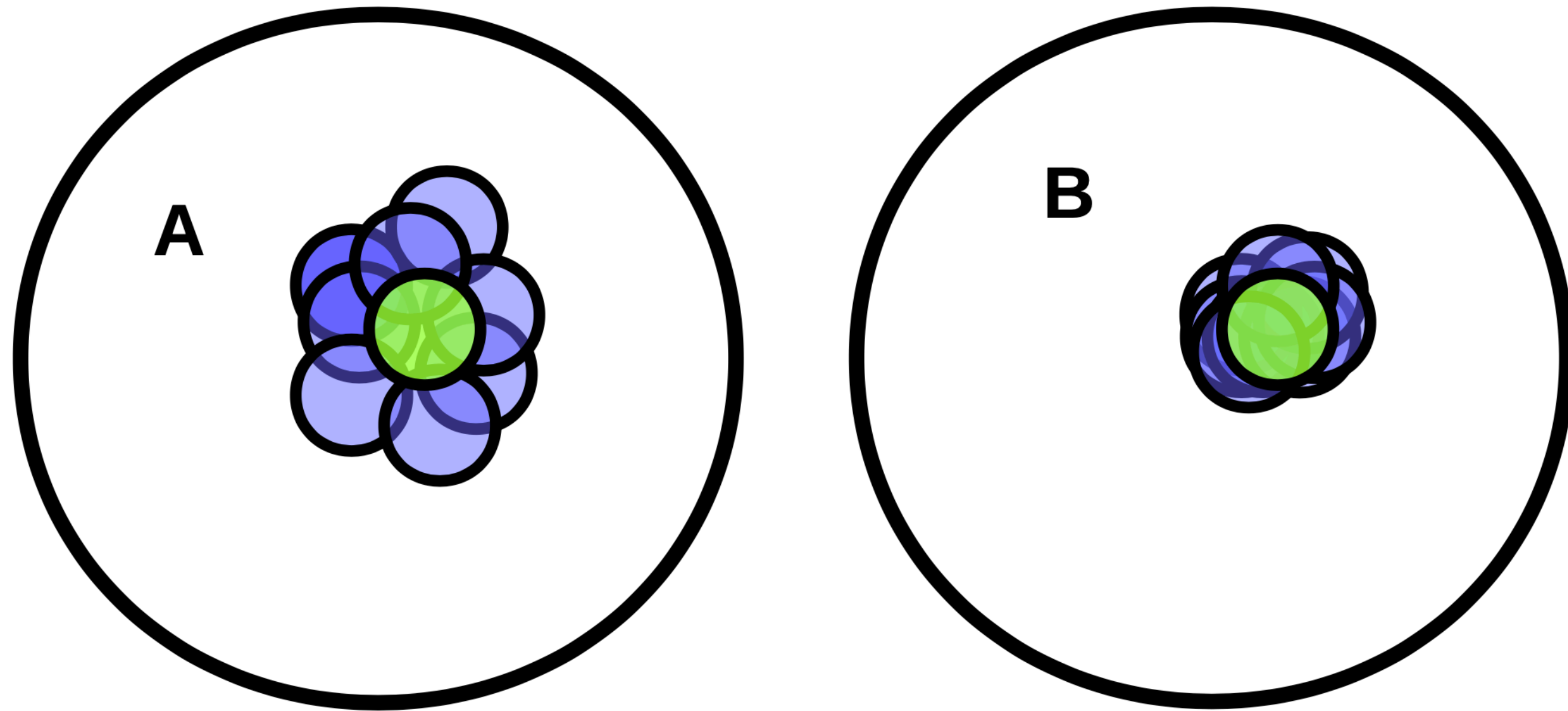
A. Olszewski, W. Broniowski, Phys. Rev. C 96, 054903 (2017)

It can help to identify the source of the azimuthal anisotropy in the experimental data

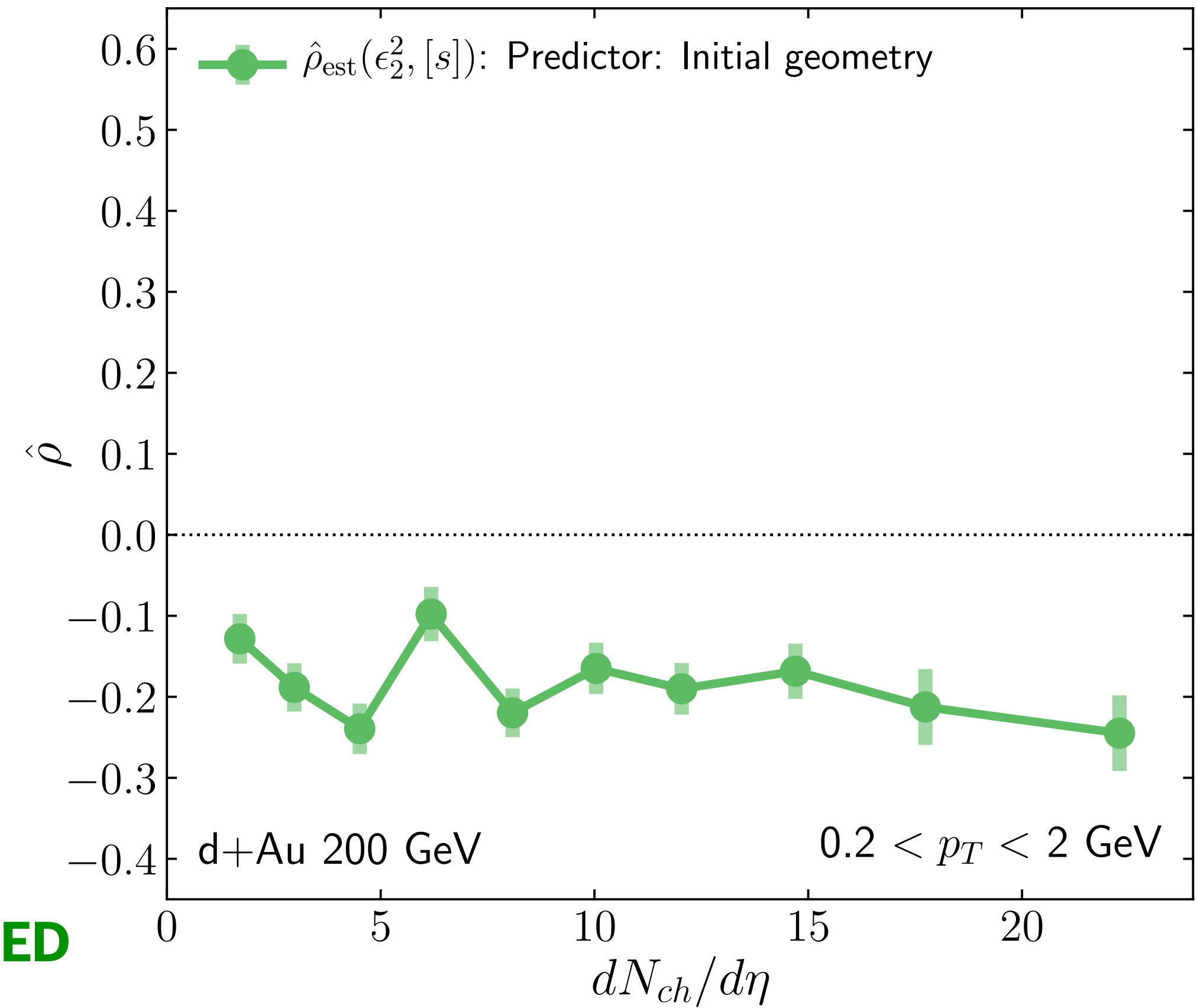
The two origins of v_2 have very distinct predictions for this correlator

SMALL SYSTEMS: CORRELATION FROM GEOMETRY

G. Giacalone, B. Schenke, C. Shen, Phys. Rev. Lett. 125 (2020) 19, 192301



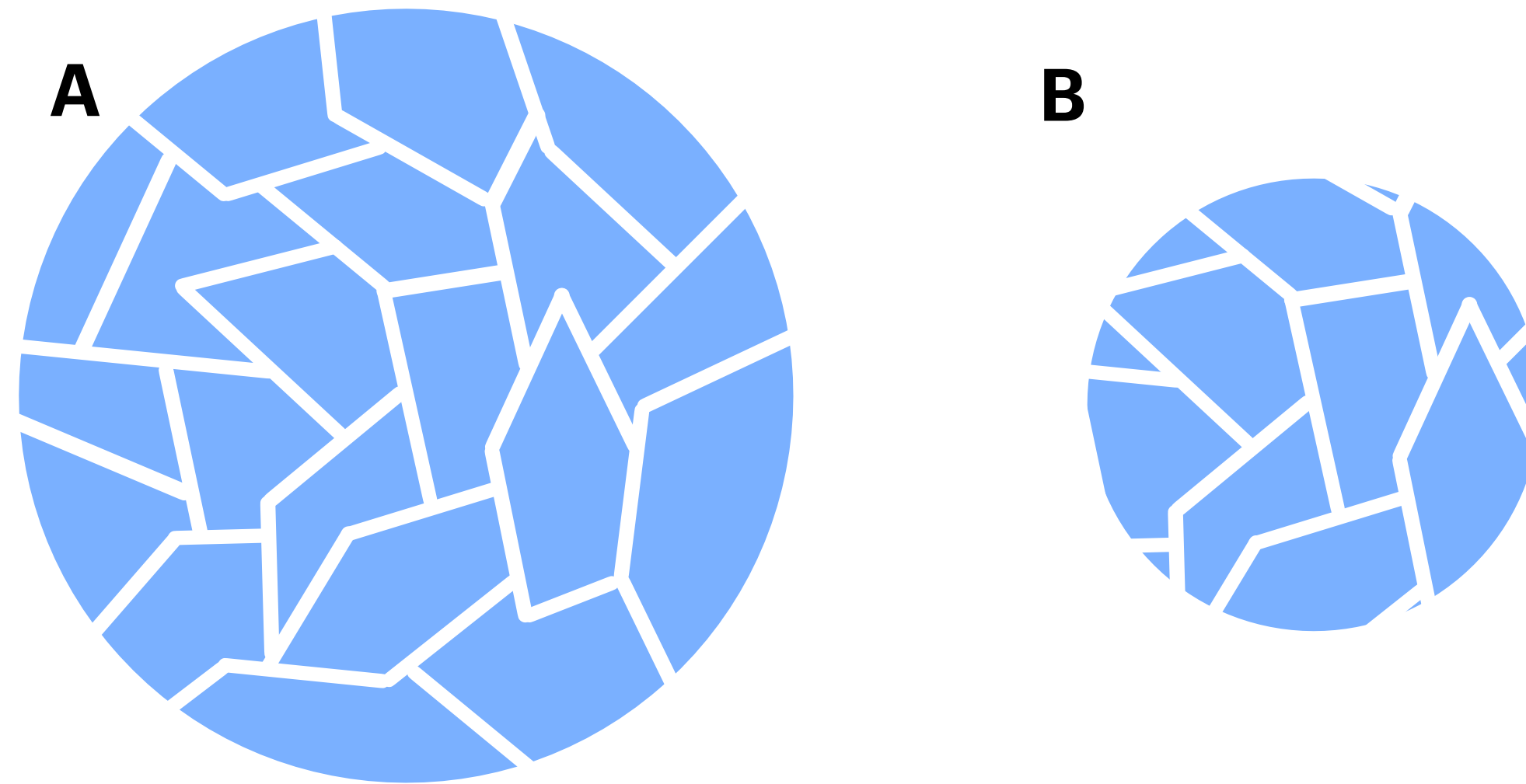
$$\left. \begin{aligned}
 R(A) &> R(B) \\
 \langle p_T \rangle(A) &< \langle p_T \rangle(B) \\
 \varepsilon_2(A) &> \varepsilon_2(B)
 \end{aligned} \right\} v_2 \text{ AND } \langle p_T \rangle \text{ ARE ANTI-CORRELATED}$$



CORRELATION FROM INITIAL MOMENTUM ANISOTROPHY

G. Giacalone, B. Schenke, C. Shen, Phys. Rev. Lett. 125 (2020) 19, 192301

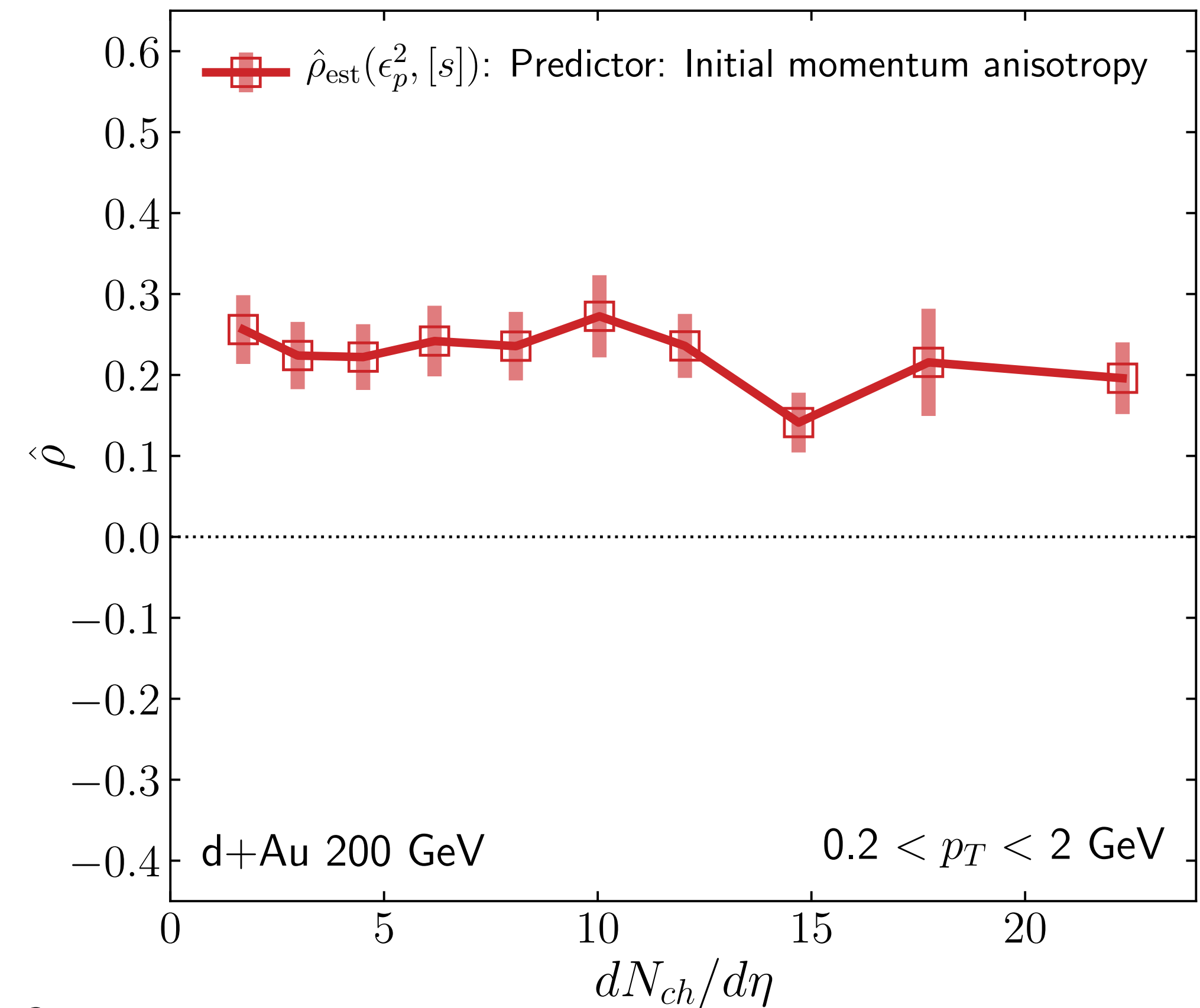
COLOR DOMAIN CARTOON (PARTICLES PRODUCED FROM ONE DOMAIN ARE CORRELATED):



$$\left. \begin{aligned}
 R(A) &> R(B) \\
 \langle p_T \rangle(A) &< \langle p_T \rangle(B) \\
 \varepsilon_p(A) &< \varepsilon_p(B)
 \end{aligned} \right\} v_2 \text{ AND } \langle p_T \rangle \text{ ARE CORRELATED}$$

BECAUSE A HAS MORE DOMAINS

NOTE: Multiplicity is dominated by projectile Q_s
 At fixed multiplicity, for the target: $Q_s(A) \approx Q_s(B) \rightarrow$ domain sizes $1/Q_s$ are the same
 $\langle p_T \rangle$ assumed to be still driven by the geometry



WHICH ONE SURVIVES?

G. Giacalone, B. Schenke, C. Shen, Phys. Rev. Lett. 125 (2020) 19, 192301

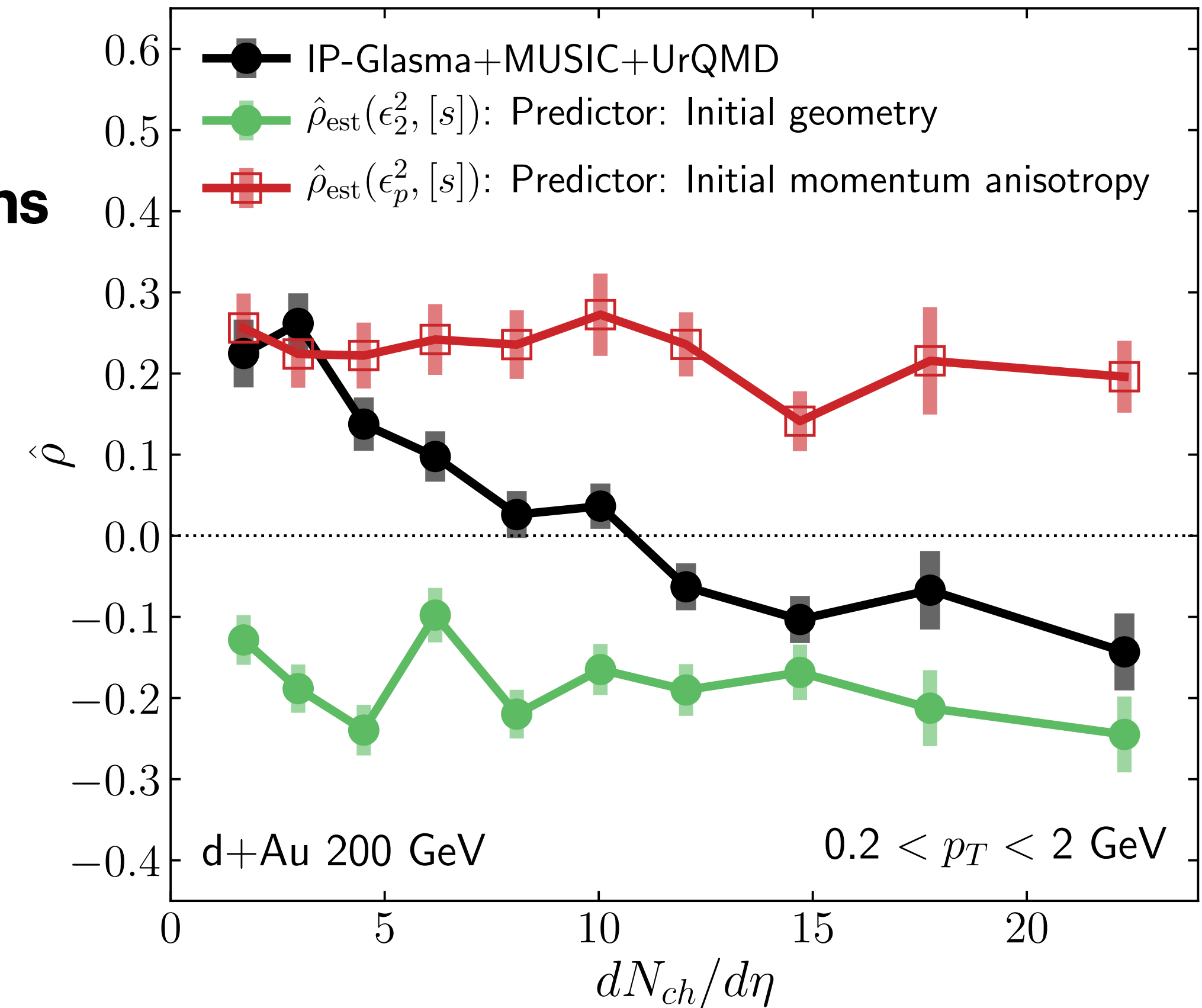
IT DEPENDS ON MULTIPLICITY

We predict a sign change of the ρ correlator with multiplicity in p/d+Au collisions at RHIC and p+Pb collisions at LHC around $dN_{ch}/d\eta \approx 10$

Below $dN_{ch}/d\eta \approx 10$
initial momentum anisotropy dominates

Above $dN_{ch}/d\eta \approx 10$
final state response to the initial geometry dominates

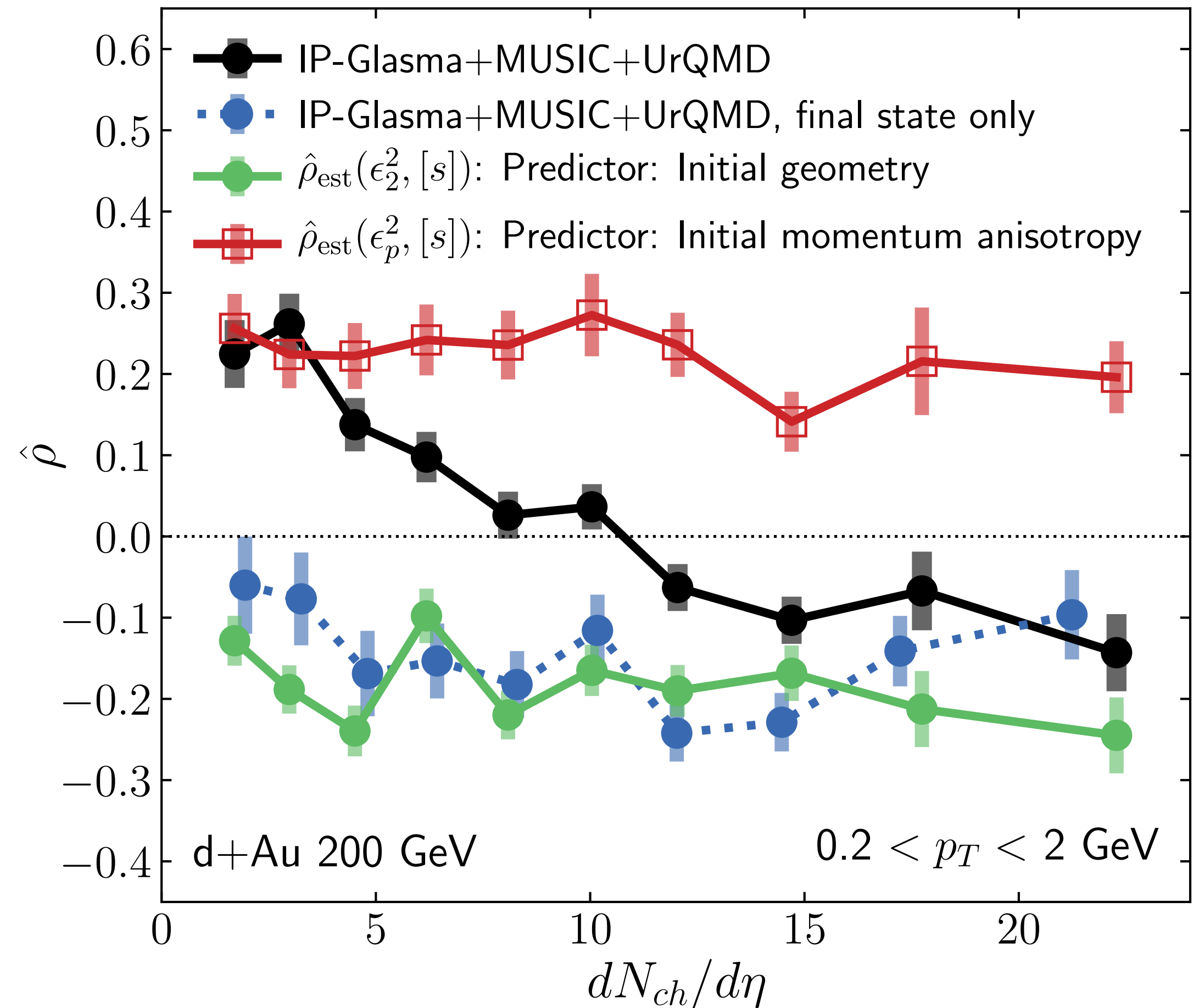
The observable moves from one predictor to the other



CHECK: REMOVE THE INITIAL STATE MOMENTUM ANISOTROPHY

G. Giacalone, B. Schenke, C. Shen, Phys. Rev. Lett. 125 (2020) 19, 192301

With no initial momentum anisotropy, our result follows the geometry predictor for all $dN_{ch}/d\eta$ as expected



CHECK: REMOVE THE INITIAL STATE MOMENTUM ANISOTROPHY

G. Giacalone, B. Schenke, C. Shen, Phys. Rev. Lett. 125 (2020) 19, 192301

With no initial momentum anisotropy, our result follows the geometry predictor for all $dN_{ch}/d\eta$ as expected

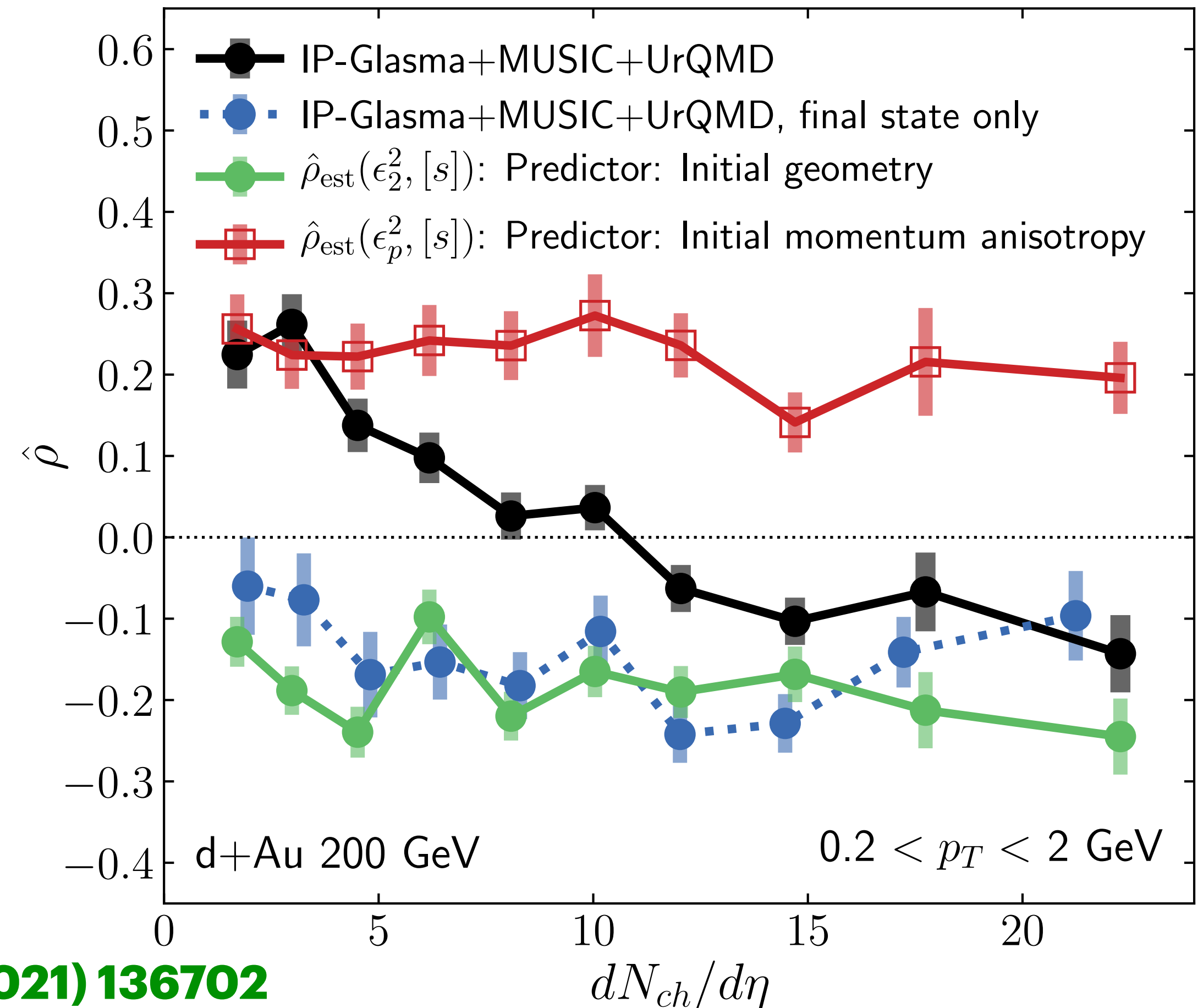
Is it detectable?

Very low multiplicity

Non-flow can mimic the signal

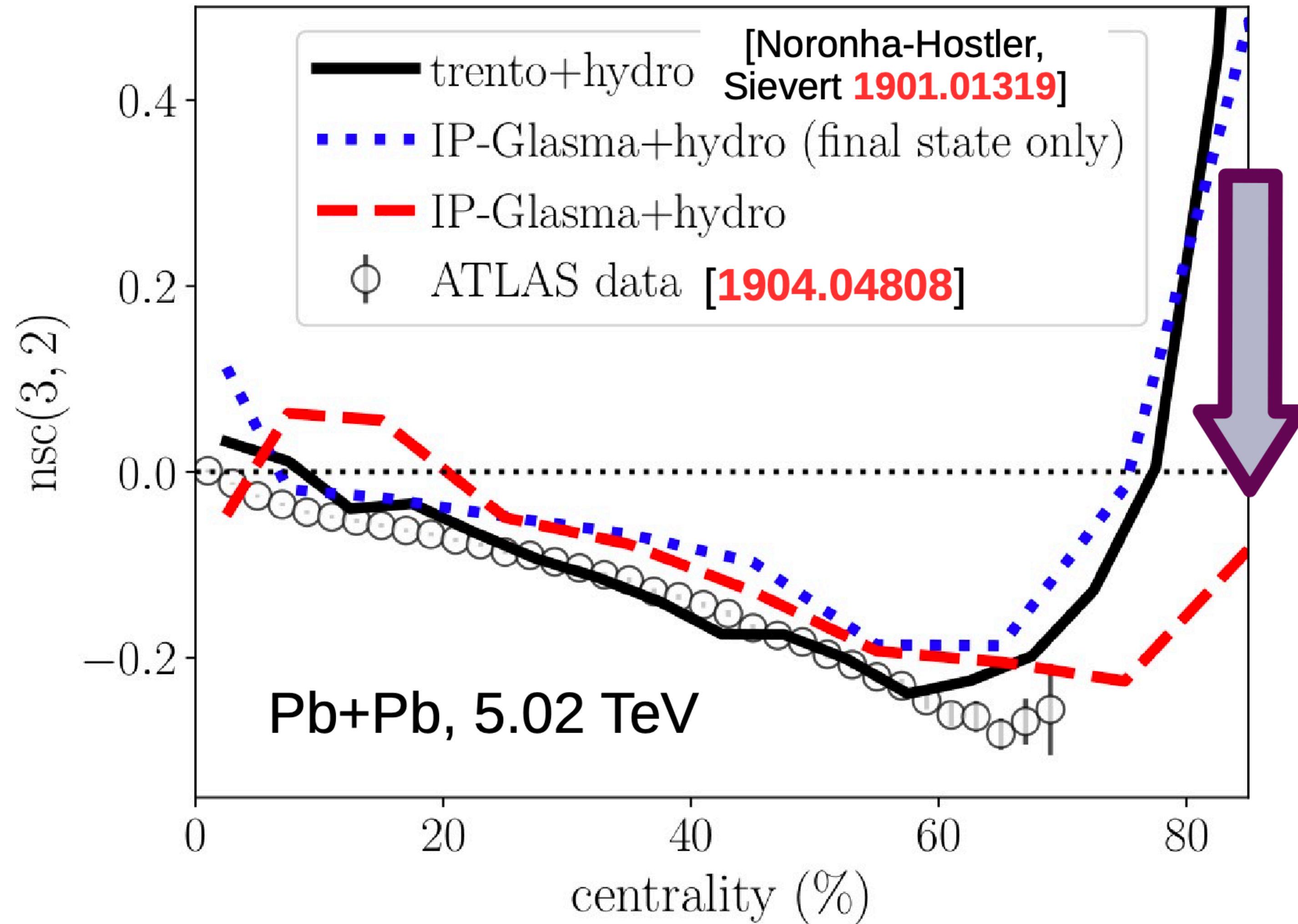
C. Zhang, A. Behera, S. Bhatta, J. Jia, Phys.Lett.B 822 (2021) 136702

S. H. Lim, J. L. Nagle, Phys.Rev.C 103 (2021) 6, 064906



CORRELATION BETWEEN v_2^2 AND v_3^2

G. Giacalone, B. Schenke, C. Shen, in preparation



BEYOND BOOST-INVARIANCE

What is the rapidity dependence of the initial momentum space anisotropy?

Does it survive the experimentally applied gap?

PART II: GOING BEYOND BOOST INVARIANCE

- **Use the CGC including JIMWLK evolution**
- **Do not assume boost invariance**

BEYOND BOOST-INVARIANCE

work in progress with Pragma Singh and Sören Schlichting

Employ JIMWLK small-x evolution to the proton and nucleus

as in B. Schenke, S. Schlichting, Phys.Lett.B 739 (2014) 313-319 and Phys.Rev.C 94 (2016) 4, 044907

$$V_{\mathbf{x}_\perp}(Y + dY) = \text{Functional Langevin equation}$$
$$\exp \left\{ -i \frac{\sqrt{\alpha_s dY}}{\pi} \int_{\mathbf{z}_\perp} K_{\mathbf{x}_\perp - \mathbf{z}_\perp} \cdot (V_{\mathbf{z}_\perp} \boldsymbol{\xi}_{\mathbf{z}_\perp} V_{\mathbf{z}_\perp}^\dagger) \right\}$$
$$\times V_{\mathbf{x}_\perp}(Y) \exp \left\{ i \frac{\sqrt{\alpha_s dY}}{\pi} \int_{\mathbf{z}_\perp} K_{\mathbf{x}_\perp - \mathbf{z}_\perp} \cdot \boldsymbol{\xi}_{\mathbf{z}_\perp} \right\}, \quad (7)$$

IR regularized JIMWLK Kernel

$$K_{\mathbf{x}_\perp - \mathbf{z}_\perp} = m |\mathbf{x}_\perp - \mathbf{z}_\perp| K_1(m |\mathbf{x}_\perp - \mathbf{z}_\perp|) \frac{\mathbf{x}_\perp - \mathbf{z}_\perp}{(\mathbf{x}_\perp - \mathbf{z}_\perp)^2}$$

Compute the energy momentum tensor in different rapidity bins after Yang-Mills evolution

Study the correlation function of the geometry and initial momentum anisotropy as a function of rapidity

EVOLUTION OF THE PROTON

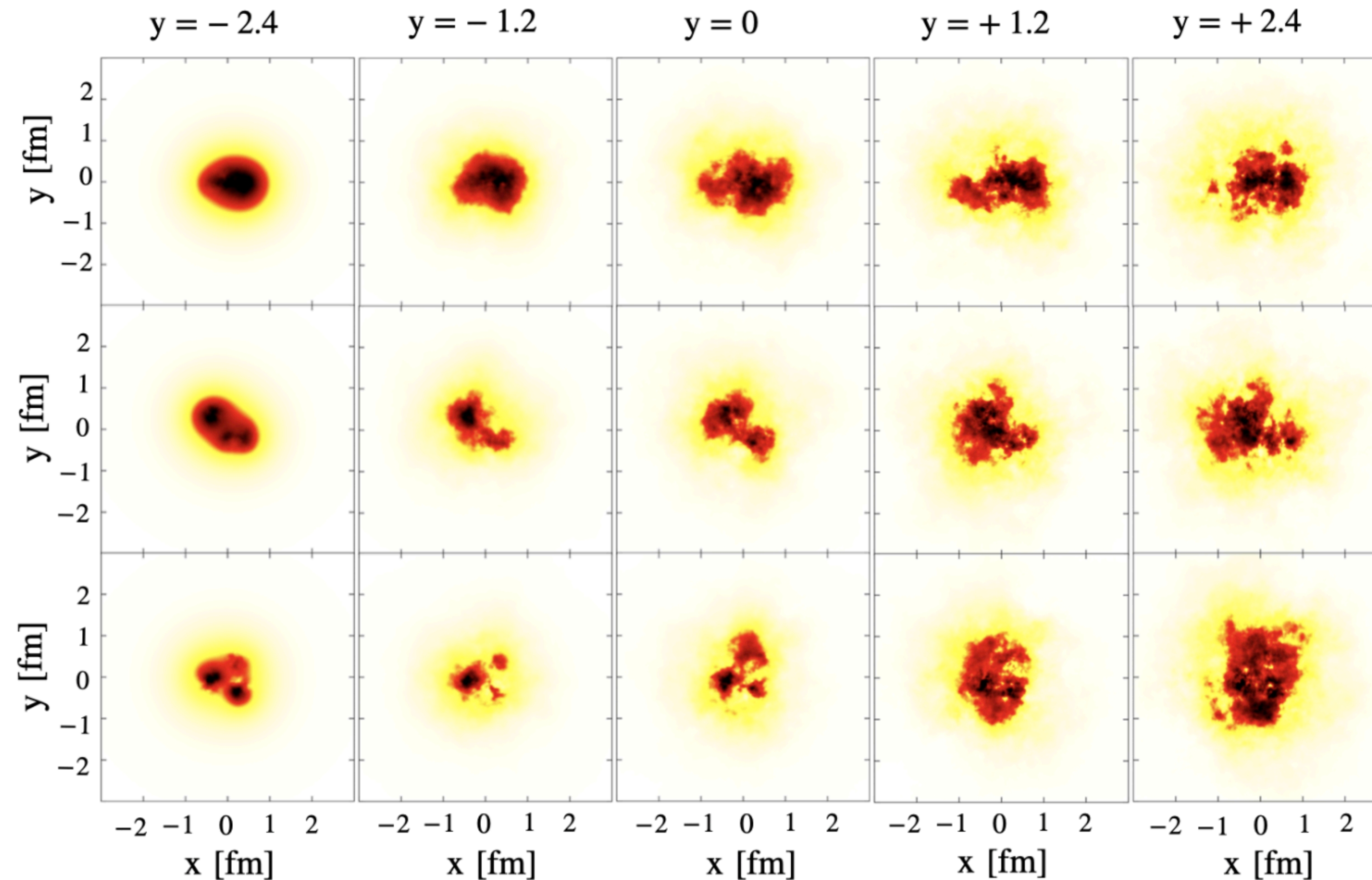
work in progress with Pragma Singh and Sören Schlichting

3 EXAMPLES

PROTON 1

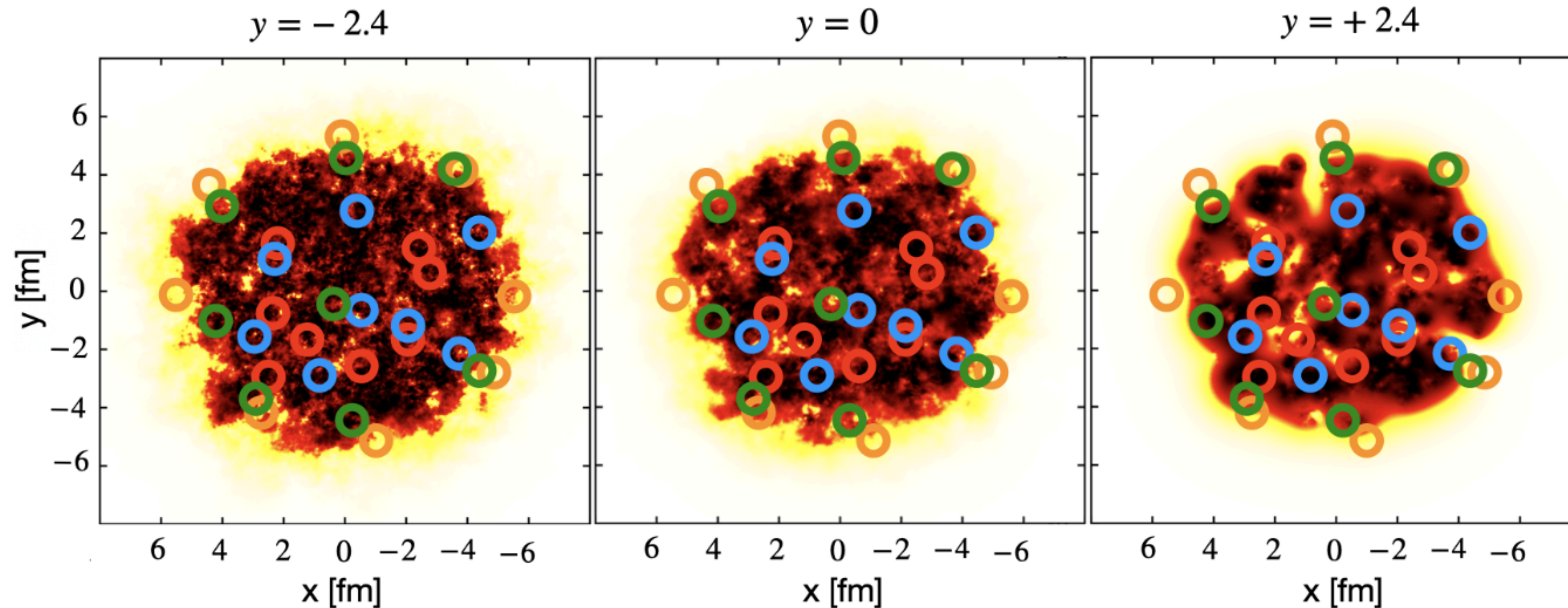
PROTON 2

PROTON 3



EVOLUTION OF THE NUCLEUS

work in progress with Pragma Singh and Sören Schlichting

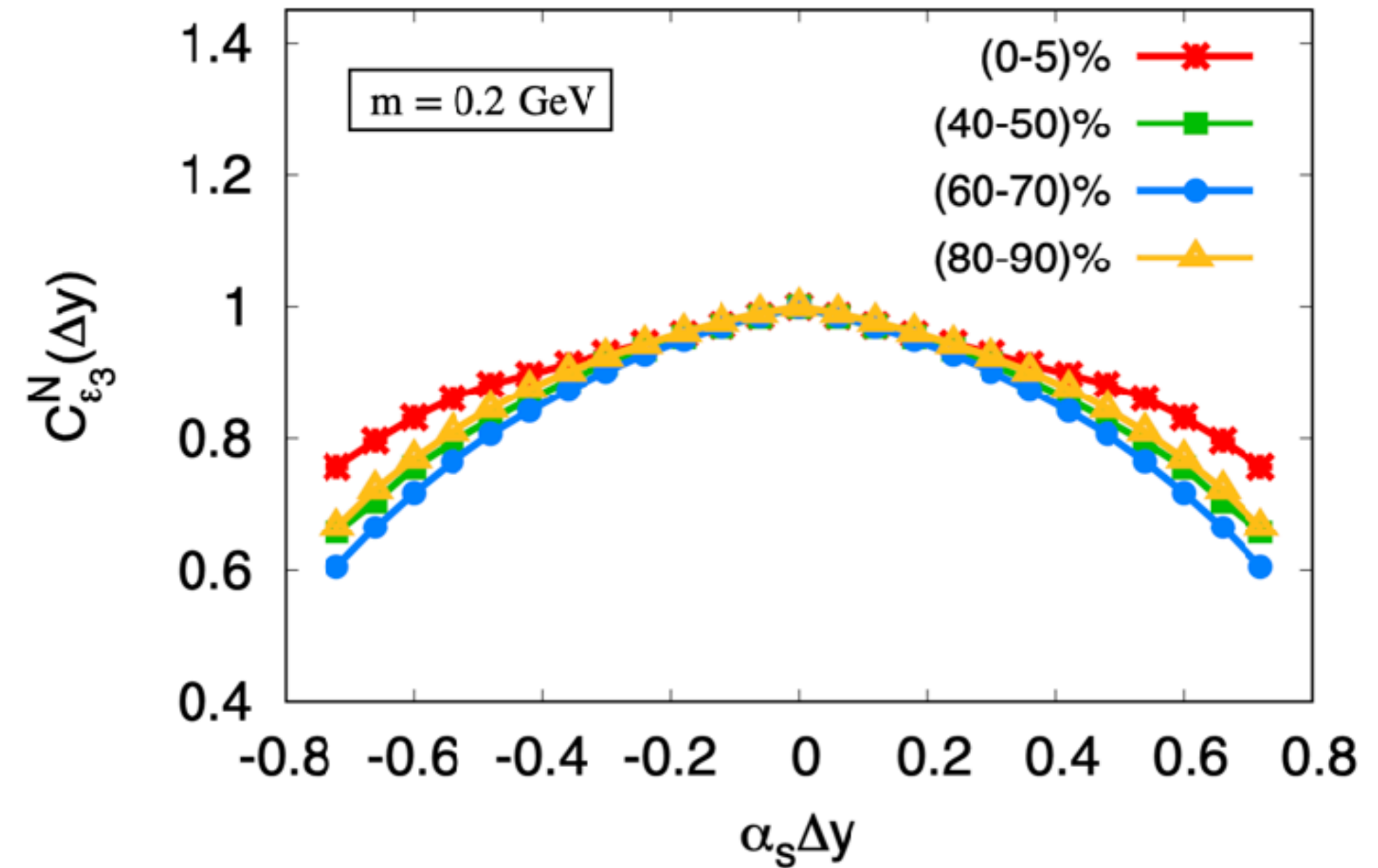
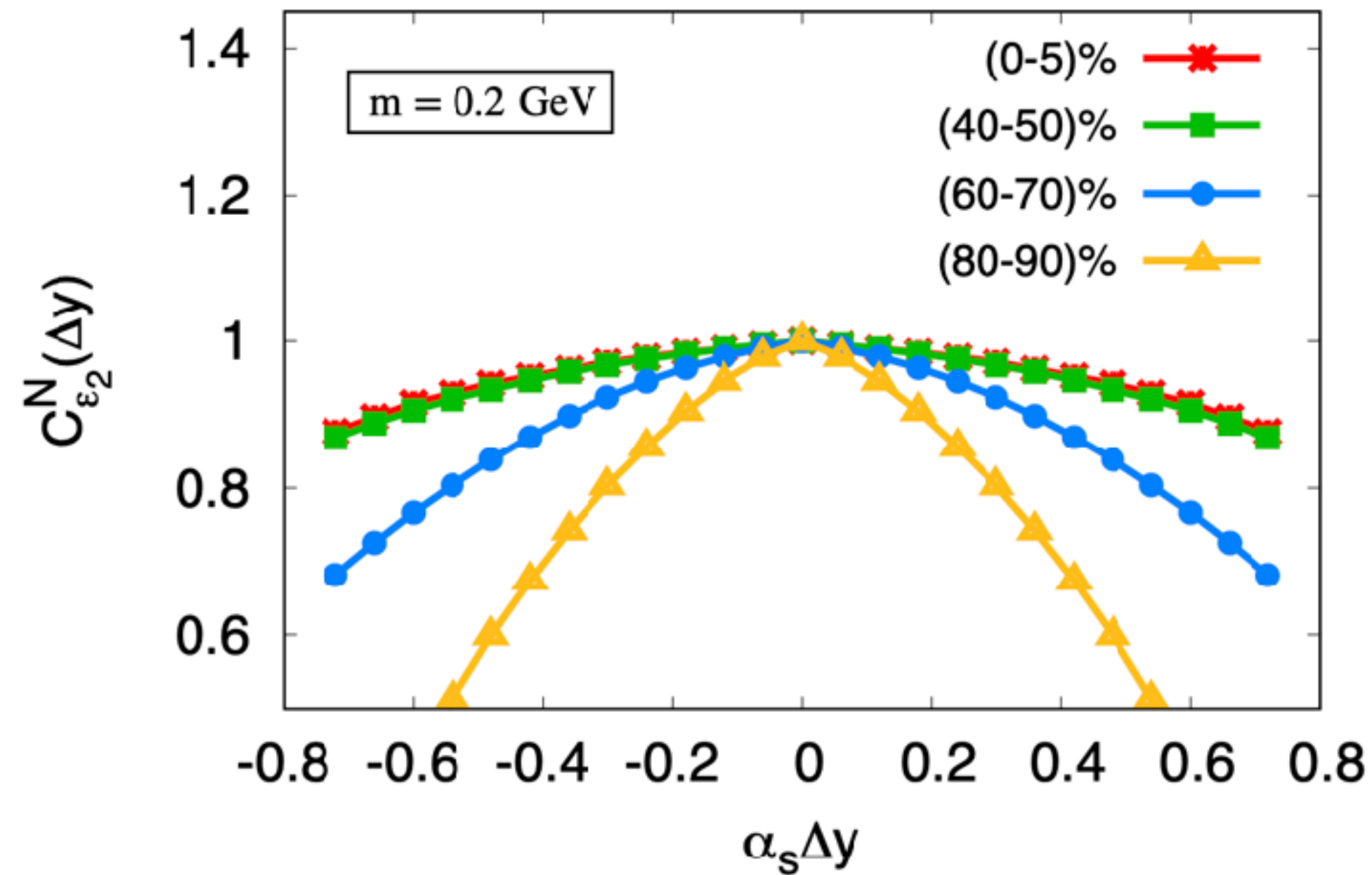


Dots indicate places where the proton hit in a given event in centrality class 0-5% (blue), 40-50% (blue), 60-70% (green), 80-90% (orange)

Centrality is determined at mid-rapidity

CORRELATION OF ECCENTRICITY

work in progress with Pragma Singh and Sören Schlichting



The geometry, quantified here with ϵ_2 and ϵ_3 , decorrelates fairly slowly, at least for not too peripheral events

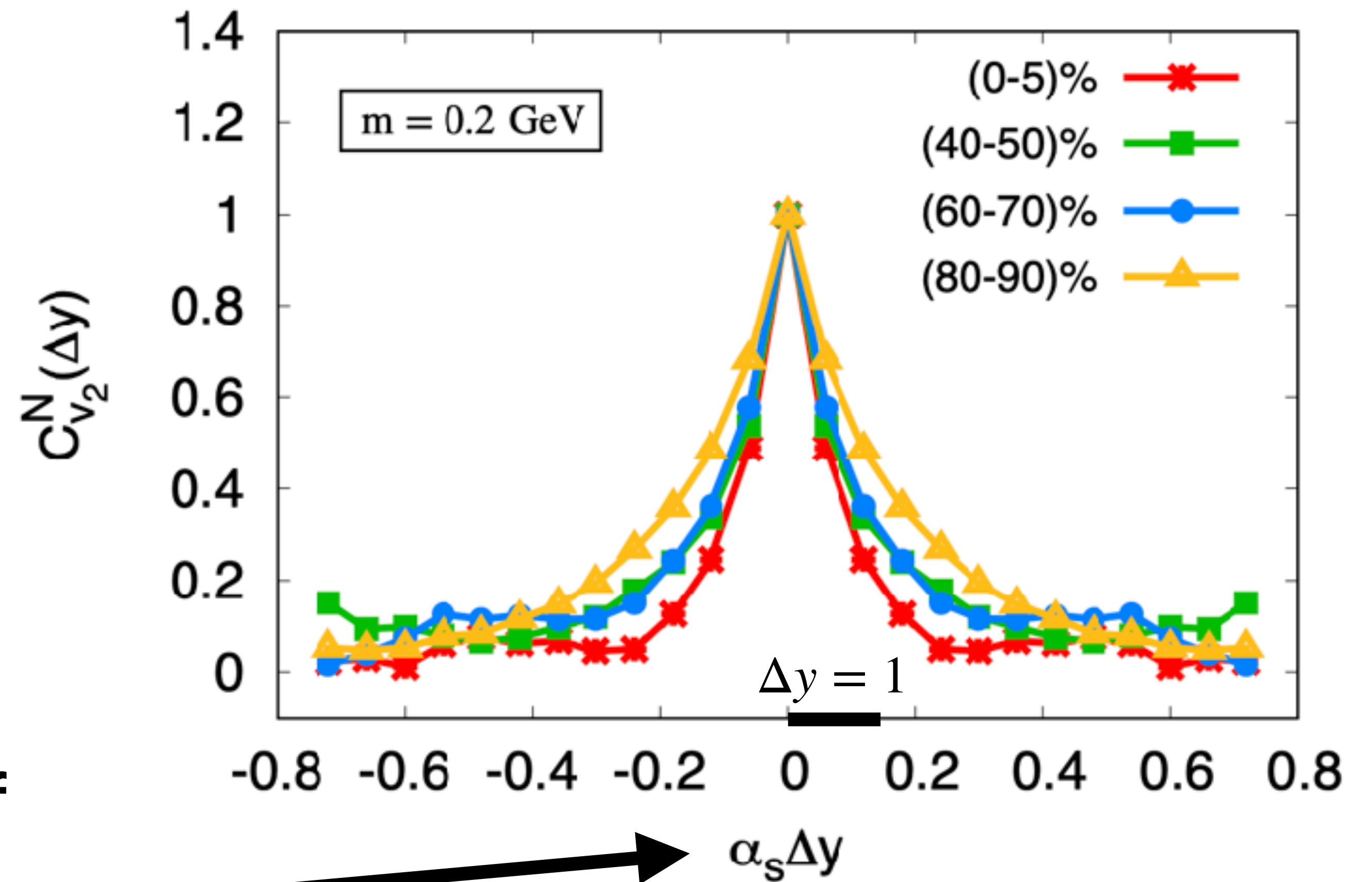
$$C_{\mathcal{O}}^N(\eta_1, \eta_2) = \frac{\langle \text{Re}(\mathcal{O}(\eta_1)\mathcal{O}^*(\eta_2)) \rangle}{\sqrt{\langle |\mathcal{O}(\eta_1)|^2 \rangle \langle |\mathcal{O}(\eta_2)|^2 \rangle}}$$

CORRELATION OF INITIAL MOMENTUM ANISOTROPHY

work in progress with Pragma Singh and Sören Schlichting

The initial momentum anisotropy, ε_p , or equivalently the initial anisotropy of the gluons, decorrelates comparatively quickly

Plug in $\alpha_s = 0.15$, which works well for the rapidity dependence of the charged hadron distribution

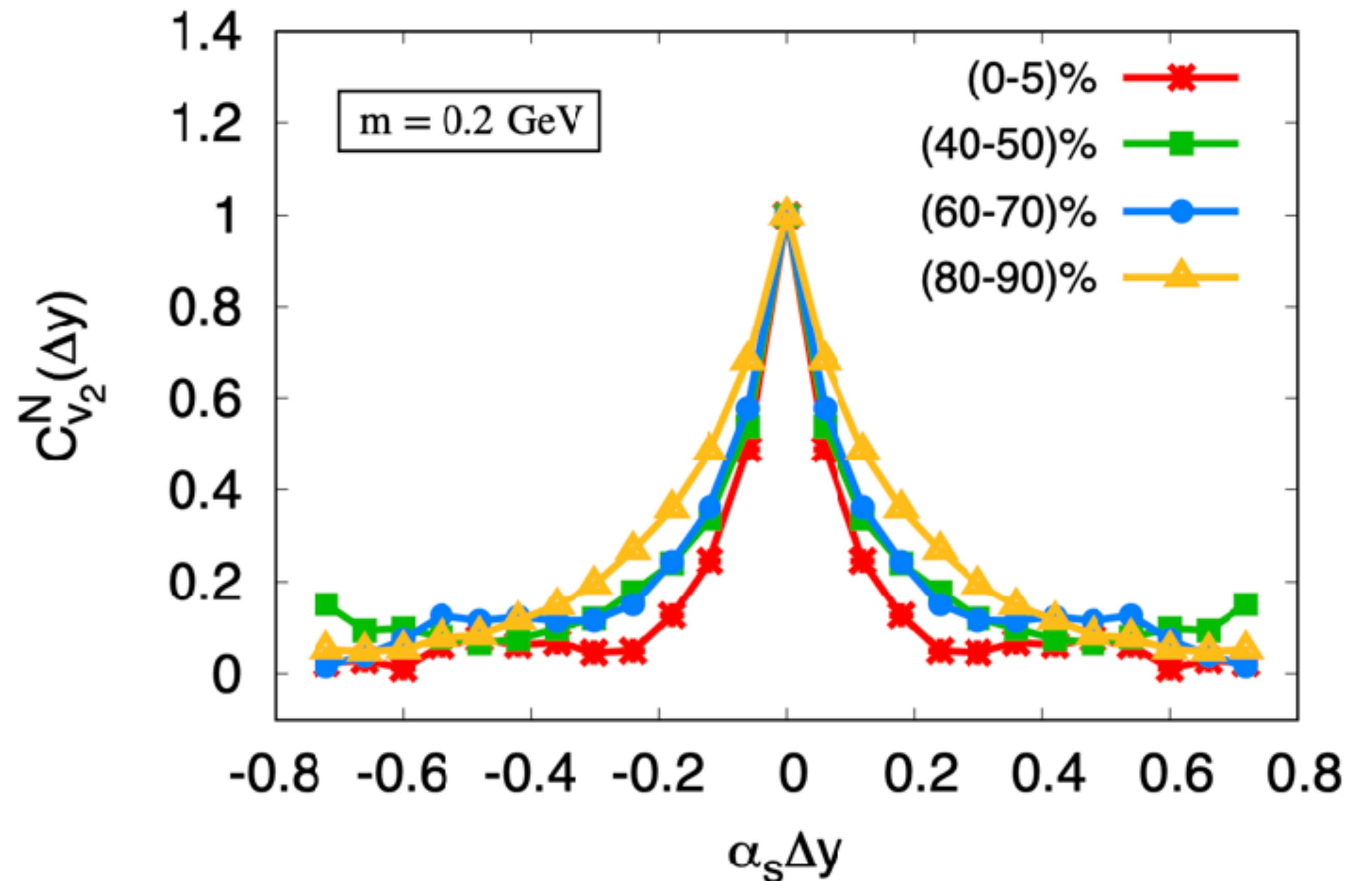


CORRELATION OF INITIAL MOMENTUM ANISOTROPHY

work in progress with Pragma Singh and Sören Schlichting

So this is a bad sign for the initial momentum anisotropy

The ρ correlator is measured using different rapidity bins for $[p_T]$ and the two particles used for v_2 . Over the rapidity range used, the signal from initial state momentum anisotropy would have decayed significantly.



PART III: FULL 3+1D HYDRO FOR LOWER ENERGIES

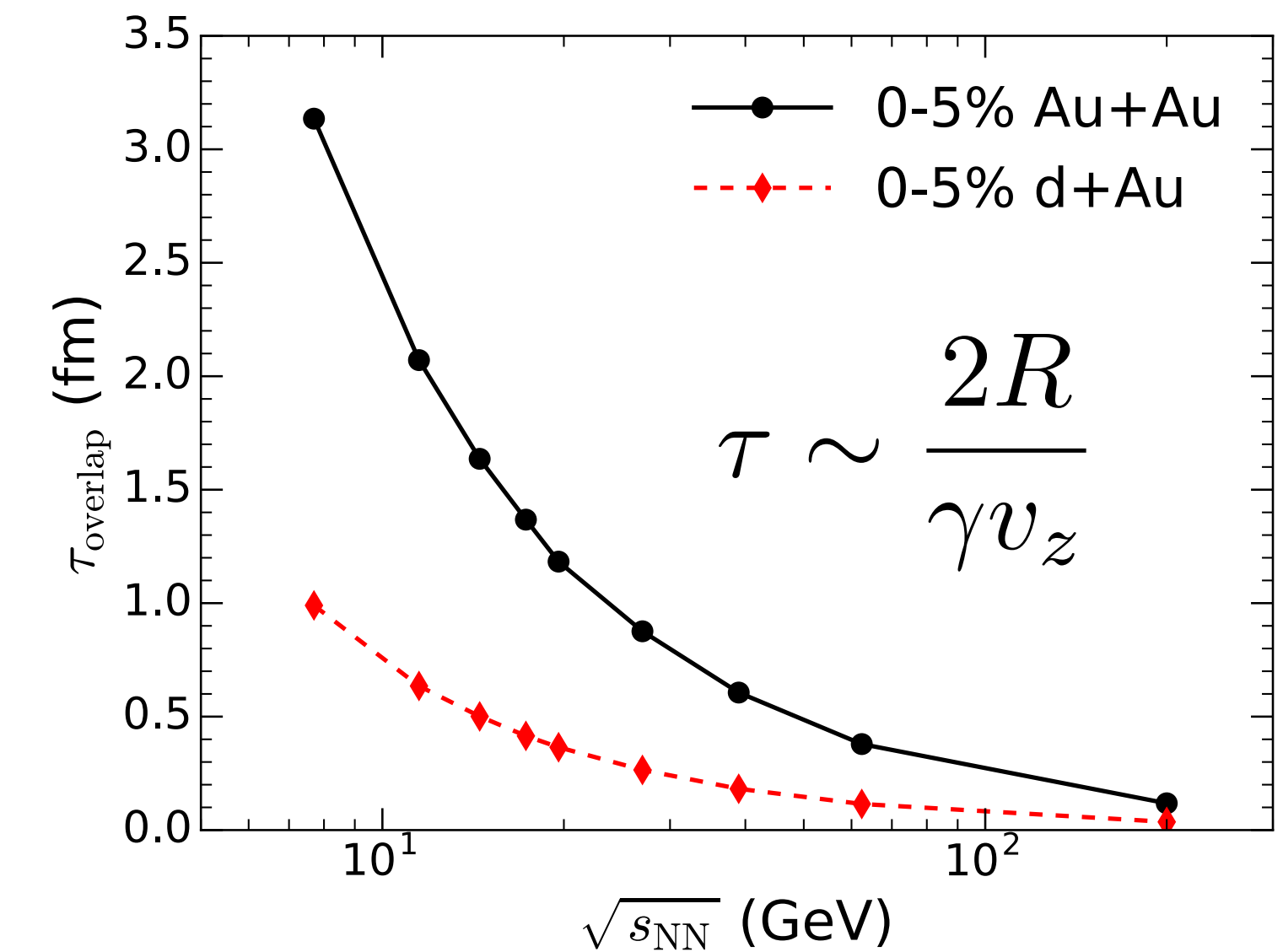
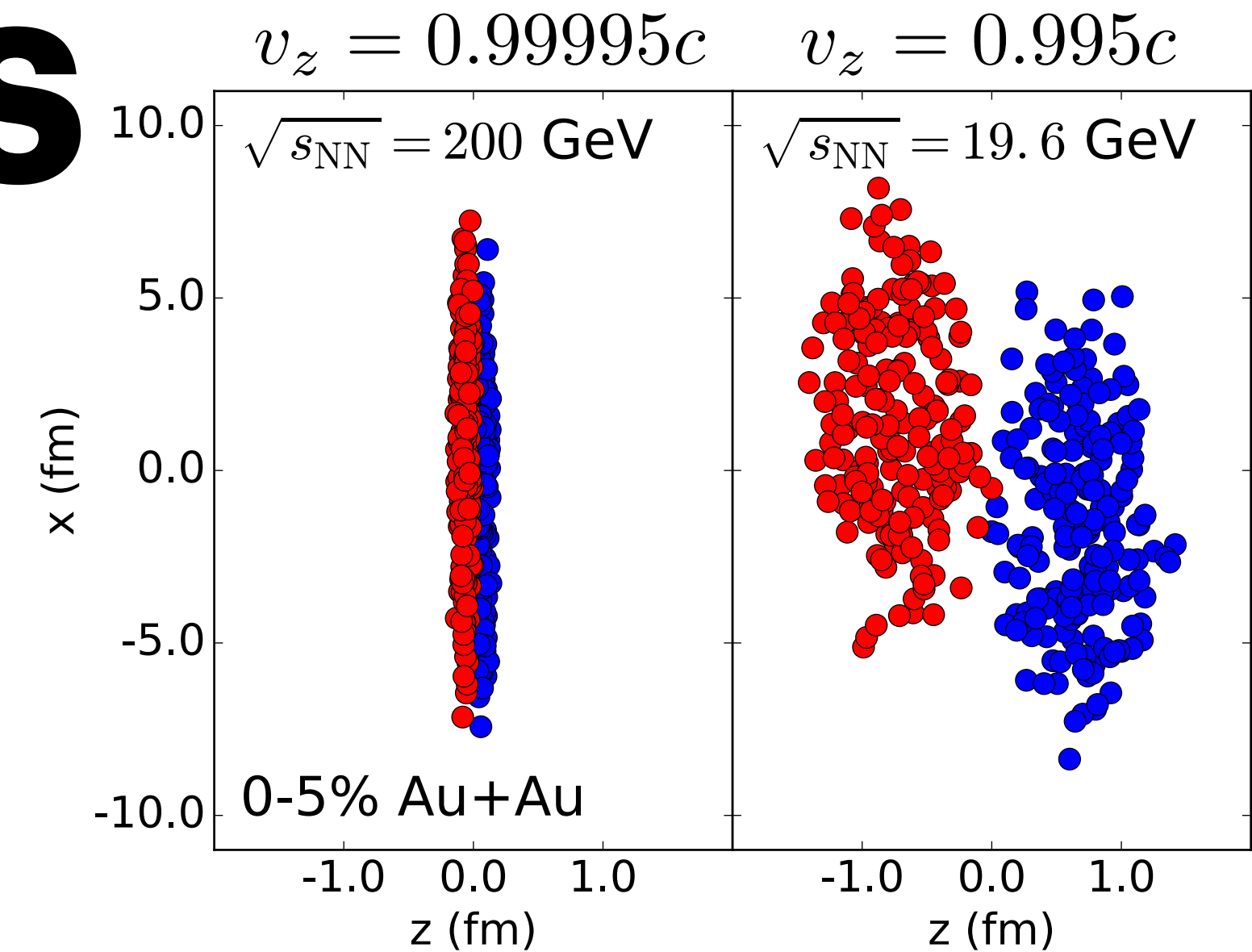
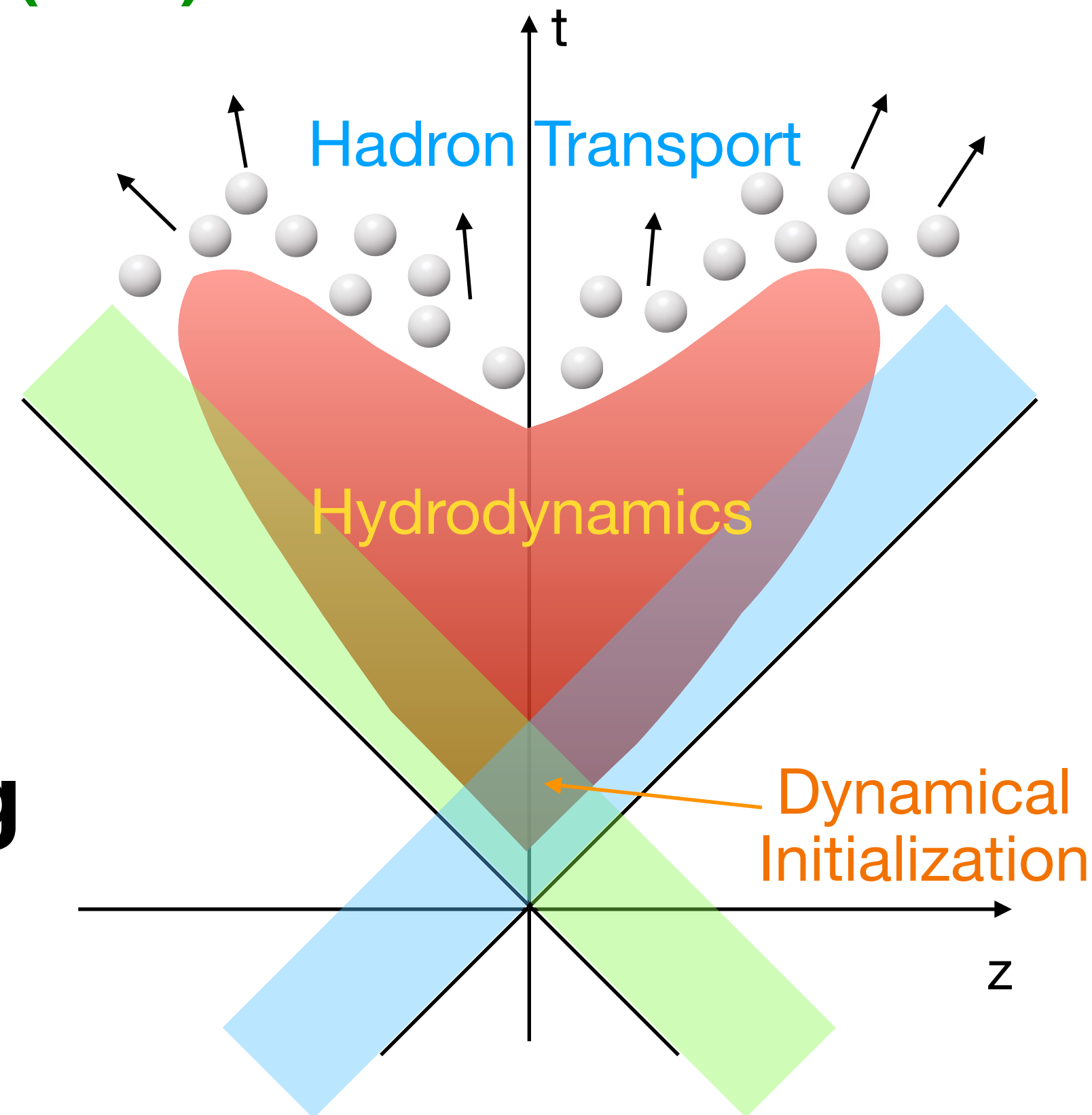
- **Do not use CGC but dynamical MC-Glauber + string model**
- **Do full 3+1D hydrodynamic calculations**

PART III: LOWER ENERGIES

C. Shen and B. Schenke, Phys.Rev. C97 (2018) 024907

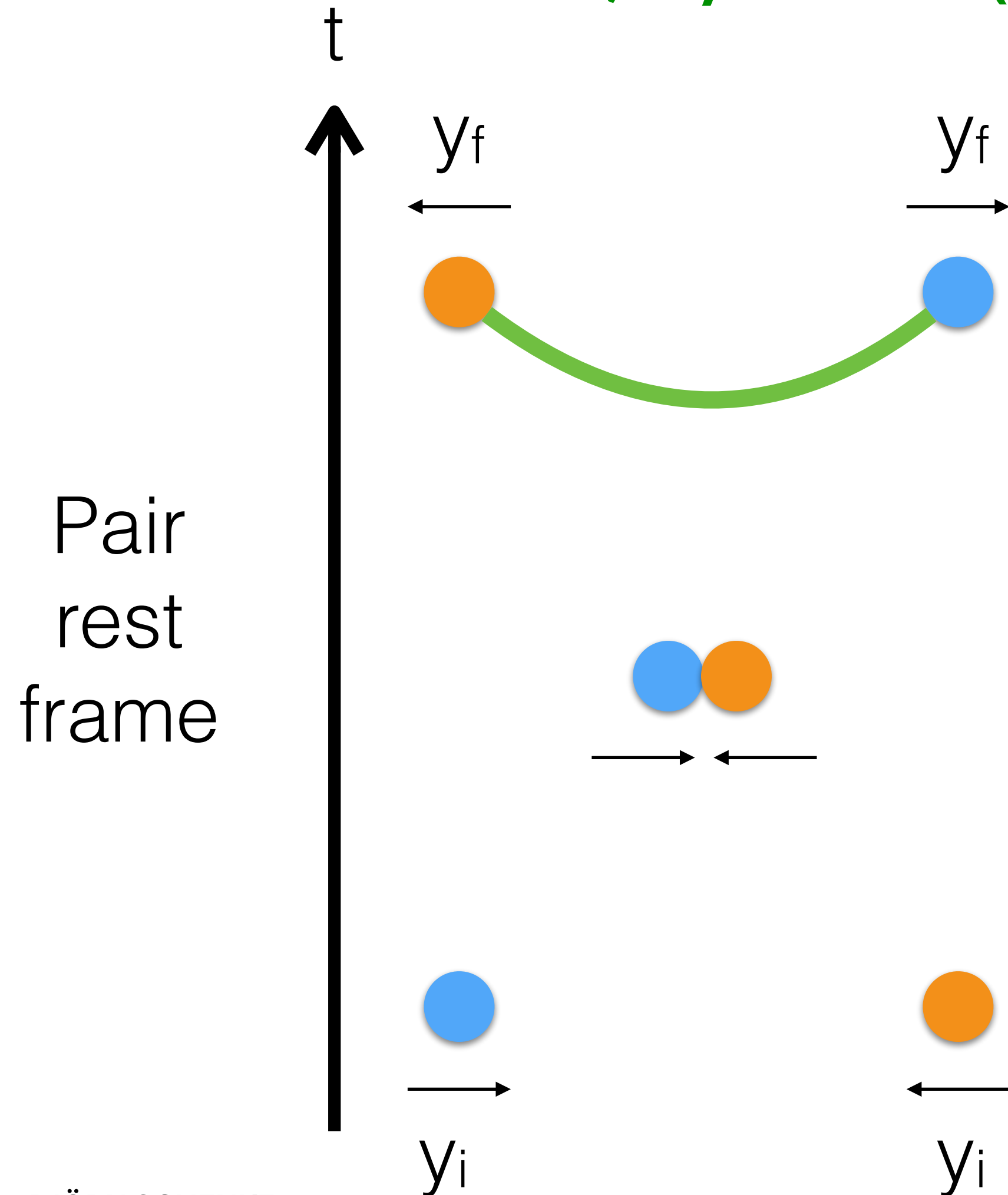
For lower energies, the CGC has very limited validity

Model the initial state within a dynamical string deceleration model



3D MC-GLAUBER + STRING MODEL

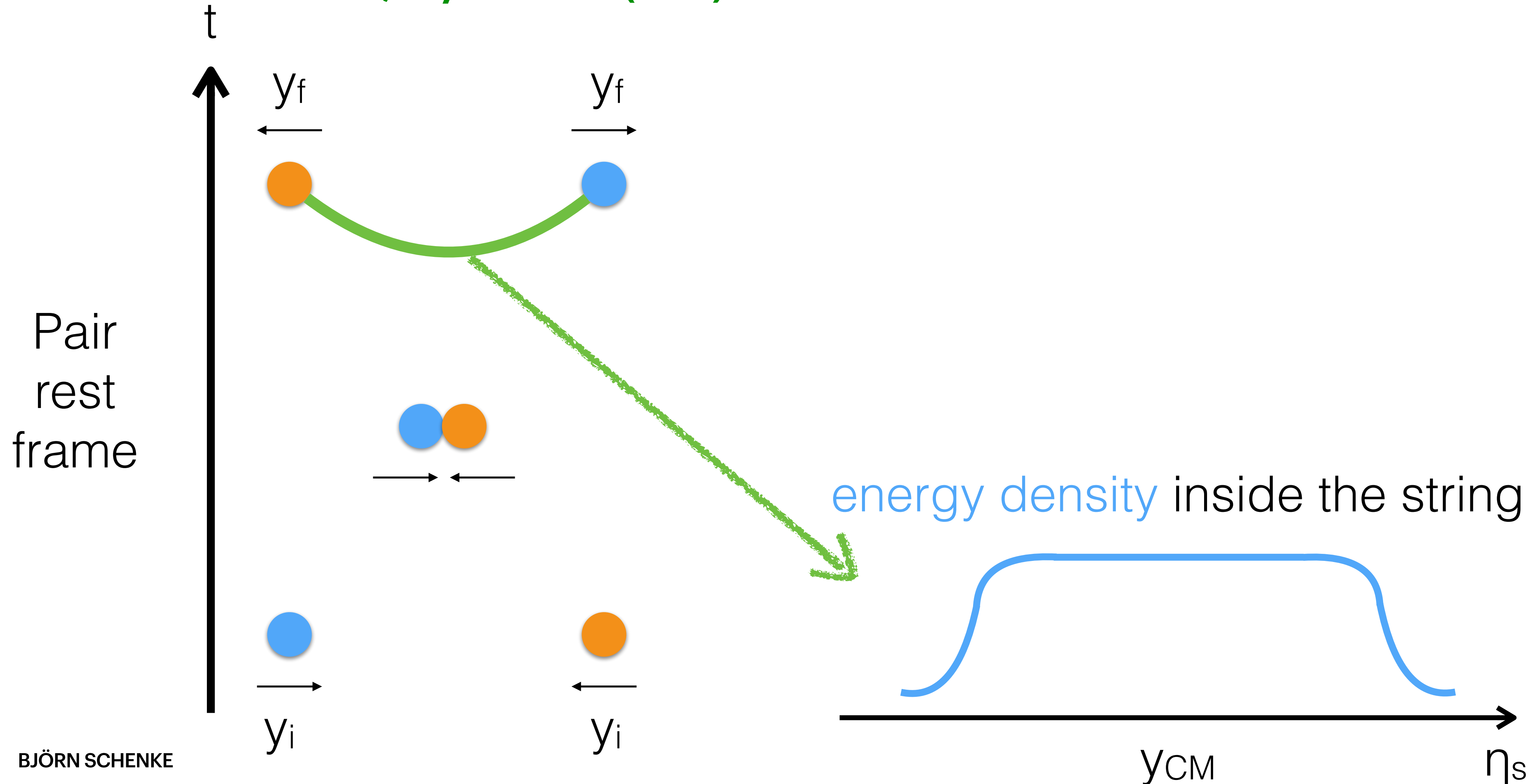
C. Shen and B. Schenke, Phys.Rev. C97 (2018) 024907



- Collision geometry is determined by MC-Glauber model
- 3 valence quarks are sampled from PDF and randomly picked to lose $\left(\sum_i x_i \leq 1\right)$ energy during a collision
- Incoming quarks are decelerated with a classical string tension,

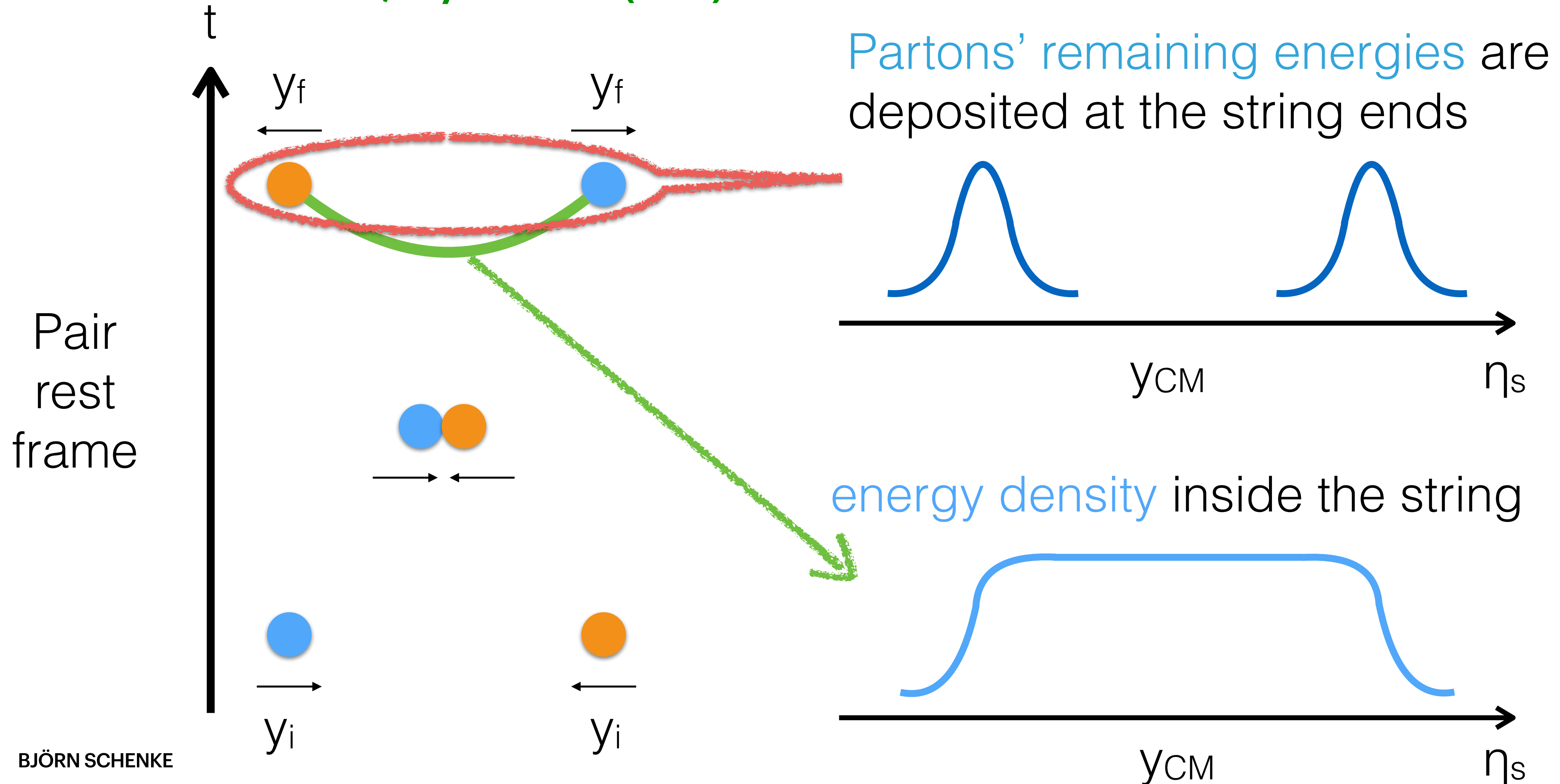
3D MC-GLAUBER + STRING MODEL

C. Shen and B. Schenke, Phys.Rev. C97 (2018) 024907



3D MC-GLAUBER + STRING MODEL

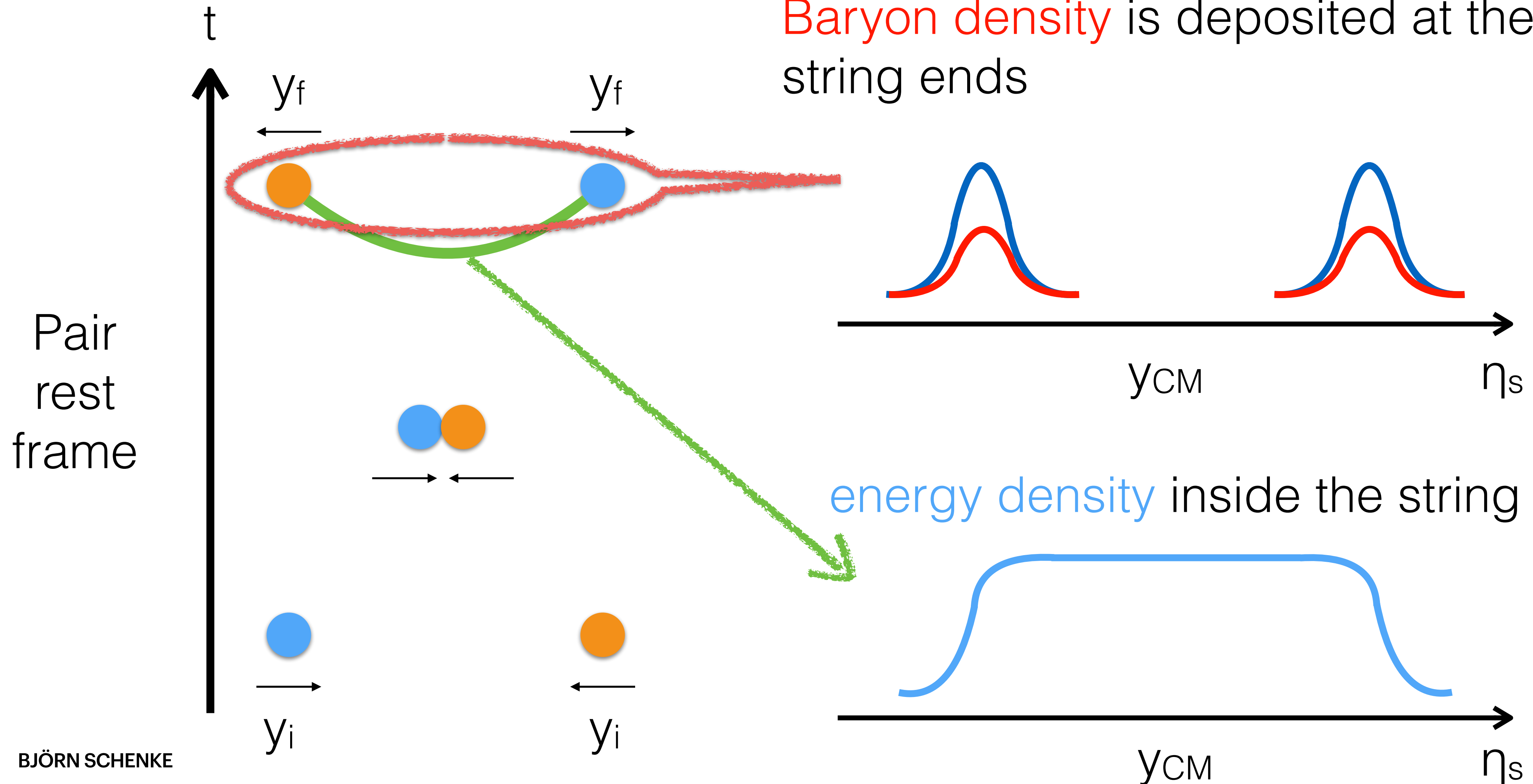
C. Shen and B. Schenke, Phys.Rev. C97 (2018) 024907



3D MC-GLAUBER + STRING MODEL

C. Shen and B. Schenke, Phys.Rev. C97 (2018) 024907

Baryon density is deposited at the string ends

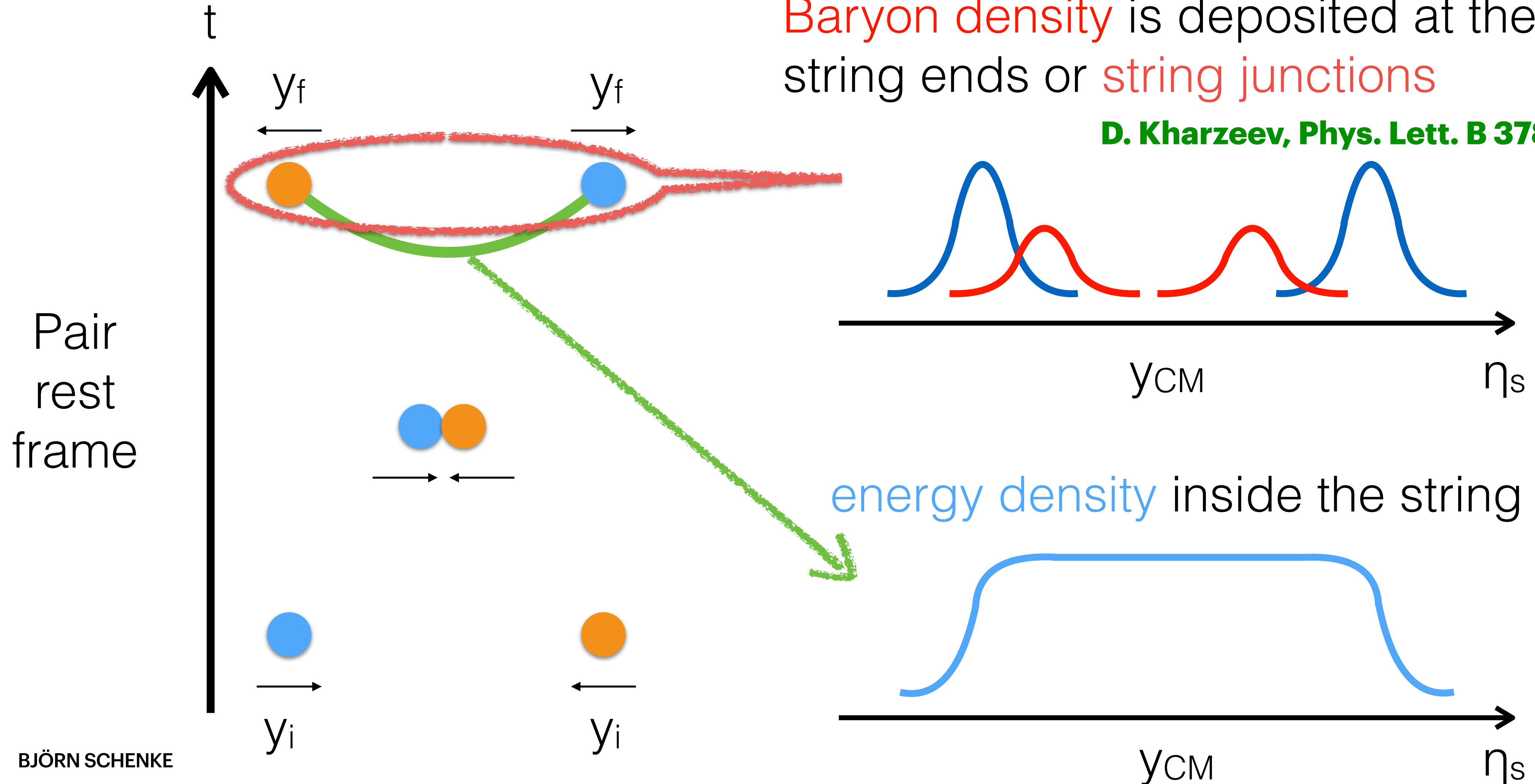


3D MC-GLAUBER + STRING MODEL

C. Shen and B. Schenke, Phys.Rev. C97 (2018) 024907

Baryon density is deposited at the string ends or string junctions

D. Kharzeev, Phys. Lett. B 378, 238 (1996)

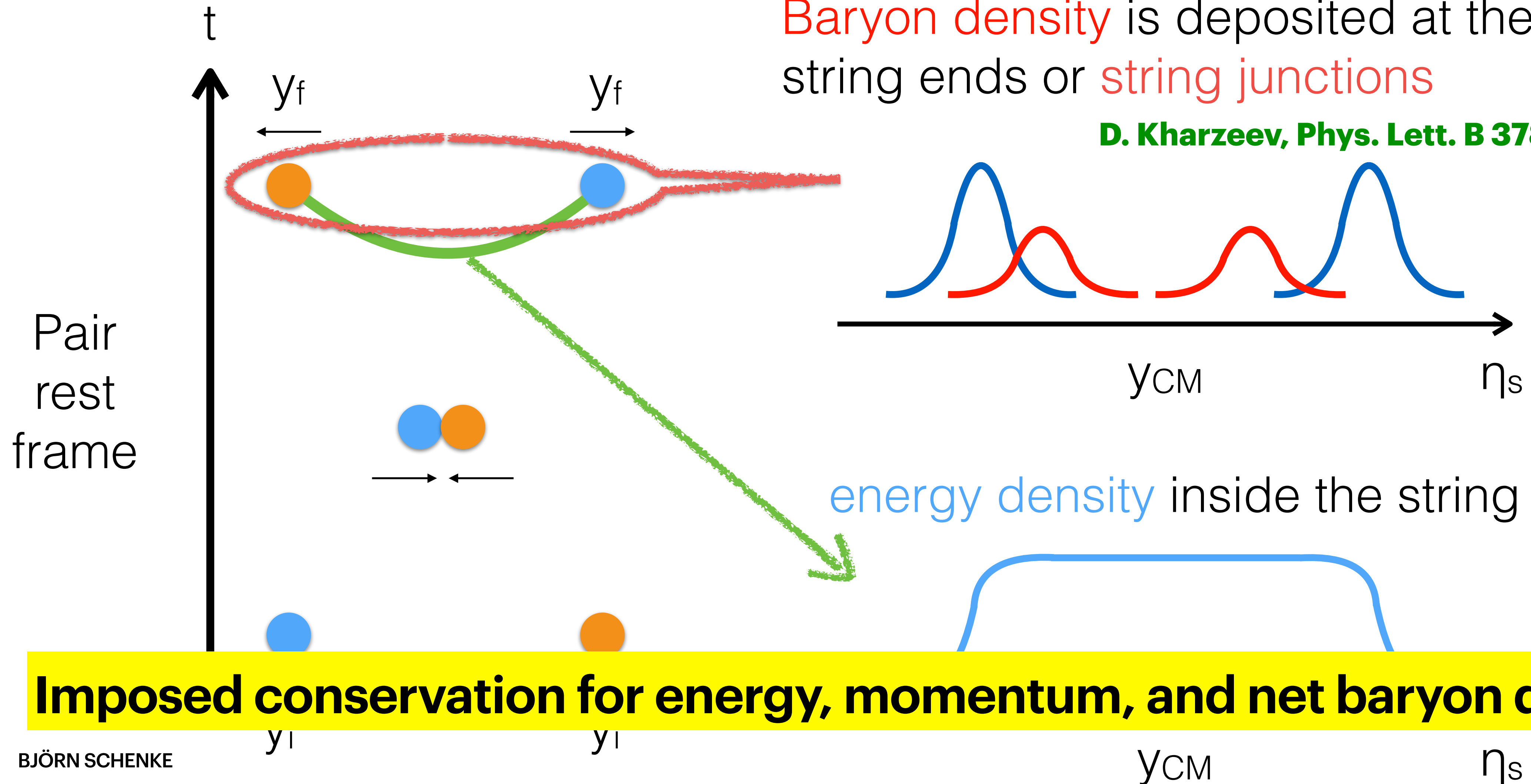


3D MC-GLAUBER + STRING MODEL

C. Shen and B. Schenke, Phys.Rev. C97 (2018) 024907

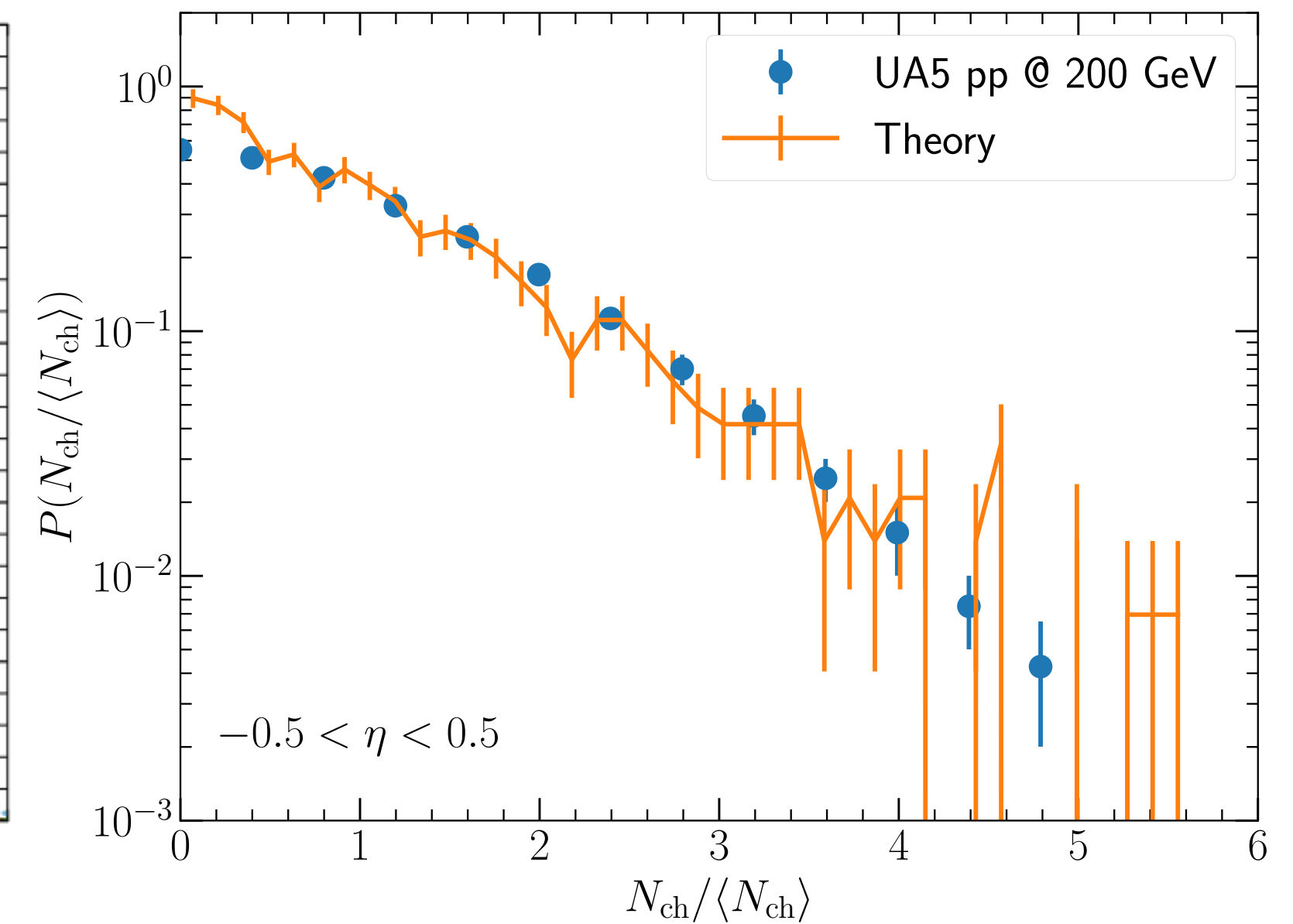
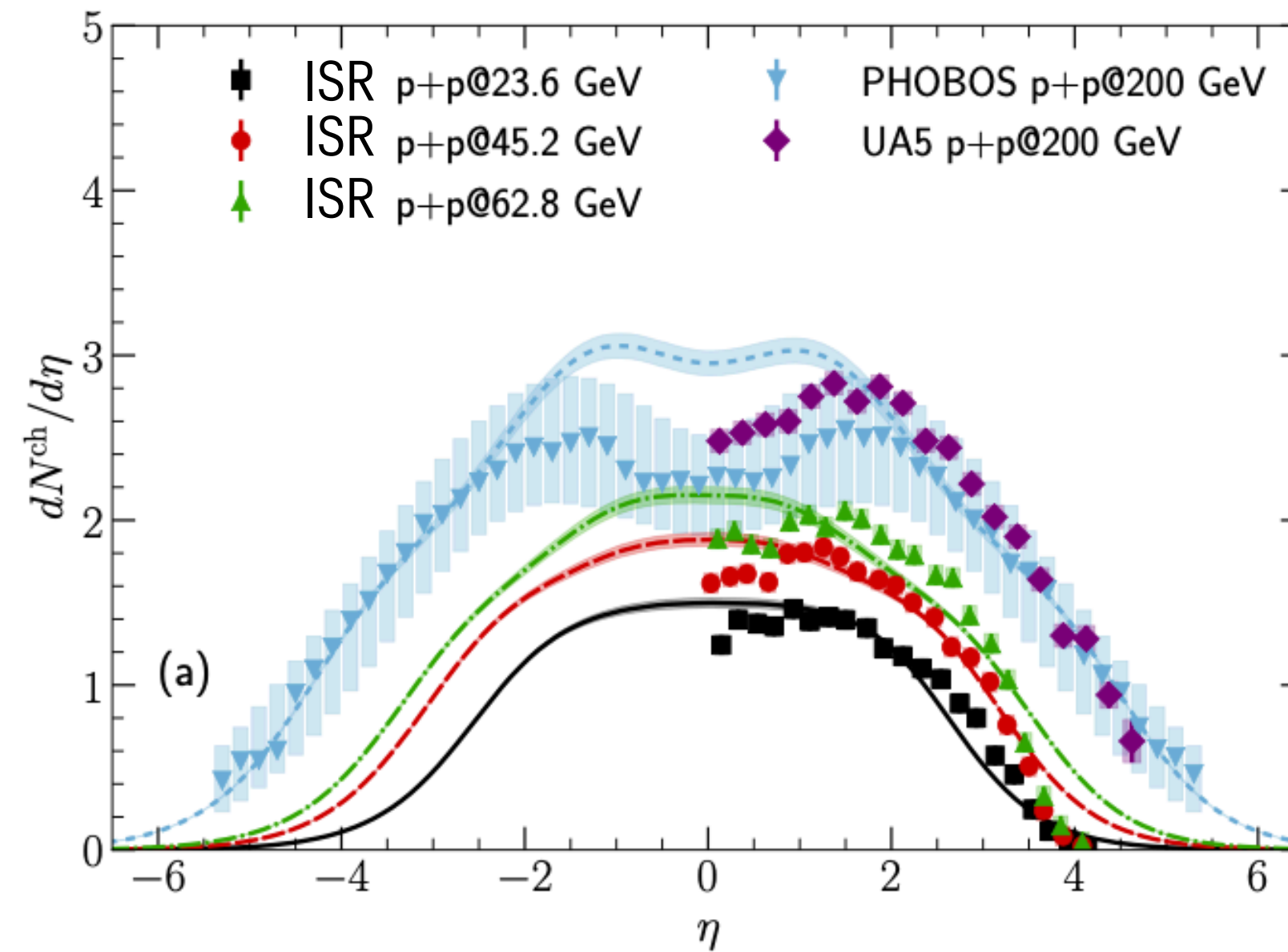
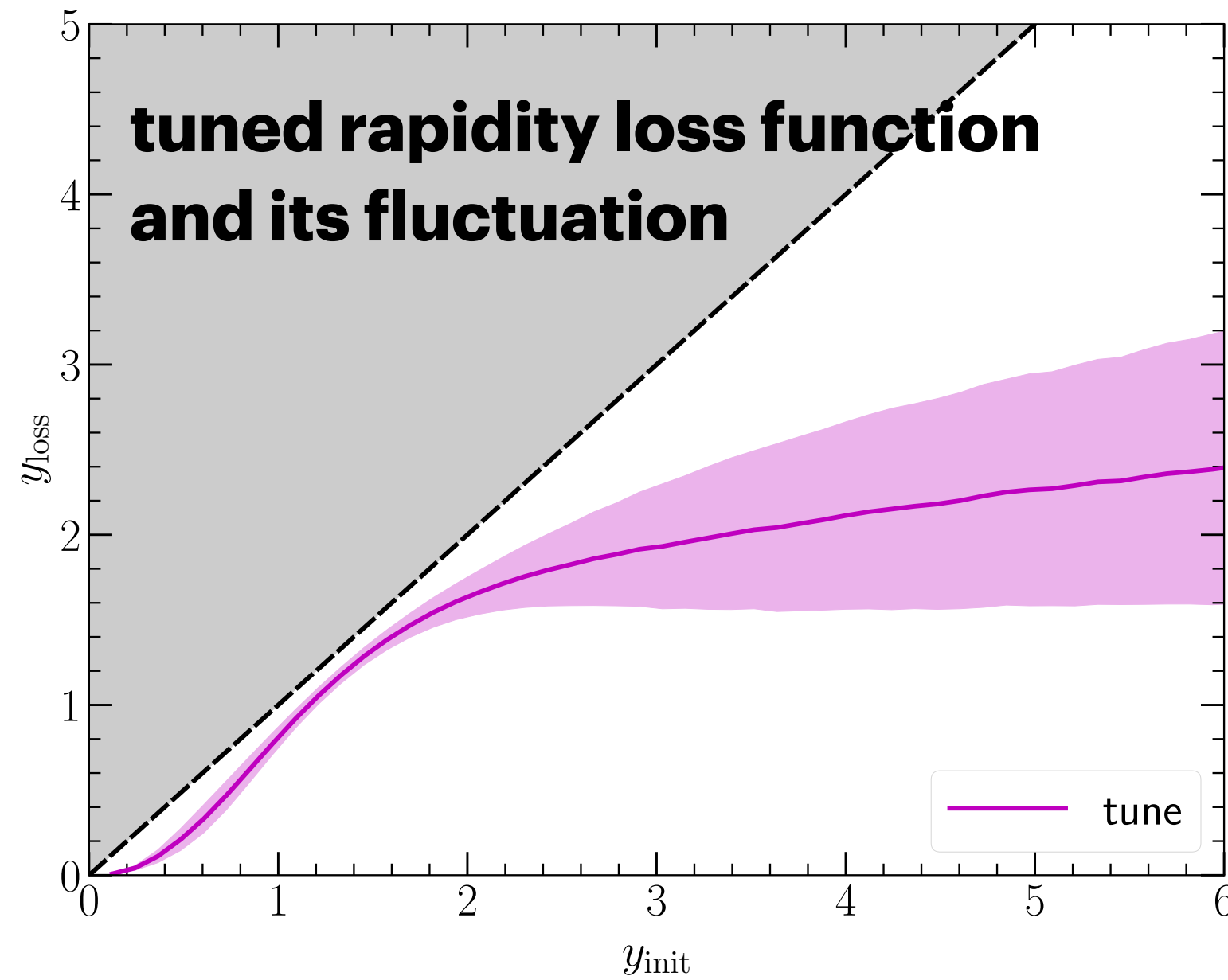
Baryon density is deposited at the string ends or string junctions

D. Kharzeev, Phys. Lett. B 378, 238 (1996)



3D MC-GLAUBER + STRING MODEL+MUSIC

C. Shen and B. Schenke, in preparation



- **Feed energy and momentum of the strings dynamically into hydrodynamics via source terms**
- **Calibrated with minimum bias pp measurements at mid-rapidity and their multiplicity distributions**

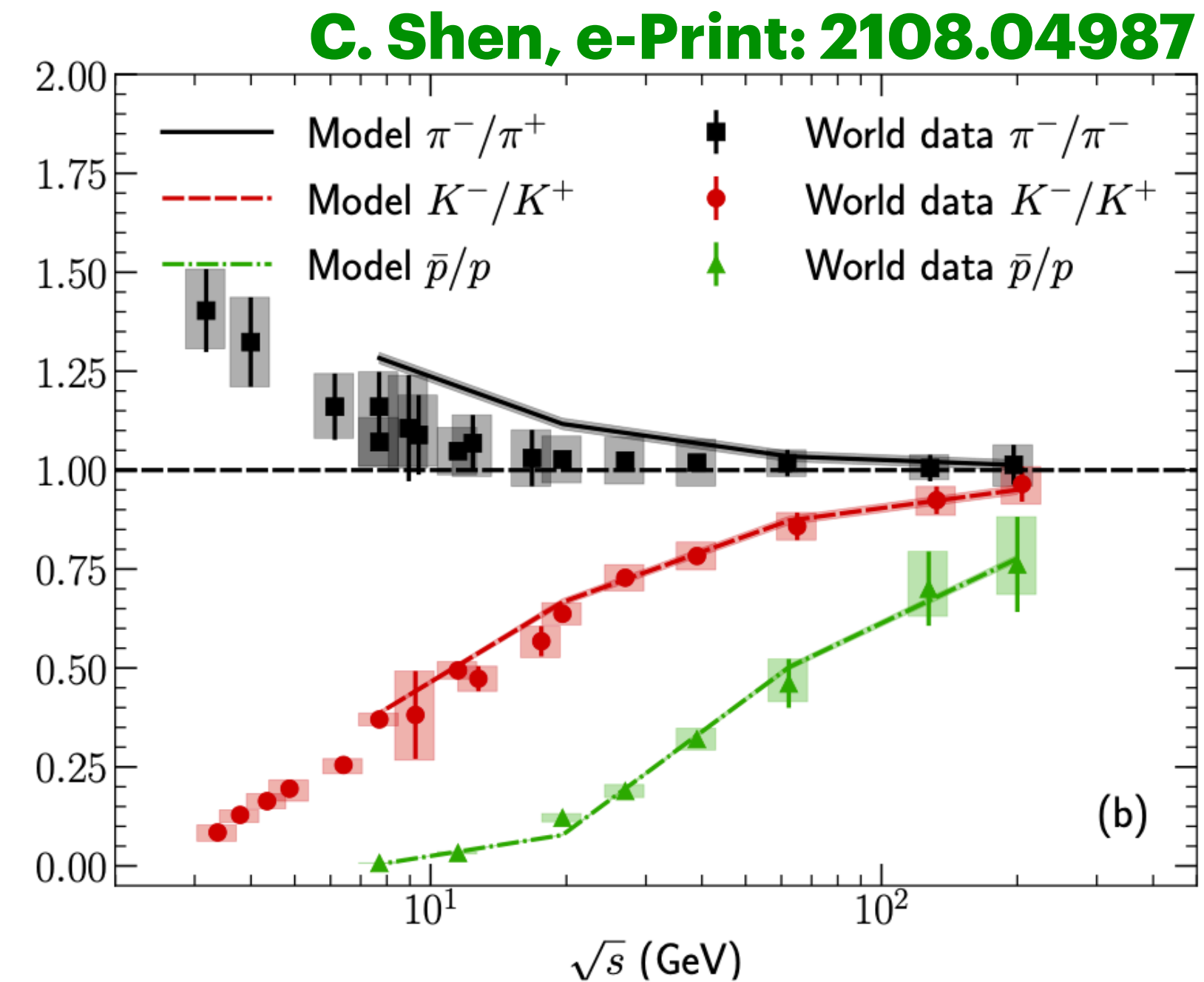
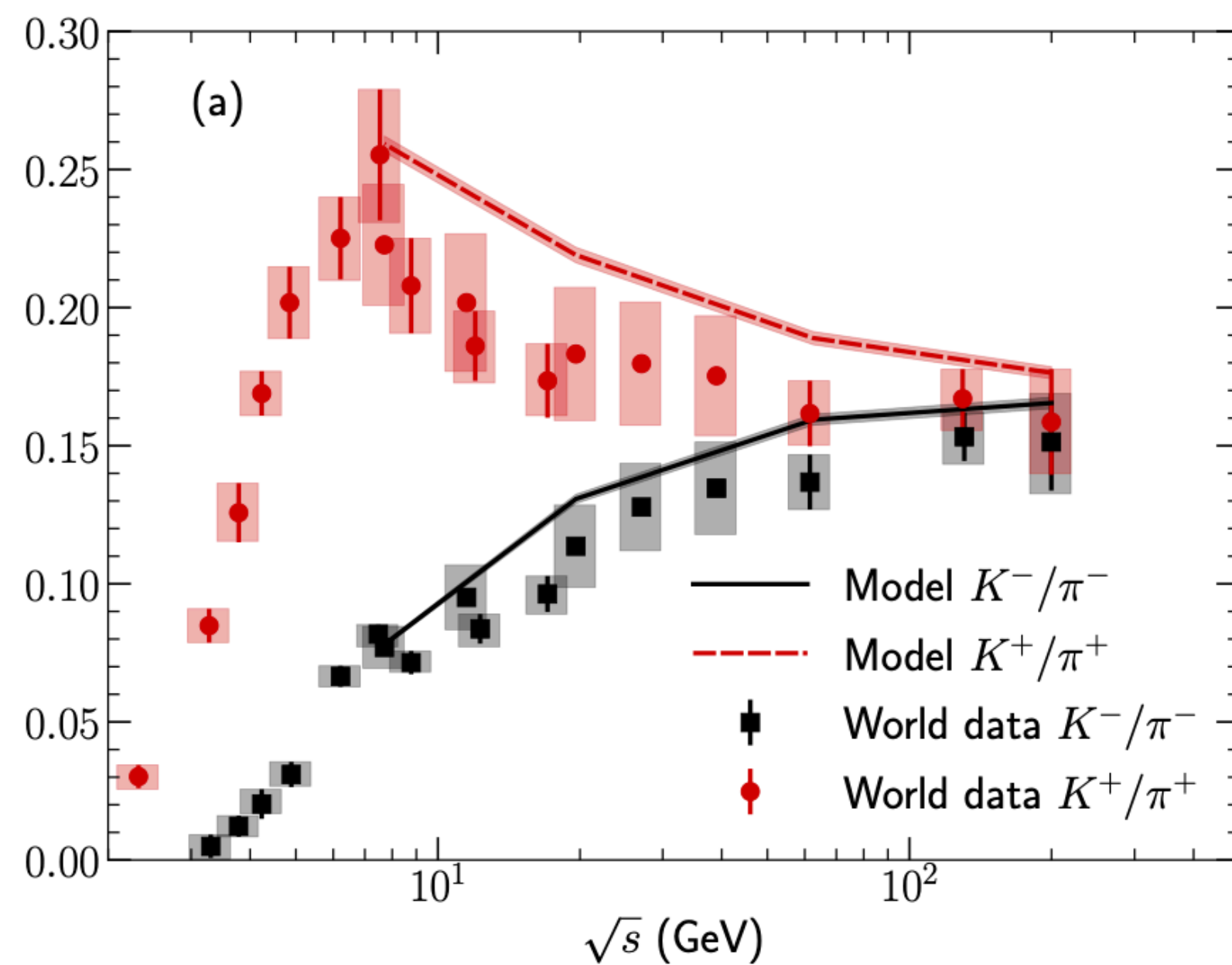
HYDRODYNAMICS AND EOS

- For the equation of state we use NEOS with finite μ_B, μ_S, μ_Q

A. Monnai, B. Schenke, C. Shen, Phys. Rev. C 100, 024907 (2019)

A. Monnai, B. Schenke, C. Shen, Int.J.Mod.Phys.A 36 (2021) 07, 2130007

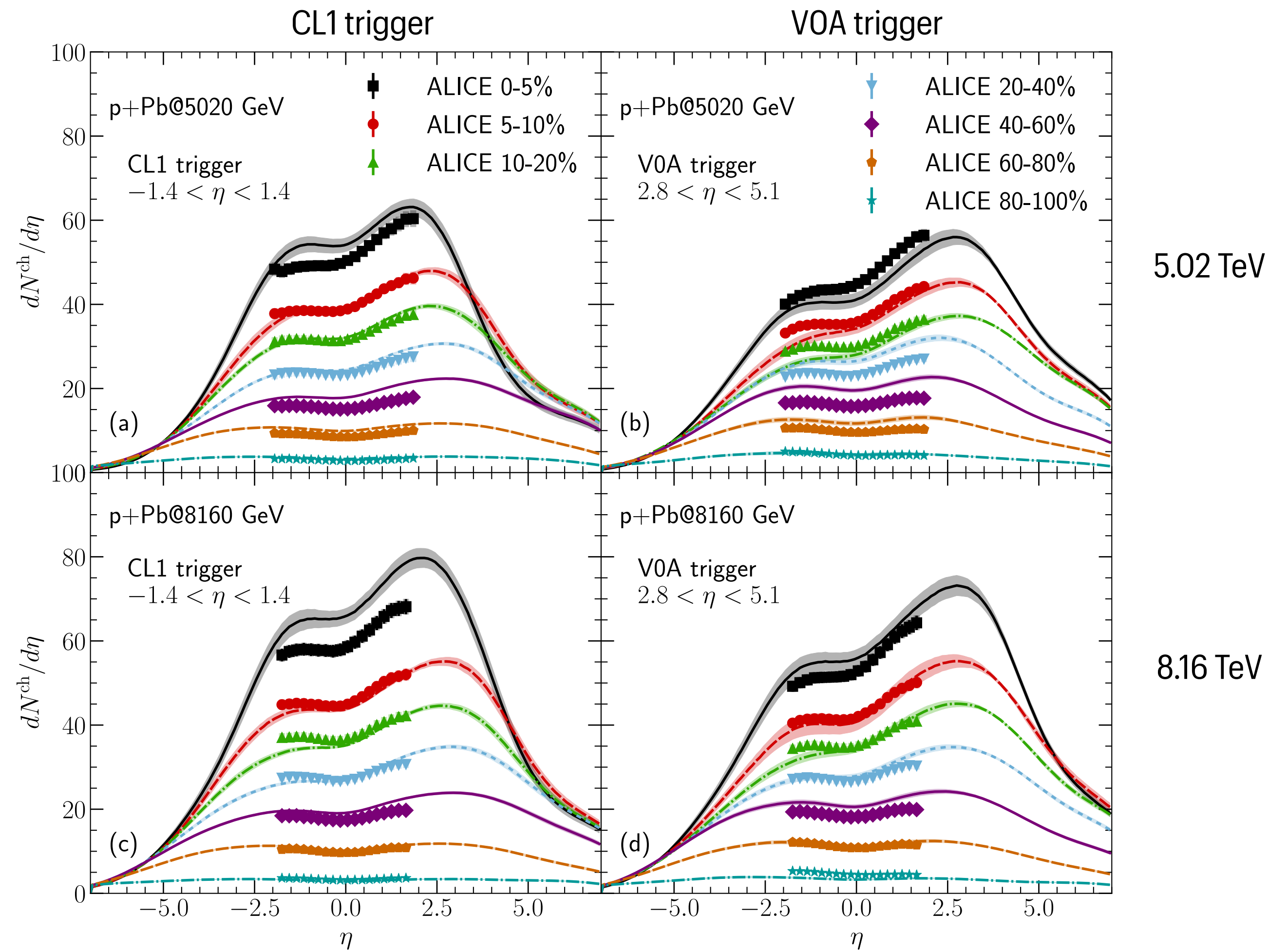
And choose $n_S = 0$ and $n_Q = 0.4n_B$ for Au+Au collisions:



CENTRALITY DEFINITION

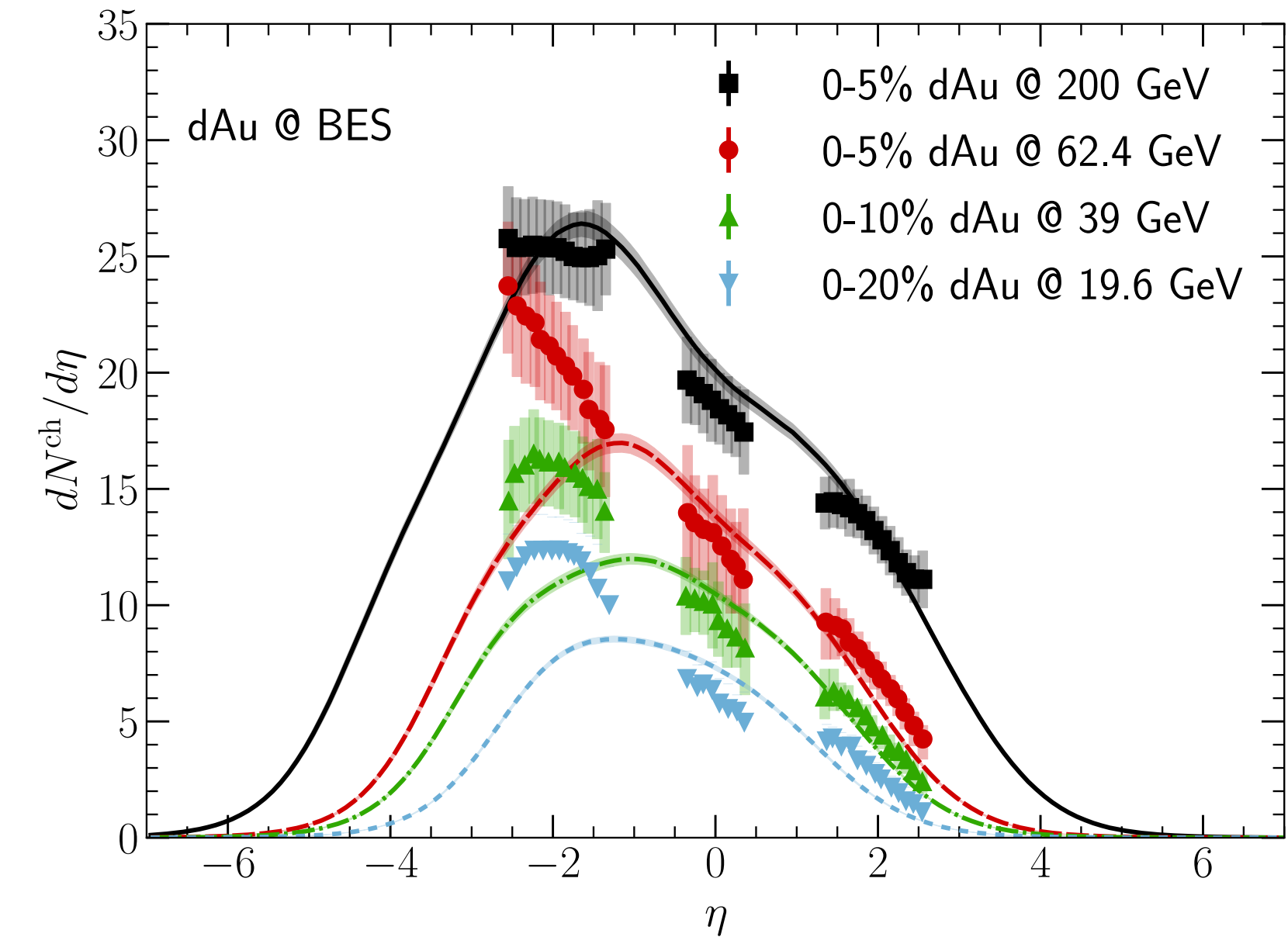
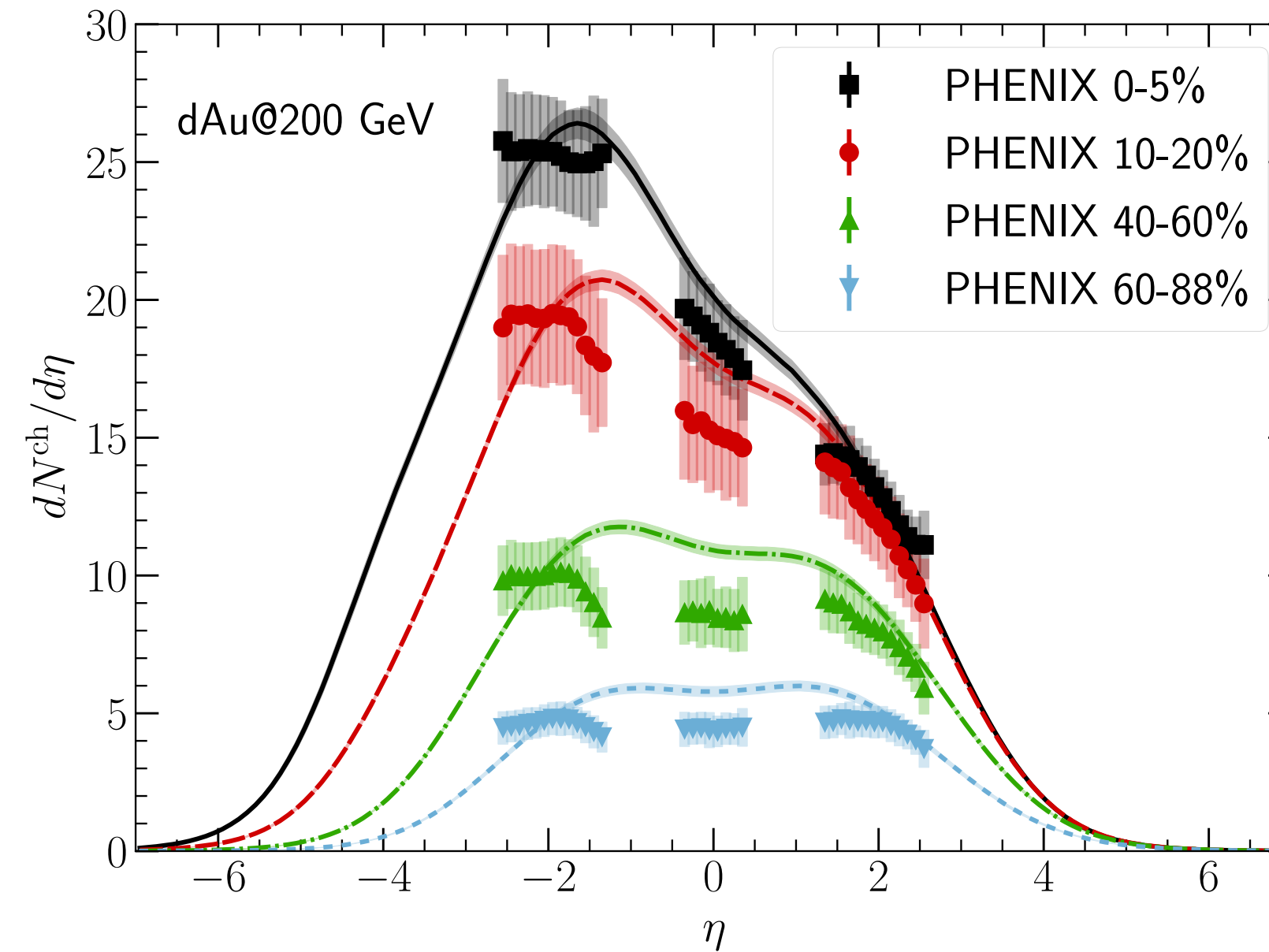
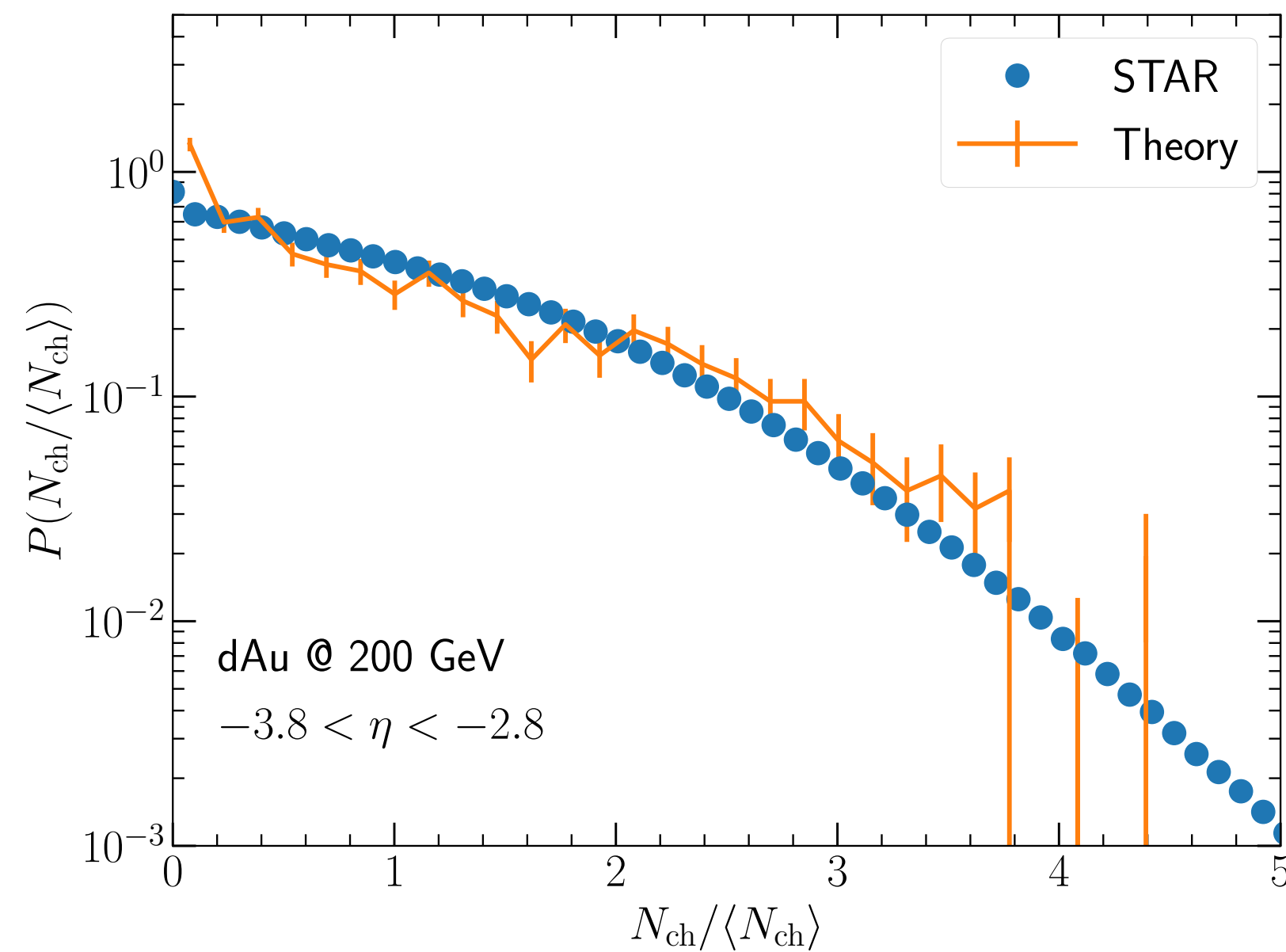
C. Shen and B. Schenke, in preparation

- **We can now determine centrality in the same rapidity bins as the experiments**
- **It does make a difference for the shape of the rapidity distribution**



MULTIPLICITY DISTRIBUTIONS

C. Shen and B. Schenke, in preparation

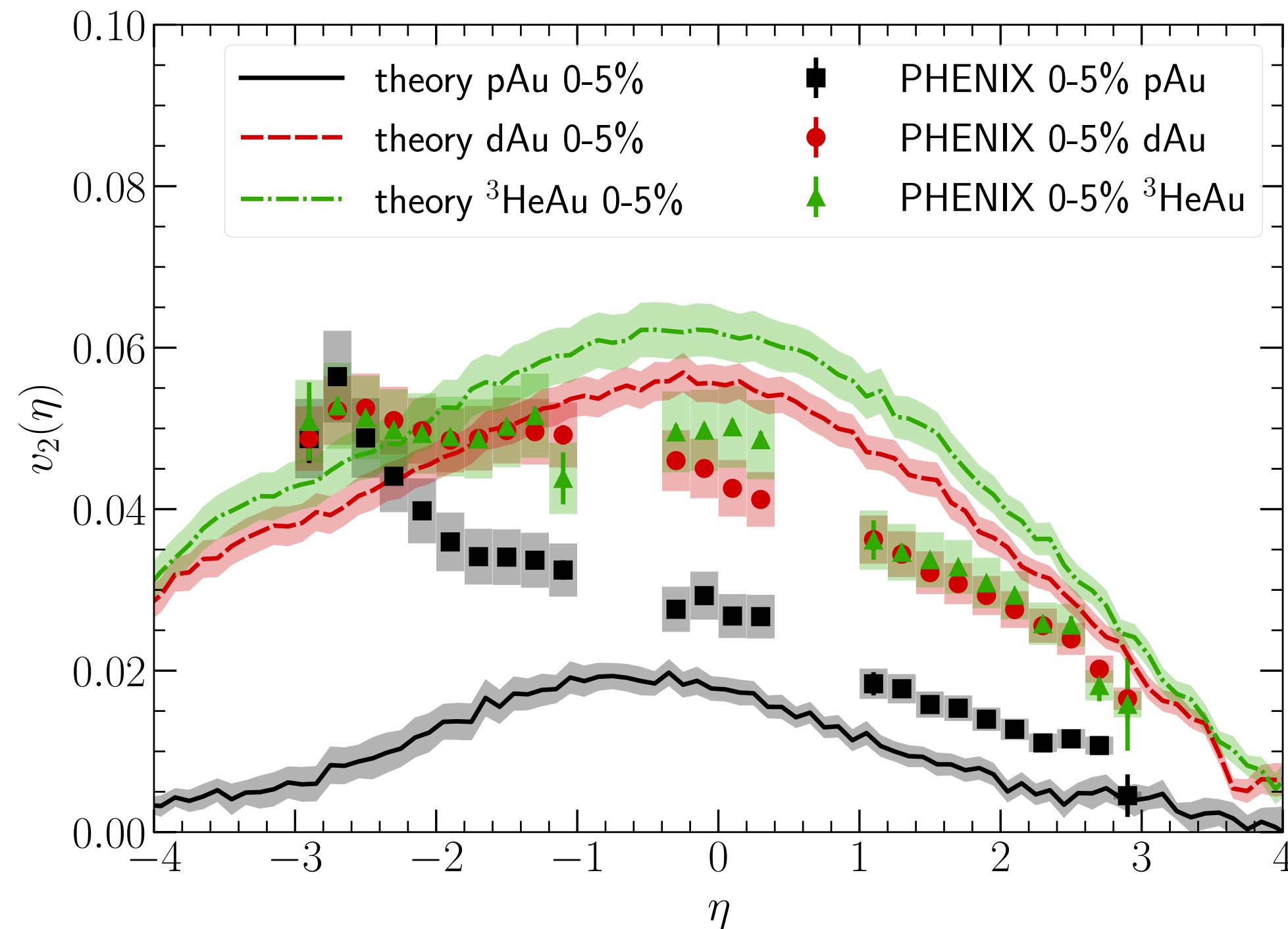


- **Model reproduces the STAR multiplicity distribution in d+Au collisions at 200 GeV**
- **The predicted charged hadron rapidity distribution agrees well with the PHENIX measurements from central to peripheral collisions**
- **The role of spectators at forward rapidity needs further investigation**

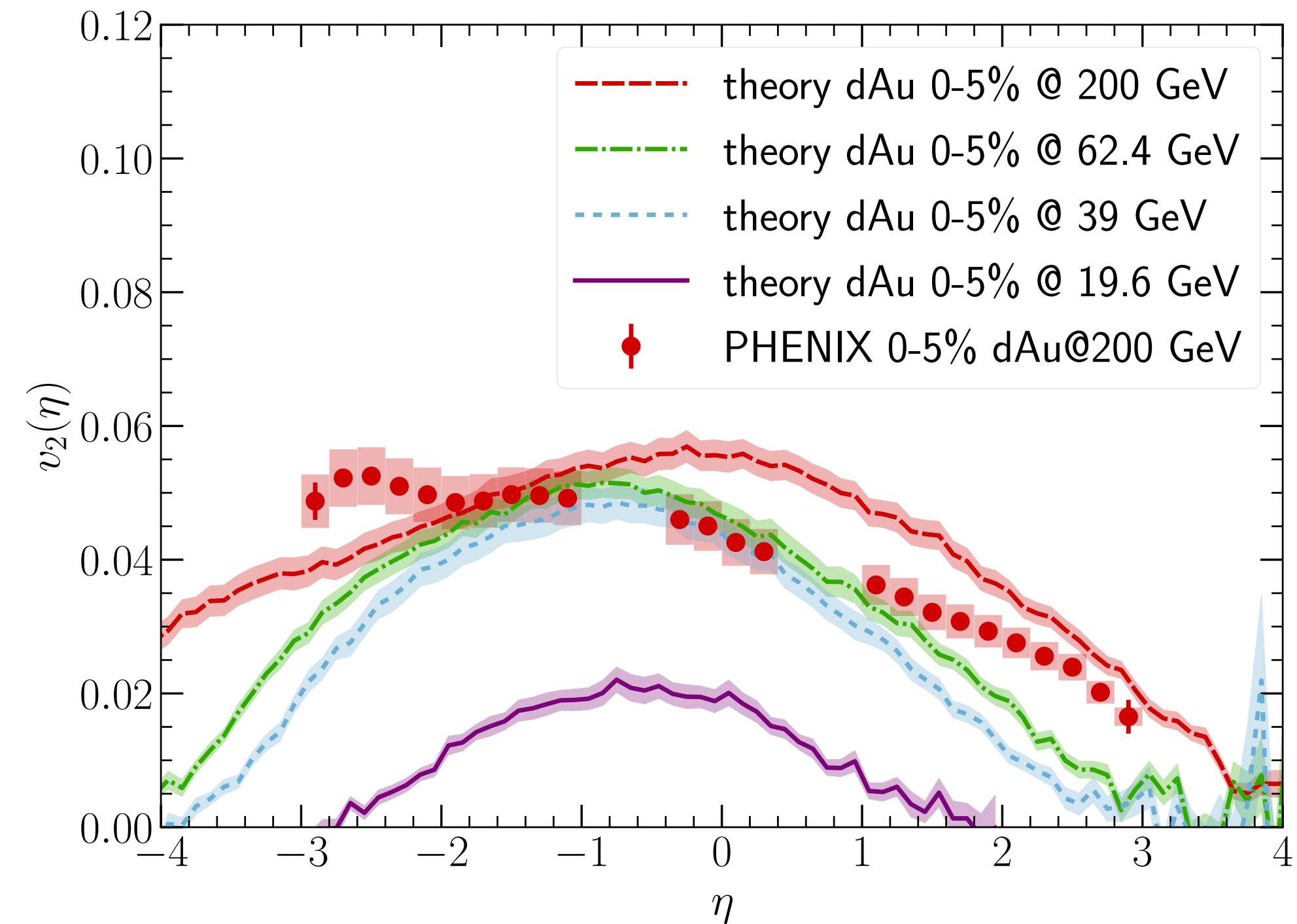
ANISOTROPIC FLOW

C. Shen and B. Schenke, in preparation

System dependence



Energy dependence



- **Discrepancies could come from different method being used in the experiment**
- **Biggest deviation from the data in p+Au in the Au going direction (non-flow?)**
- **PHENIX event plane method with event plane at y in $[-3.9, -3.1]$**

SUMMARY

- **High energies: Boost-invariant hybrid model with IP-Glasma initial state and sub-nucleon fluctuations can describe bulk properties over a wide range of collision systems**
- **Especially for small systems, observables that use large rapidity gaps cannot be compared to boost invariant calculations**
- **IP-Glasma+JIMWLK evolution: Geometry decorrelates with rapidity (faster for low multiplicity); initial state anisotropy decorrelates more quickly (faster for high multiplicity)**
- **Low energies: 3+1D dynamic initial state and 3+1D hydrodynamics needed: Allows the calculation of rapidity dependent observables and use of the experimental rapidity gaps and proper centrality definitions. Need these calculations to be ready for BESII data.**

CODES - ALL PUBLIC

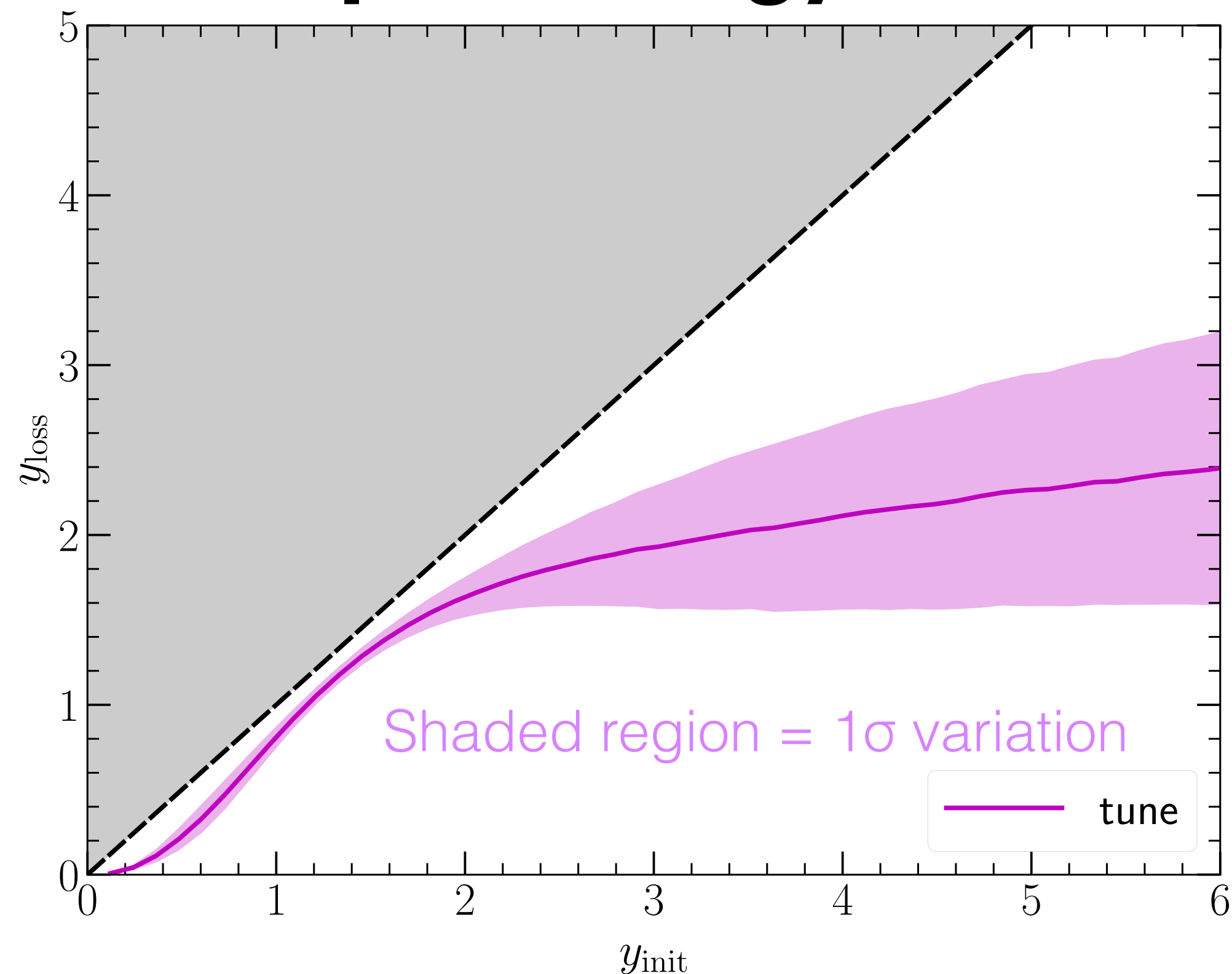
- The iEBE-MUSIC framework integrates individual physical models which describe different stages of relativistic heavy-ion collisions. This work uses v1.0 of this framework, which can be downloaded from <https://github.com/chunshen1987/iEBE-MUSIC/releases>
- The official code repository of the IP-Glasma initial conditions is <https://github.com/schenke/ipglasma> . Here we used v1.0: <https://github.com/schenke/ipglasma/releases>
- MUSIC is the numerical implementation of (3+1)D relativistic viscous hydrodynamic simulations for high energy heavy-ion collisions. Its official website is <http://www.physics.mcgill.ca/music> . This work uses the version 3.0 of MUSIC, which can be downloaded from <https://github.com/MUSIC-fluid/MUSIC/releases>
- The iSS code package is an open-source particle sampler based on the Cooper-Frye freeze-out prescription. It converts fluid cells to particle samples. This work uses v1.0 of the iSS, which can be downloaded from <https://github.com/chunshen1987/iSS/releases>
- We use the official UrQMD v3.4 and set it up to run as the afterburner mode https://bitbucket.org/Chunshen1987/urqmd_afterburner/src/master/
- The hadronic afterburner toolkit is a code package which performs analysis of particle spectra, flow observables, and their correlations using the outputs from hadronic transport models. This work uses v1.0 of the code which can be downloaded from https://github.com/chunshen1987/hadronic_afterburner_toolkit/releases
- The NEOS equation of state v0.11: <https://sites.google.com/view/qcdneos/>

BACKUP

3D MC-GLAUBER + STRING MODEL

C. Shen and B. Schenke, in preparation

Parametrize the valence quark energy loss



$$\langle y_{\text{loss}} \rangle = A y_{\text{init}}^{\alpha_2} [\tanh(y_{\text{init}})]^{\alpha_1 - \alpha_2}$$

- A : the slope
- At small y : $\langle y_{\text{loss}} \rangle \propto y_{\text{init}}^{\alpha_1}$
- At large y : $\langle y_{\text{loss}} \rangle \propto y_{\text{init}}^{\alpha_2}$
- Std of y_{loss} fluctuations: σ_y
($y_{\text{loss}} \in [0, y_{\text{init}}]$)

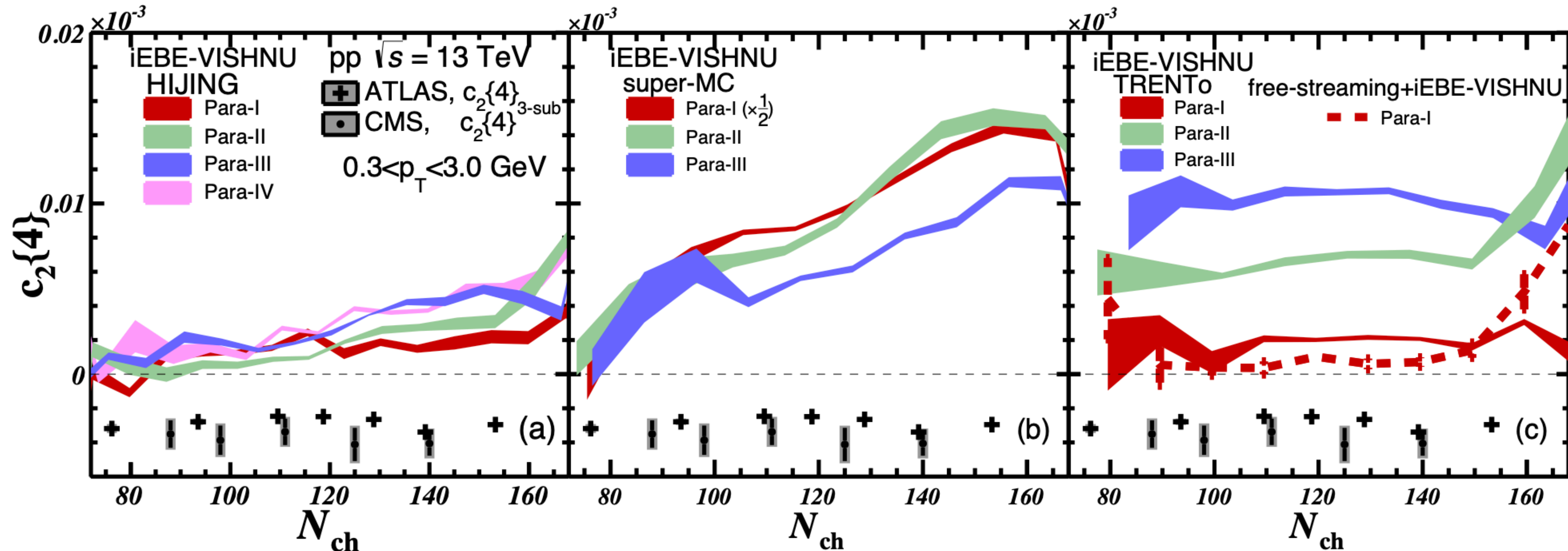
...motivated by the baryon stopping extracted by the BRAHMS Collaboration

I. C. Arsene et al. (BRAHMS), Phys. Lett. B677, 267–271 (2009)

A WORD ON p+p

Multi-particle single and mixed harmonics cumulants can not be described by hydrodynamics with HIJING, super-MC or TRENTo initial conditions, even for the signs in a few cases

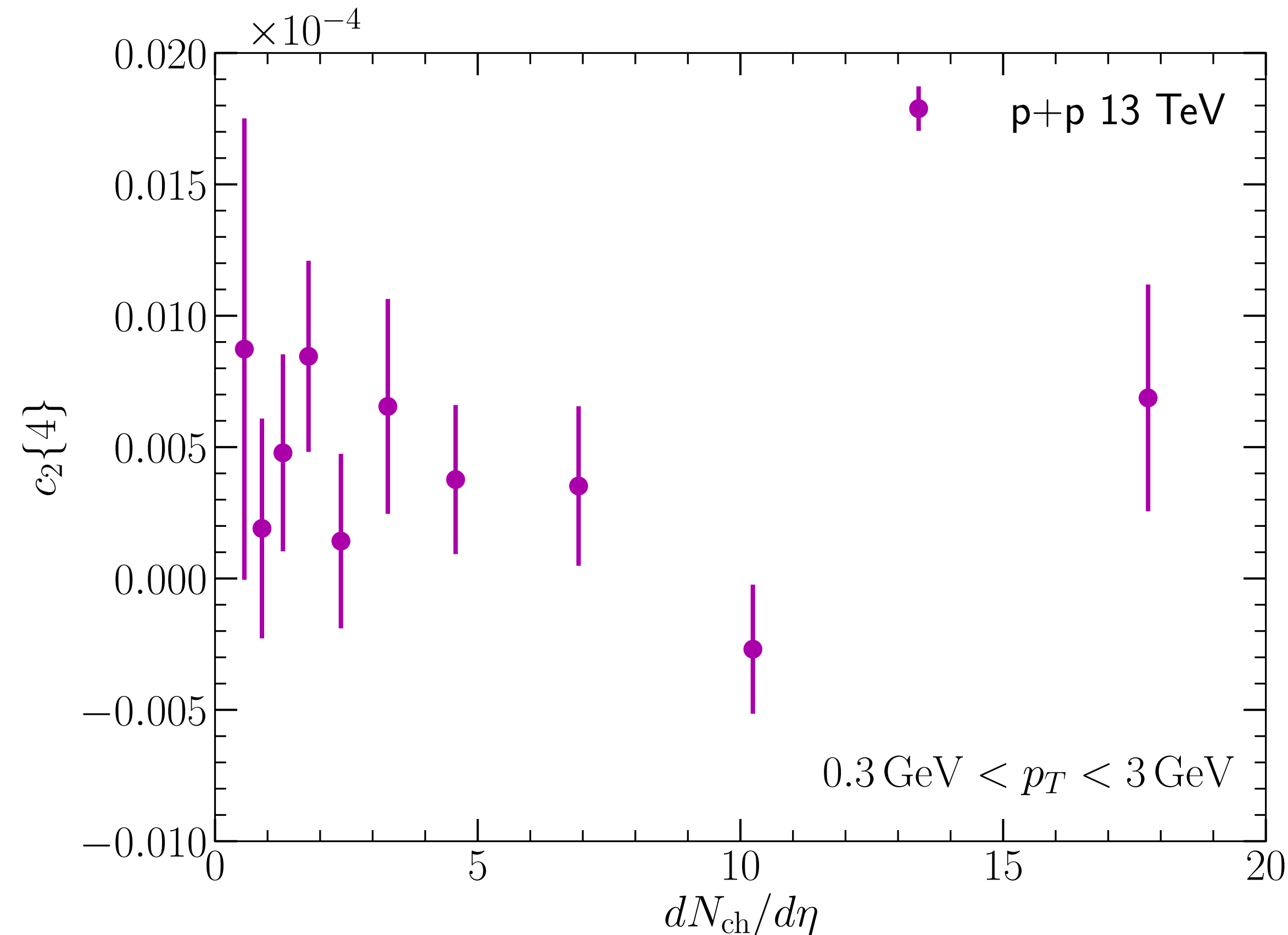
Y. Zhou, W. Zhao, K. Murase, H. Song, Nucl.Phys.A 1005 (2021) 121908



So, it is very hard to generate initial conditions that produce negative $c_2\{4\}$ in p+p collisions

A WORD ON p+p: IP-GLASMA + MUSIC + URQMD

preliminary



Errors still large, but looks positive as well. However, we do not have more central results yet. Need to “trigger” on even more high multiplicity events. Ongoing...

THE MODEL: IP-GLASMA

B. Schenke, C. Shen, P. Tribedy, Phys. Rev. C 102 (2020) 4, 044905

$$\rho(r, \theta) = \frac{\rho_0}{1 + \exp[(r - R'(\theta))/a]},$$

with $R'(\theta) = R[1 + \beta_2 Y_2^0(\theta) + \beta_4 Y_4^0(\theta)]$, and ρ_0 the nuclear density at the center of the nucleus. R is the radius parameter, a the skin depth.

Nucleus	R [fm]	a [fm]	β_2	β_4
^{238}U	6.81	0.55	0.28	0.093
^{208}Pb	6.62	0.546	0	0
^{197}Au	6.37	0.535	-0.13	-0.03
^{129}Xe	5.42	0.57	0.162	-0.003
^{96}Ru	5.085	0.46	0.158	0
^{96}Zr	5.02	0.46	0	0

Sample nucleons, determine thickness functions, then compute $x = x(\mathbf{b}_\perp) = \bar{Q}_s(x, \mathbf{b}_\perp) / \sqrt{s_{\text{NN}}}$

Using $g^2 \mu_i(x, \mathbf{b}_\perp) = c Q_s^i(x, \mathbf{b}_\perp)$ sample color charges with zero mean and variance: $\langle \rho_i^a(\mathbf{b}_\perp) \rho_i^b(\mathbf{x}_\perp) \rangle = g^2 \mu_i^2(x, \mathbf{b}_\perp) \delta^{ab} \delta^{(2)}(\mathbf{b}_\perp - \mathbf{x}_\perp)$

Sampled color charges yield currents moving on the light cone $J_i^\nu = \delta^{\nu\pm} \rho_i(x^\mp, \mathbf{x}_\perp) = \delta^{\nu\pm} \rho_i^a(x^\mp, \mathbf{x}_\perp) t^a$

which are sources in the Yang-Mills equations $[D_\mu, F^{\mu\nu}] = J^\nu$

THE MODEL: IP-GLASMA

B. Schenke, C. Shen, P. Tribedy, Phys. Rev. C 102 (2020) 4, 044905

Yang-Mills equations $[D_\mu, F^{\mu\nu}] = J^\nu$

are solved in Lorenz gauge to yield $A_i^\pm = -\frac{\rho_i(x^\mp, \mathbf{x}_\perp)}{\nabla_\perp^2 - m^2}$ with $m=0.2$ GeV

The field from both nuclei in Fock-Schwinger gauge reads $A^j(\mathbf{x}_\perp) = \theta(x^-)\theta(-x^+) \frac{i}{g} V_P(\mathbf{x}_\perp) \partial^j V_P^\dagger(\mathbf{x}_\perp) + \theta(x^+)\theta(-x^-) \frac{i}{g} V_T(\mathbf{x}_\perp) \partial^j V_T^\dagger(\mathbf{x}_\perp)$

where $V_i(\mathbf{x}_\perp) = P \exp \left(-ig \int dx^\mp \frac{\rho_i(x^\mp, \mathbf{x}_\perp)}{\nabla_\perp^2 - m^2} \right)$

$$A^j = A_P^j + A_T^j,$$

The fields in the forward light-cone are then $A^\eta = -\frac{ig}{2} [A_{Pj}, A_T^j],$

$$\partial_\tau A^j = 0,$$

$$\partial_\tau A^\eta = 0.$$

THE MODEL: IP-GLASMA

B. Schenke, C. Shen, P. Tribedy, *Phys. Rev. C* **102** (2020) 4, 044905

Yang-Mills evolution in the forward light cone is given by the discretized equations of motion ($\pi = E^\eta$, $\phi = A_\eta$)

$$\dot{U}_j = i \frac{g^2}{\tau} E^j U_j \quad (\text{no sum over } j) \quad (29)$$

$$\dot{\phi} = \tau \pi \quad (30)$$

$$\begin{aligned} \dot{E}^1 = & \frac{i\tau}{2g^2} [U_{(1,2)} + U_{(1,-2)} - U_{(1,2)}^\dagger - U_{(1,-2)}^\dagger - T_1] \\ & + \frac{i}{\tau} [\tilde{\phi}_1, \phi] \end{aligned} \quad (31)$$

$$\begin{aligned} \dot{E}^2 = & \frac{i\tau}{2g^2} [U_{(2,1)} + U_{(2,-1)} - U_{(2,1)}^\dagger - U_{(2,-1)}^\dagger - T_2] \\ & + \frac{i}{\tau} [\tilde{\phi}_2, \phi] \end{aligned} \quad (32)$$

$$\dot{\pi} = \frac{1}{\tau} \sum_j [\tilde{\phi}_j + \tilde{\phi}_{-j} - 2\phi], \quad (33)$$

One can then compute $T^{\mu\nu}$. The $\tau\tau$ component for example reads

$$\begin{aligned} T^{\tau\tau}(s) = & \frac{g^2}{2\tau^2} \text{Tr}[(E^1)^2(s) + (E^1)^2(s + \hat{e}_2) \\ & + (E^2)^2(s) + (E^2)^2(s + \hat{e}_1)] \\ & + \frac{1}{2\tau^2} \text{Tr}[(\phi(s) - \tilde{\phi}_1(s))^2 \\ & + (\phi(s + \hat{e}_2) - \tilde{\phi}_1(s + \hat{e}_2))^2 \\ & + (\phi(s) - \tilde{\phi}_2(s))^2 \\ & + (\phi(s + \hat{e}_1) - \tilde{\phi}_2(s + \hat{e}_1))^2] \\ & + \frac{1}{4} \text{Tr}[\pi^2(s) + \pi^2(s + \hat{e}_1) \\ & + \pi^2(s + \hat{e}_2) + \pi^2(s + \hat{e}_1 + \hat{e}_2)] \\ & + \frac{2}{g^2} \left(N_c - \text{ReTr}[U_{(1,2)}(s)] \right). \end{aligned}$$

THE MODEL: MUSIC

B. Schenke, C. Shen, P. Tribedy, Phys. Rev. C 102 (2020) 4, 044905

$T^{\mu\nu}$ is matched to hydrodynamics, which solves $\partial_\mu T^{\mu\nu} = 0$

We decompose $T^{\mu\nu} = eu^\mu u^\nu - (P + \Pi)\Delta^{\mu\nu} + \pi^{\mu\nu}$

We use the DNMR formalism that has constitutive relations

$$\begin{aligned} \tau_\Pi \dot{\Pi} + \Pi &= -\zeta \theta - \delta_{\Pi\Pi} \Pi \theta + \lambda_{\Pi\pi} \pi^{\mu\nu} \sigma_{\mu\nu} \\ \tau_\pi \dot{\pi}^{\langle\mu\nu\rangle} + \pi^{\mu\nu} &= 2\eta \sigma^{\mu\nu} - \delta_{\pi\pi} \pi^{\mu\nu} \theta + \varphi_7 \pi_\alpha^{\langle\mu} \pi^{\nu\rangle\alpha} \\ &\quad - \tau_{\pi\pi} \pi_\alpha^{\langle\mu} \sigma^{\nu\rangle\alpha} + \lambda_{\pi\Pi} \Pi \sigma^{\mu\nu}, \end{aligned}$$

$$\sigma^{\mu\nu} = \frac{1}{2} \left[\nabla^\mu u^\nu + \nabla^\nu u^\mu - \frac{2}{3} \Delta^{\mu\nu} (\nabla_\alpha u^\alpha) \right]$$

$$\tau_\pi = \frac{5\eta}{e + P},$$

$$\tau_\Pi = \frac{\zeta}{15 \left(\frac{1}{2} - c_s^2\right)^2 (e + P)}$$

$\tau_{\pi\pi} [\tau_\pi]$	$\delta_{\pi\pi} [\tau_\pi]$	$\varphi_7 P$	$\lambda_{\pi\Pi} [\tau_\pi]$	$\lambda_{\Pi\pi} [\tau_\Pi]$	$\delta_{\Pi\Pi} [\tau_\Pi]$
10/7	4/3	9/70	6/5	$8(1/3 - c_s^2)/5$	2/3

G. S. Denicol, H. Niemi, E. Molnar, and D. H. Rischke, Phys. Rev. **D85**, 114047 (2012), [Erratum: Phys. Rev.D91,no.3,039902(2015)], arXiv:1202.4551 [nucl-th].
G. S. Denicol, S. Jeon, and C. Gale, Phys. Rev. **C90**, 024912 (2014), arXiv:1403.0962 [nucl-th].

THE MODEL: PARTICLE SAMPLING

B. Schenke, C. Shen, P. Tribedy, Phys. Rev. C 102 (2020) 4, 044905

When converting to particles, we use viscous corrections

$$\delta f_{\text{shear}}^i(x^\mu, p^\mu) = f_0^i(1 \pm f_0^i) \frac{\pi^{\mu\nu} p_\mu p_\nu}{2T^2(e + P)},$$

and

$$\delta f_{\text{bulk}}^i(x^\mu, p^\mu) = f_0^i(1 \pm f_0^i) \left(-\frac{\Pi}{\hat{\zeta}} \right) \frac{(p \cdot u)}{T} \\ \times \left[\frac{m_i^2}{3(p \cdot u)^2} - \left(\frac{1}{3} - c_s^2 \right) \right]$$

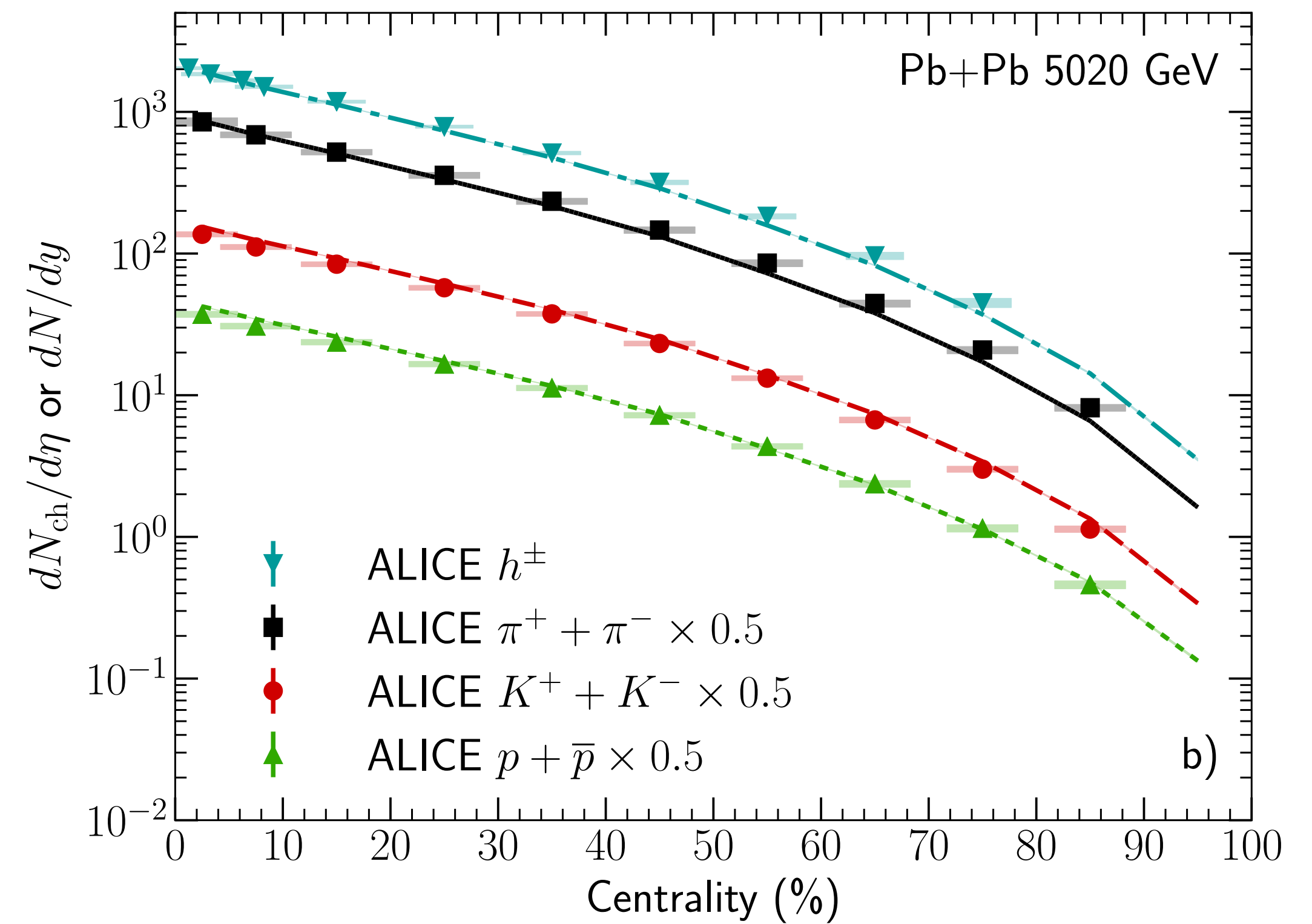
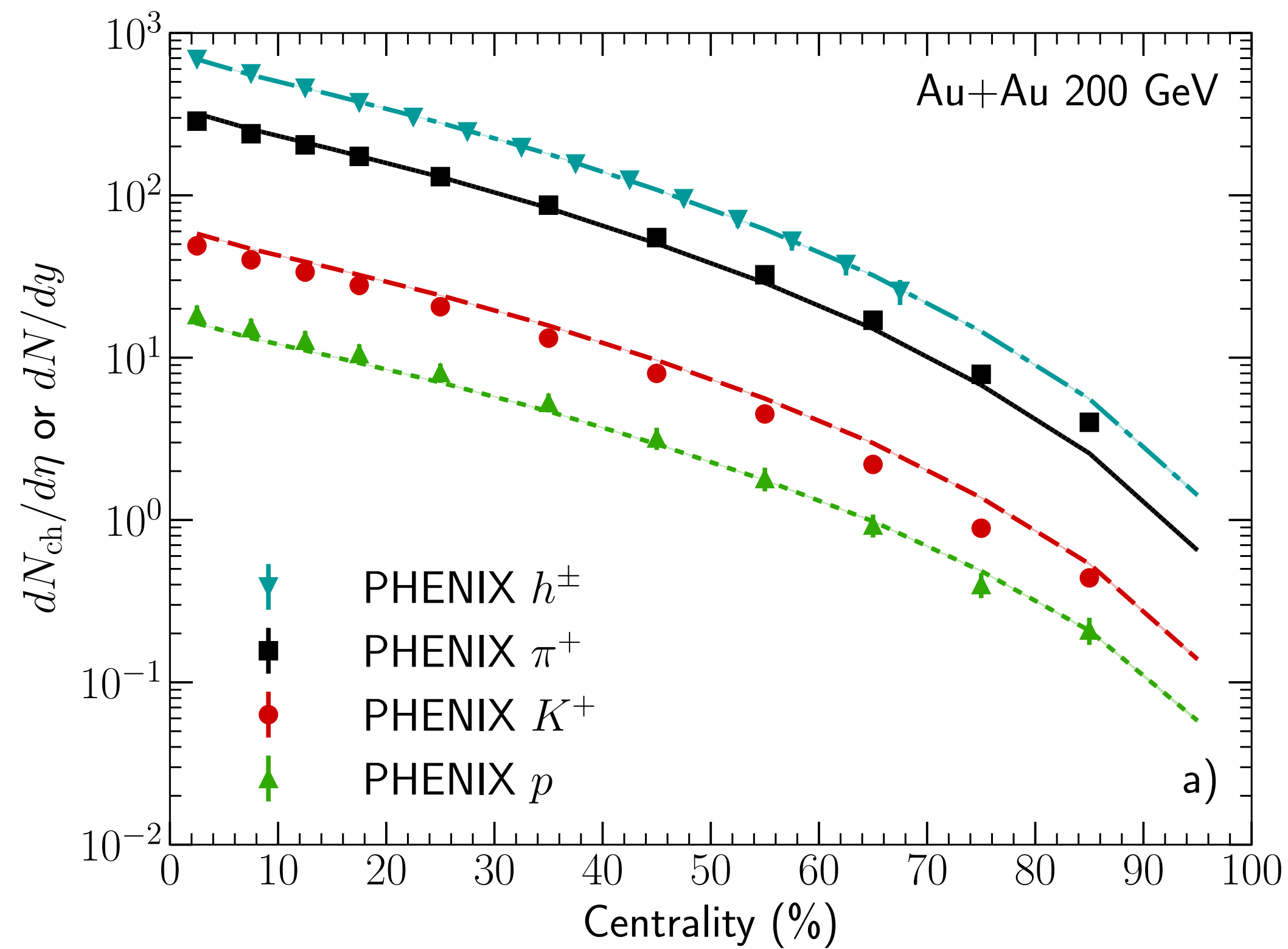
where

$$\hat{\zeta} = \frac{1}{3T} \sum_i \frac{g_i}{(2\pi)^3} m_i^2 \int \frac{d^3k}{E} f_0^i(1 \pm f_0^i) \\ \times E \left[\frac{m_i^2}{3E^2} - \left(\frac{1}{3} - c_s^2 \right) \right]$$

Should the value of any δf be larger than that of the equilibrium distribution, we set the distribution to zero,

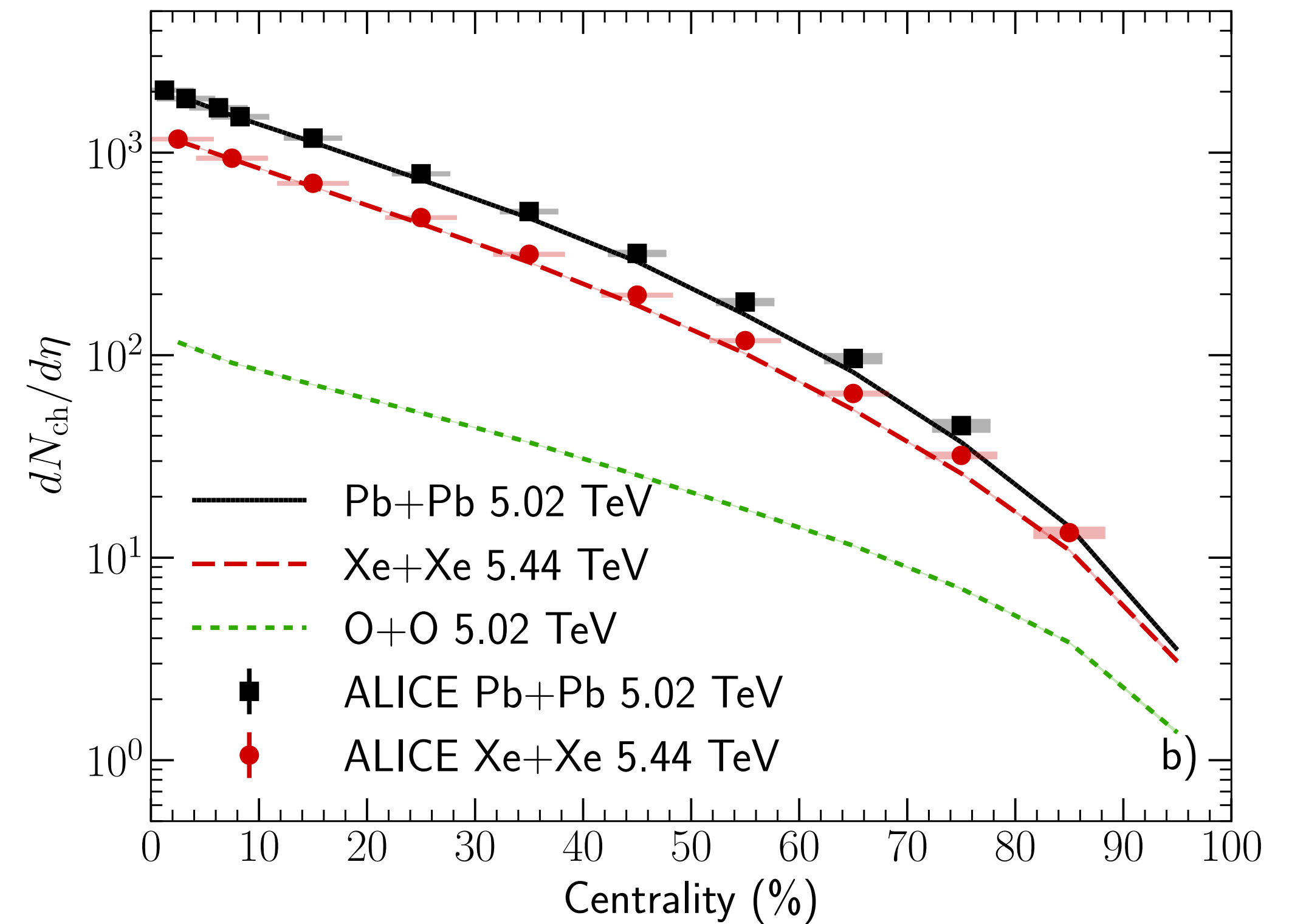
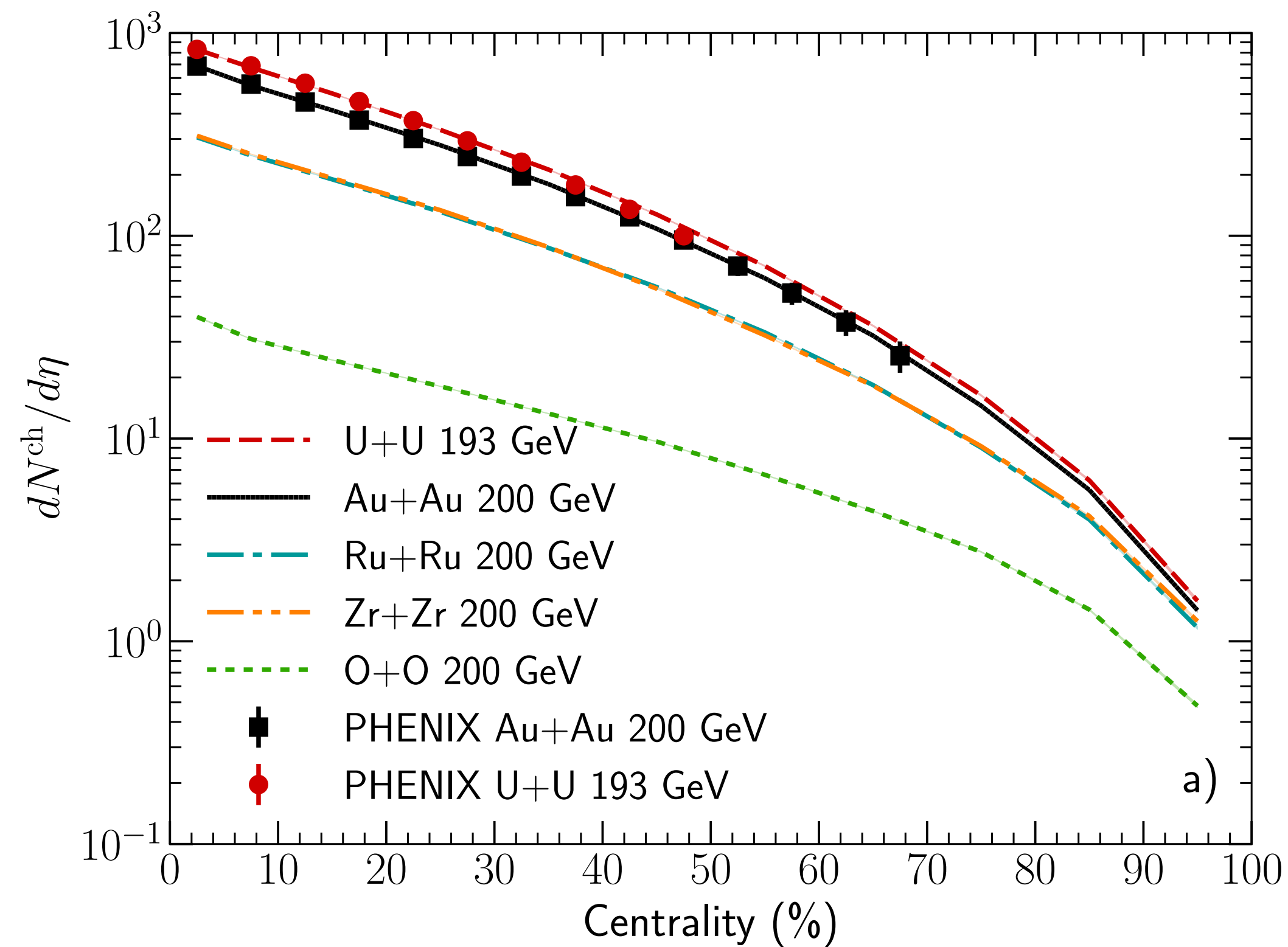
BACKUP: Model validation

B. Schenke, C. Shen, P. Tribedy, Phys. Rev. C 102 (2020) 4, 044905



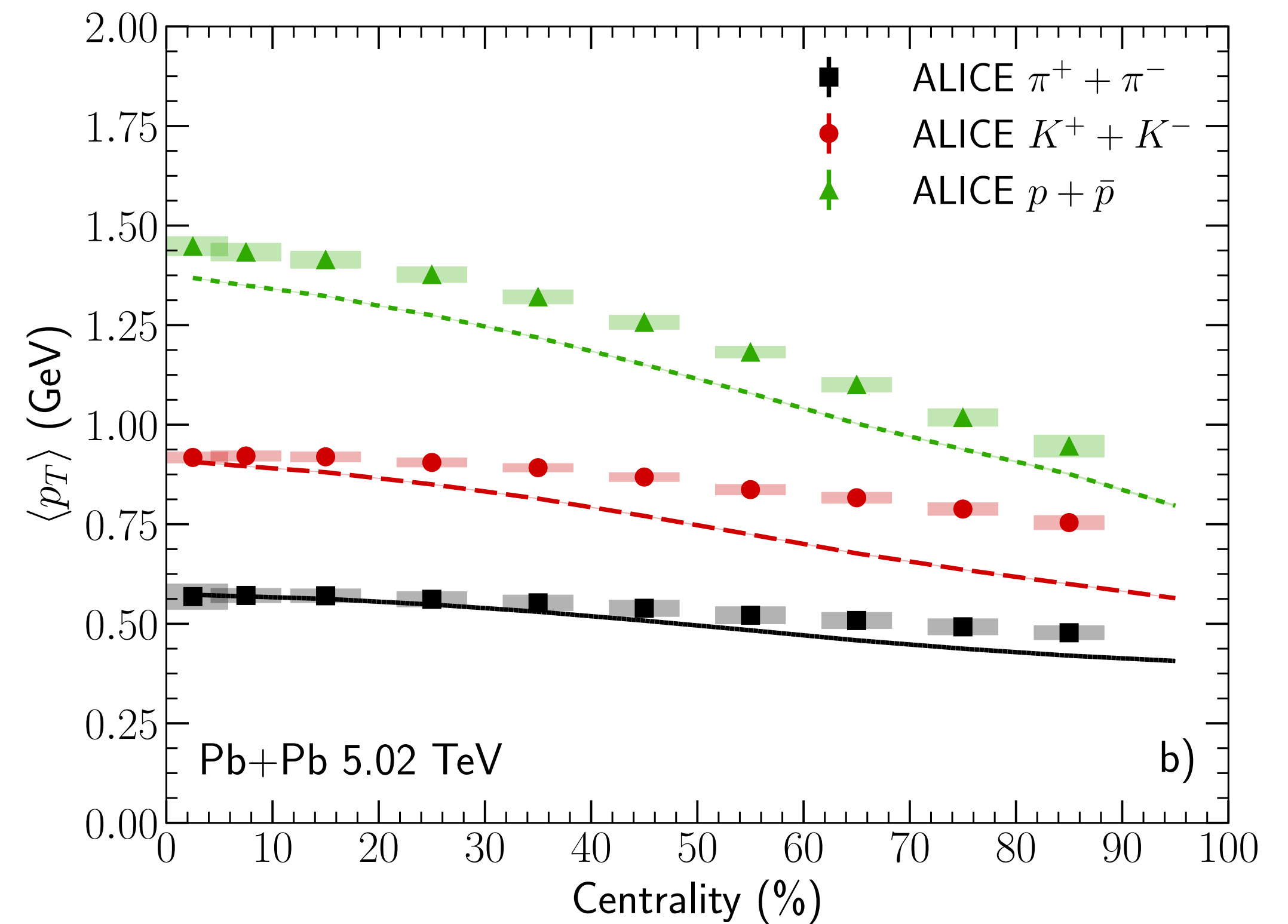
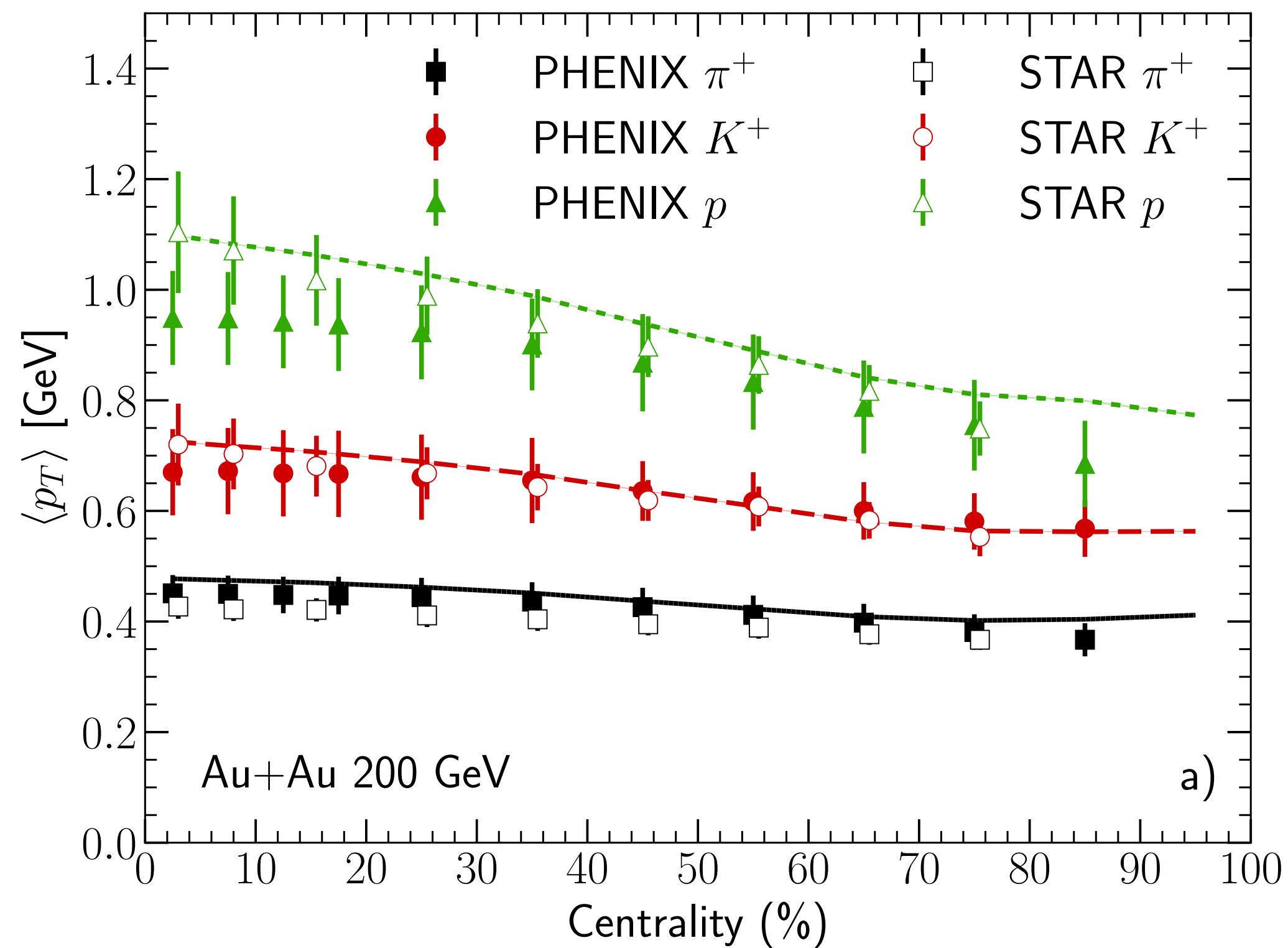
BACKUP: Model validation

B. Schenke, C. Shen, P. Tribedy, Phys. Rev. C 102 (2020) 4, 044905



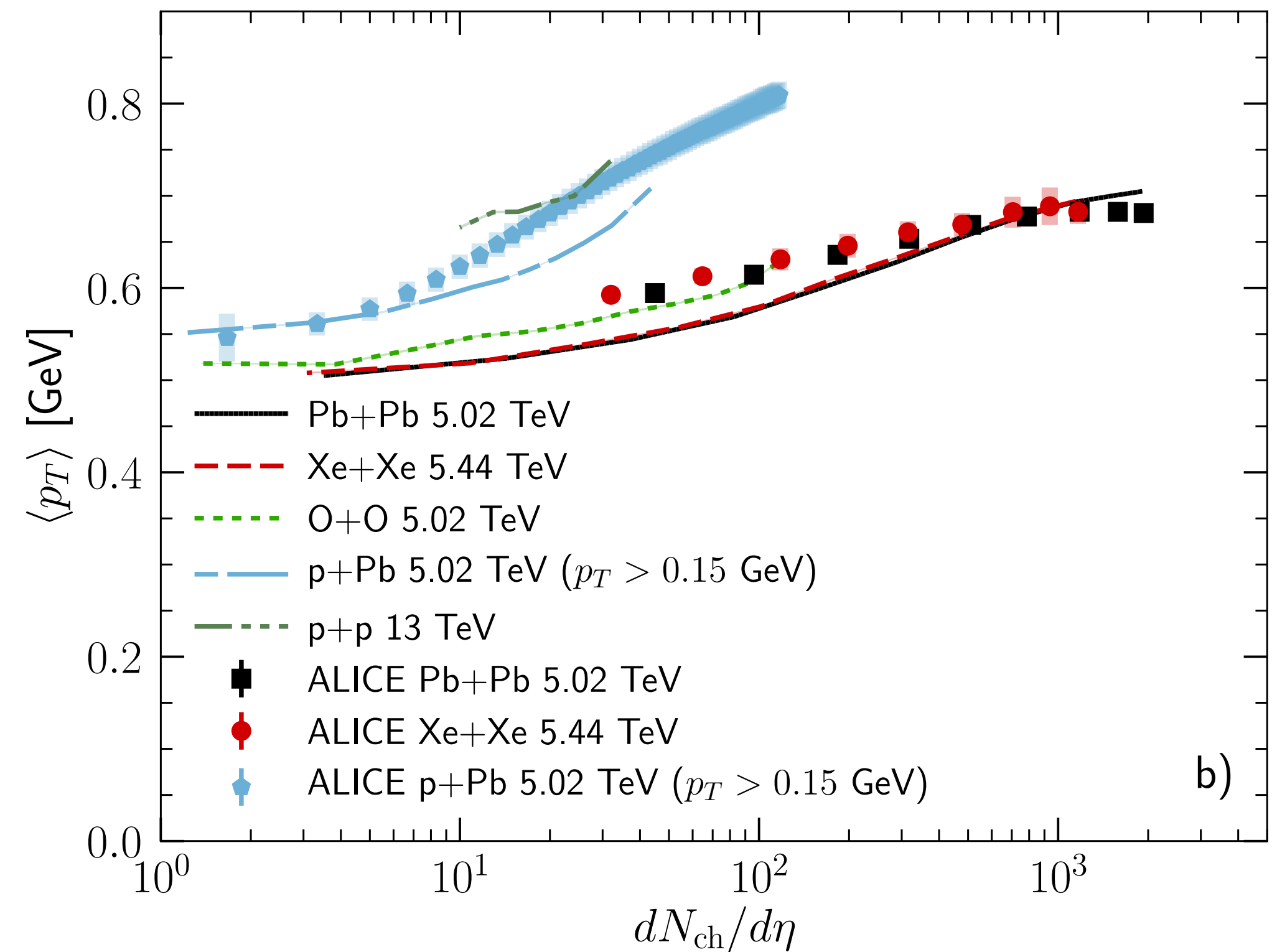
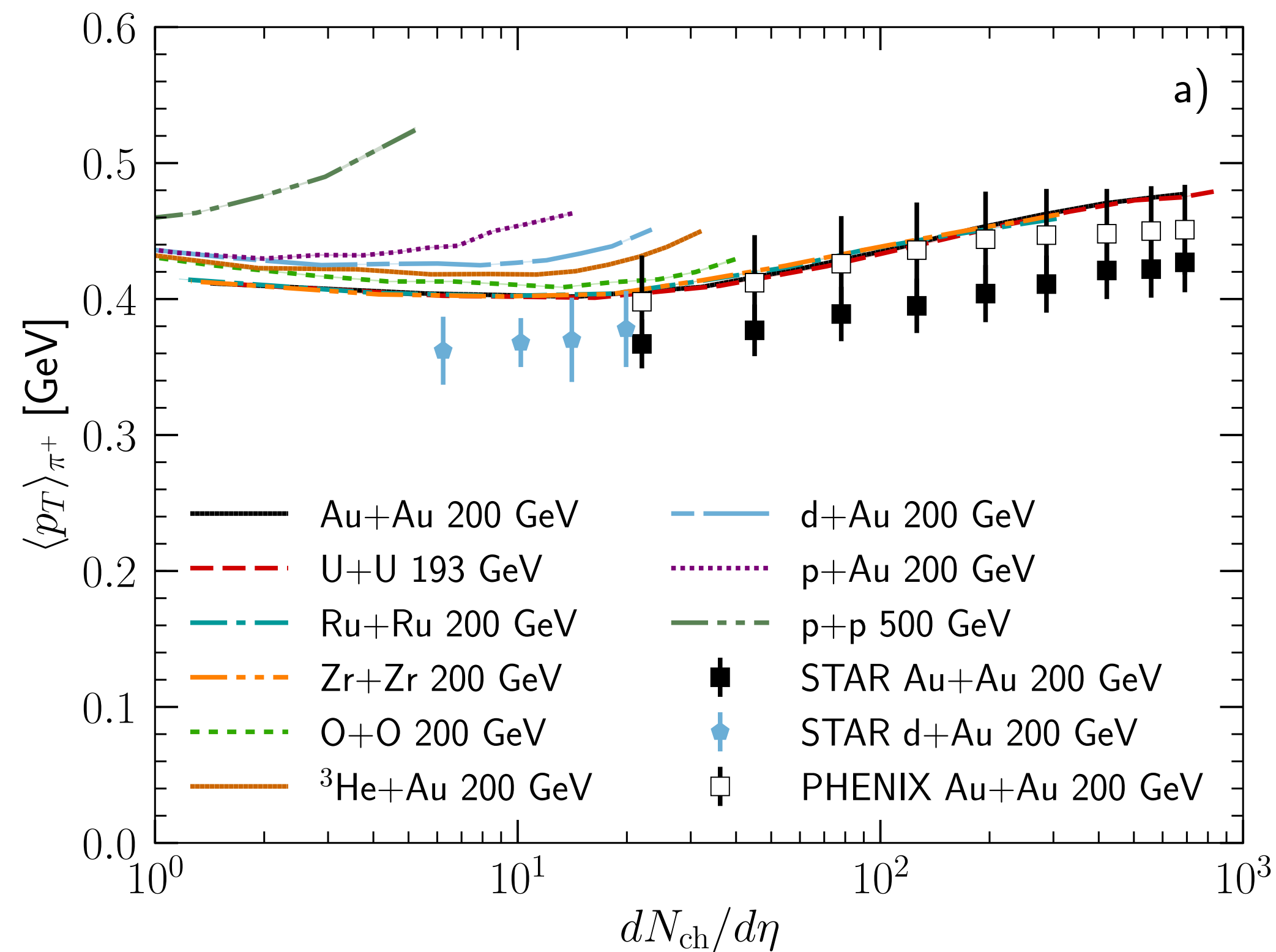
BACKUP: Model validation

B. Schenke, C. Shen, P. Tribedy, Phys. Rev. C 102 (2020) 4, 044905



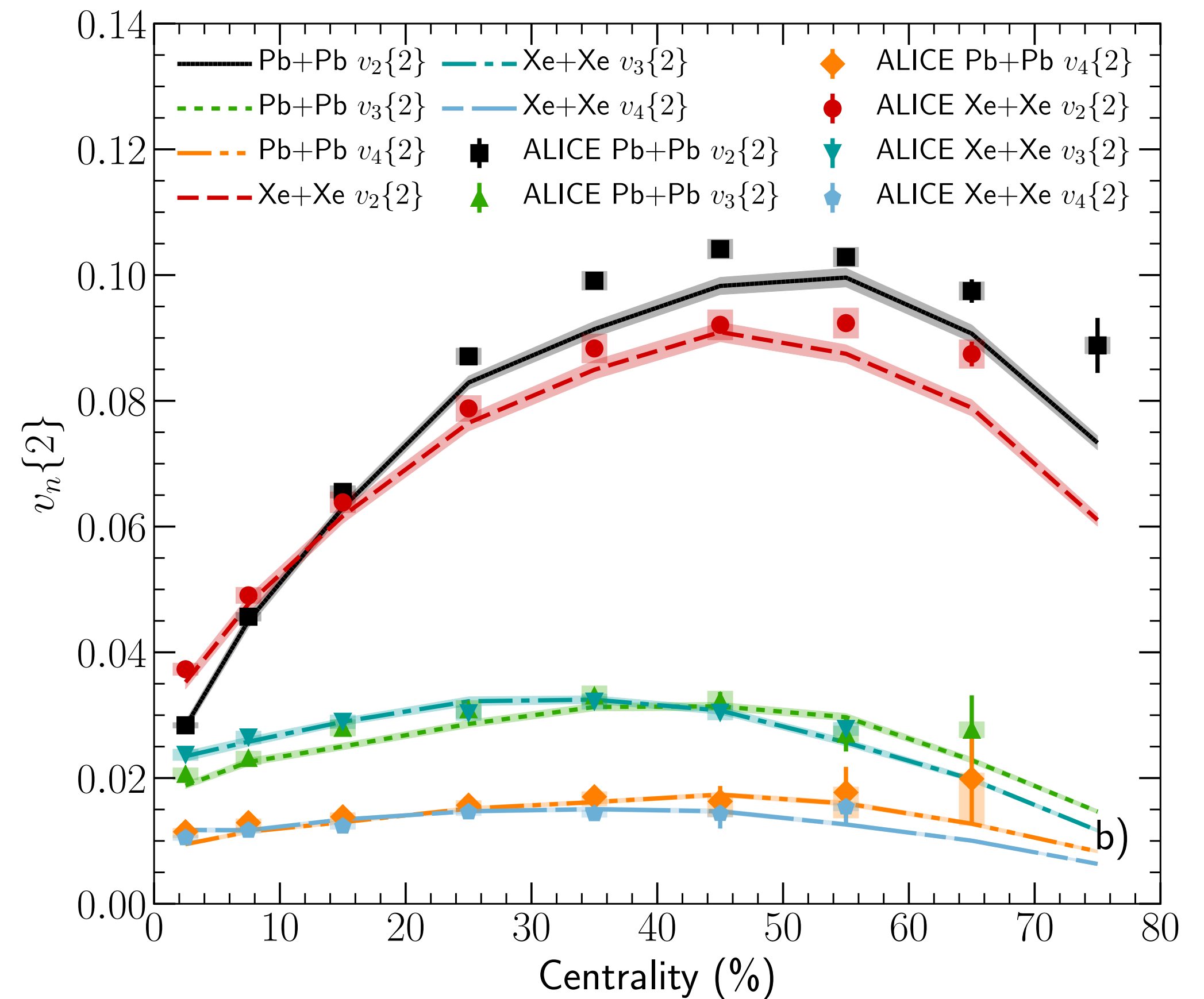
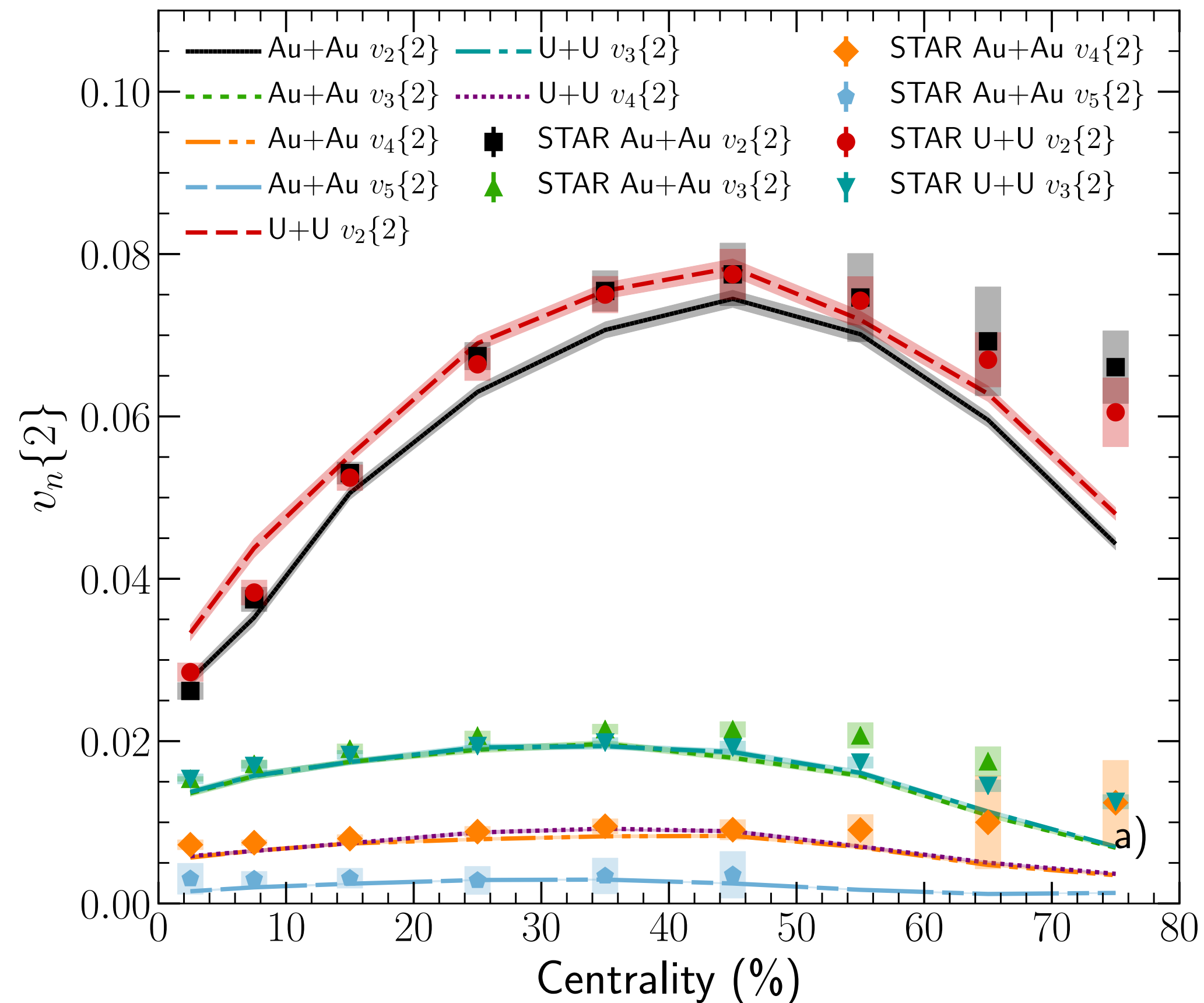
BACKUP: Model validation

B. Schenke, C. Shen, P. Tribedy, Phys. Rev. C 102 (2020) 4, 044905



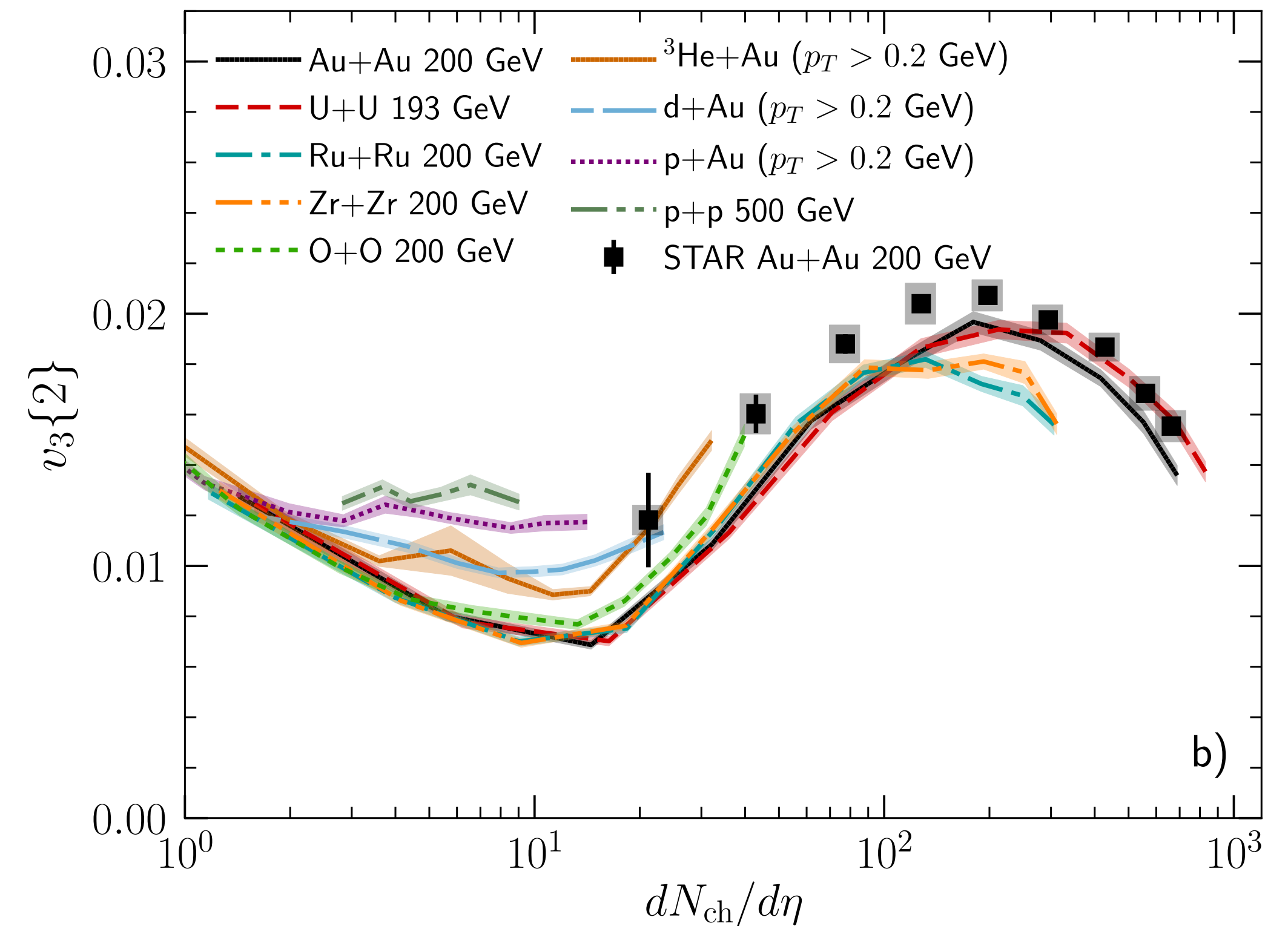
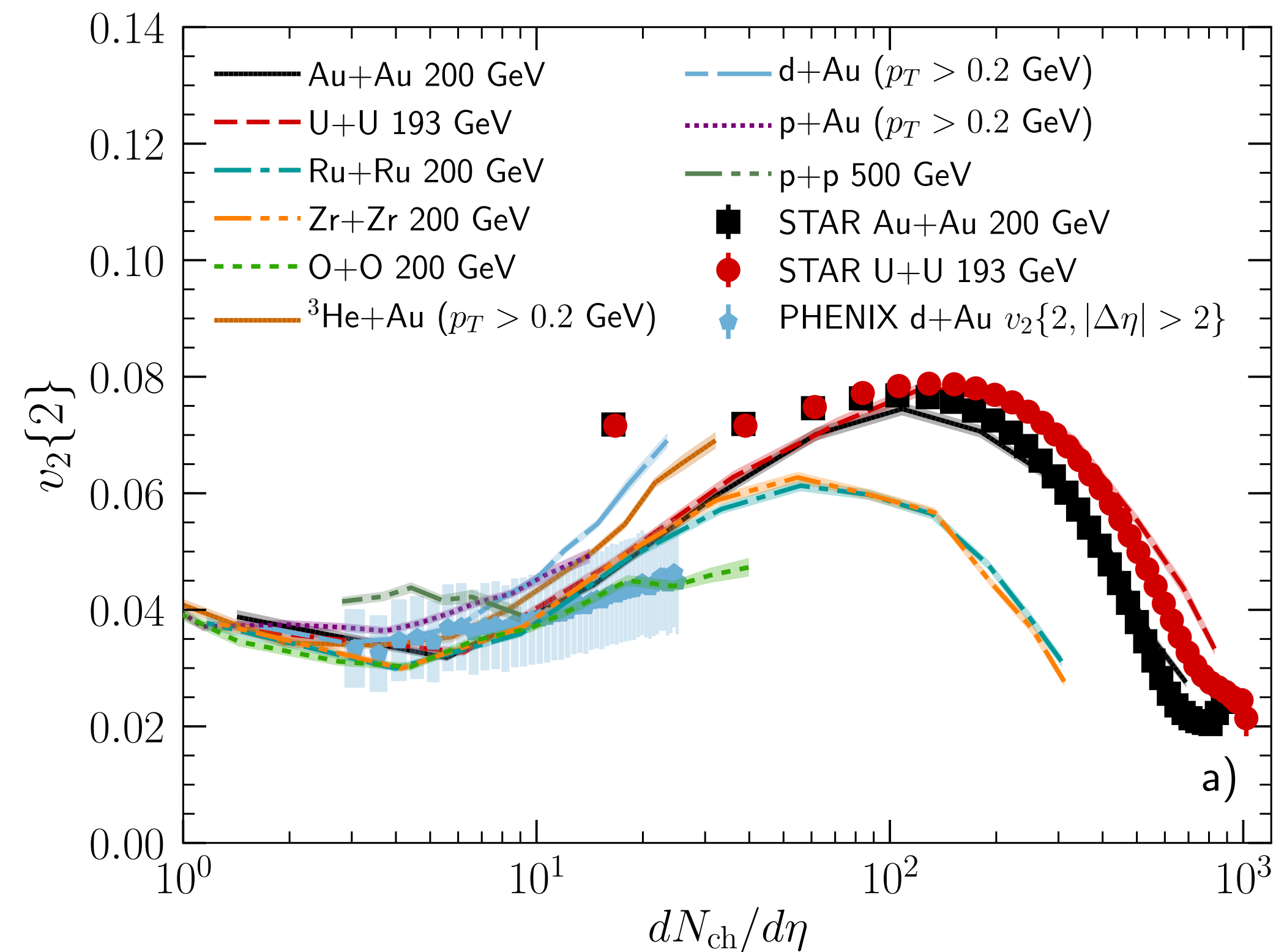
BACKUP: Model validation

B. Schenke, C. Shen, P. Tribedy, Phys. Rev. C 102 (2020) 4, 044905



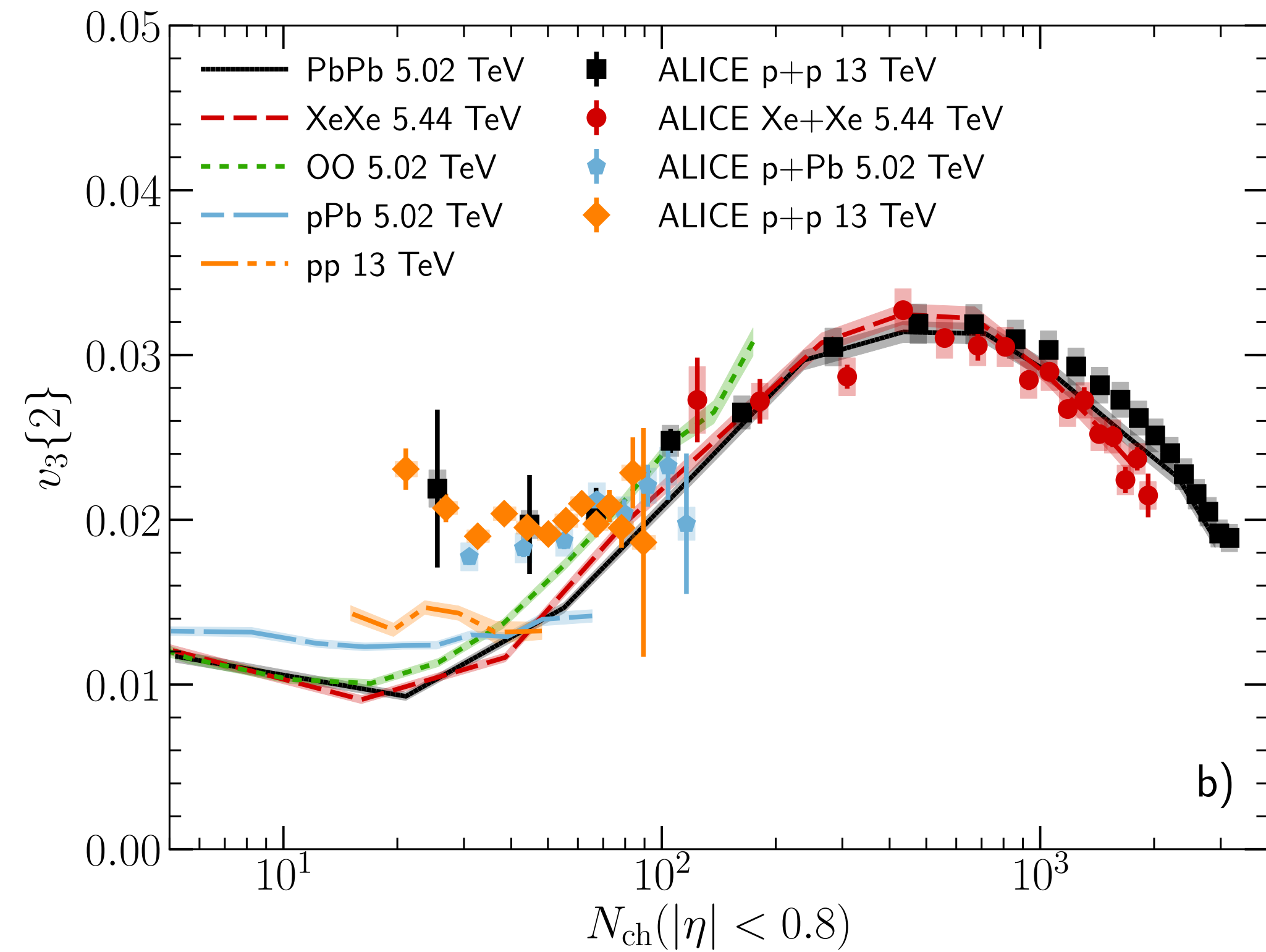
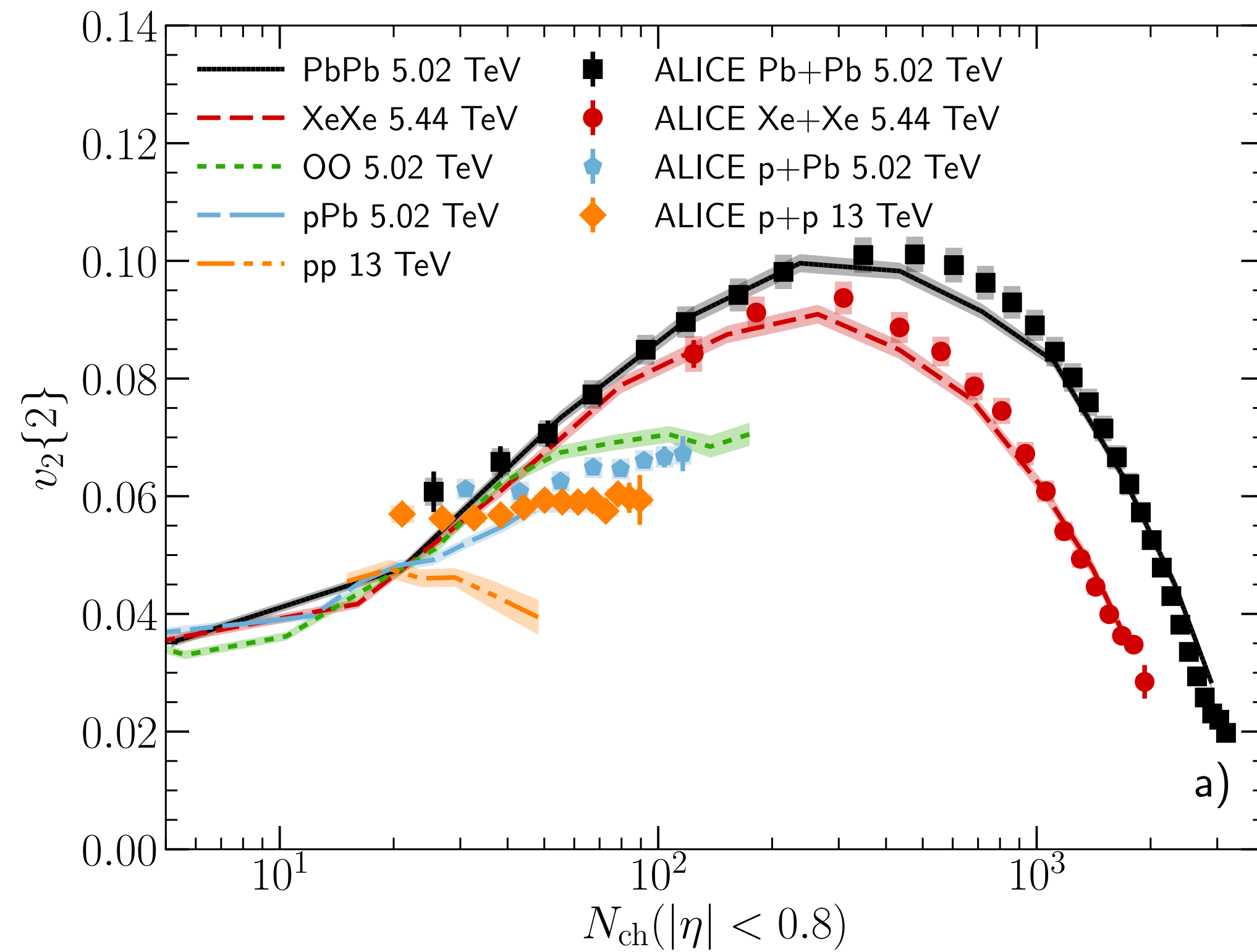
BACKUP: Model validation

B. Schenke, C. Shen, P. Tribedy, Phys. Rev. C 102 (2020) 4, 044905



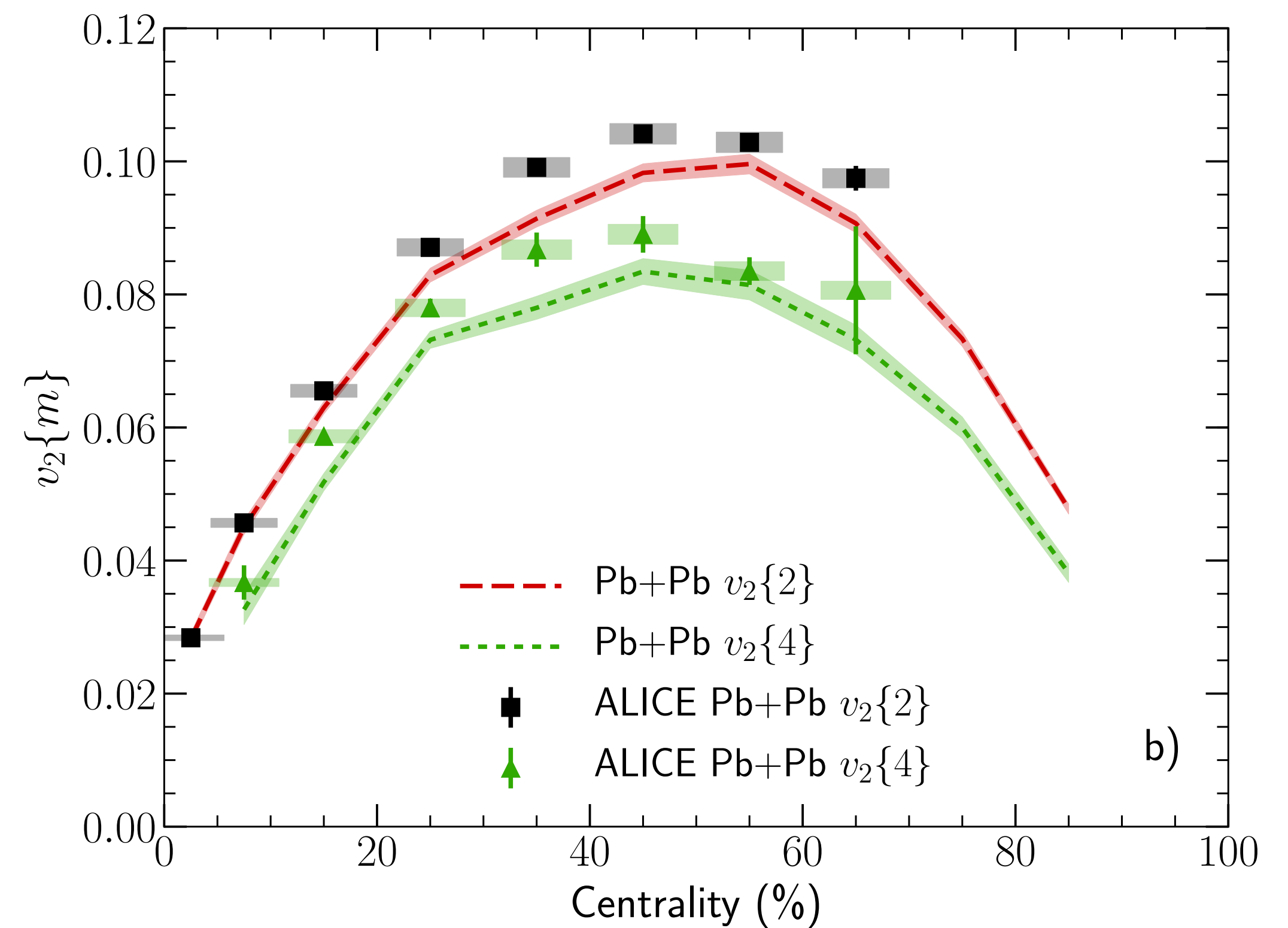
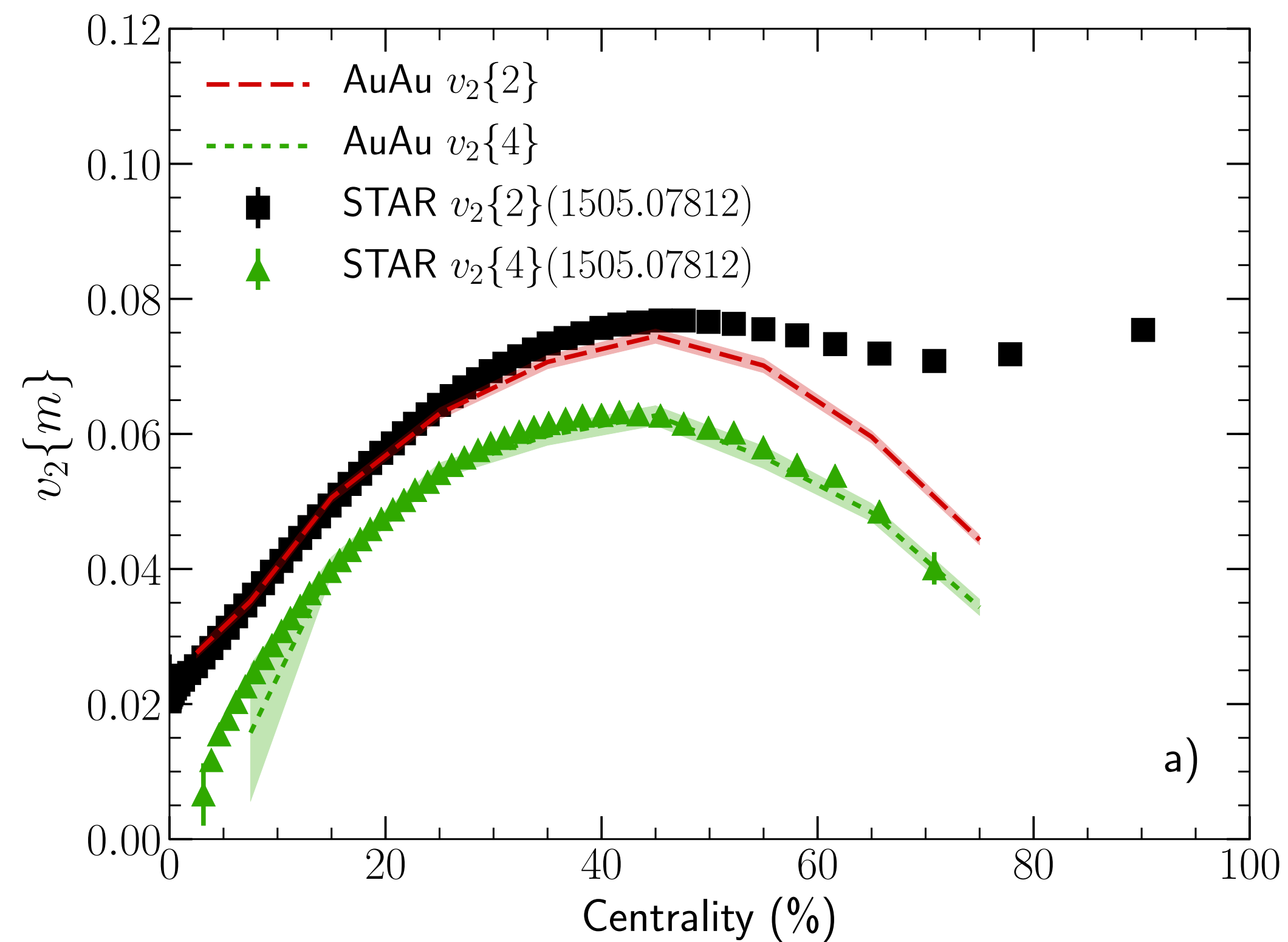
BACKUP: Model validation

B. Schenke, C. Shen, P. Tribedy, Phys. Rev. C 102 (2020) 4, 044905



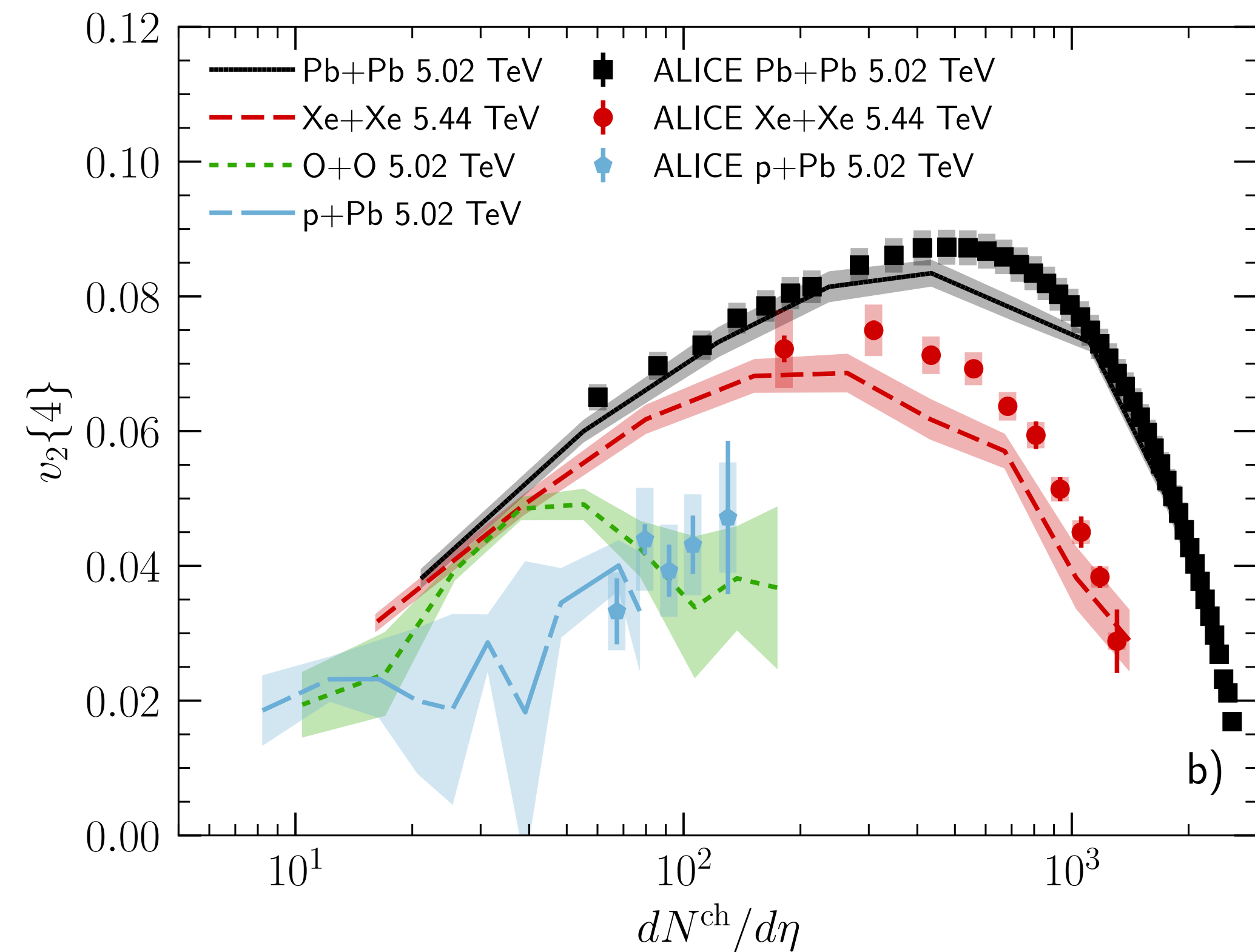
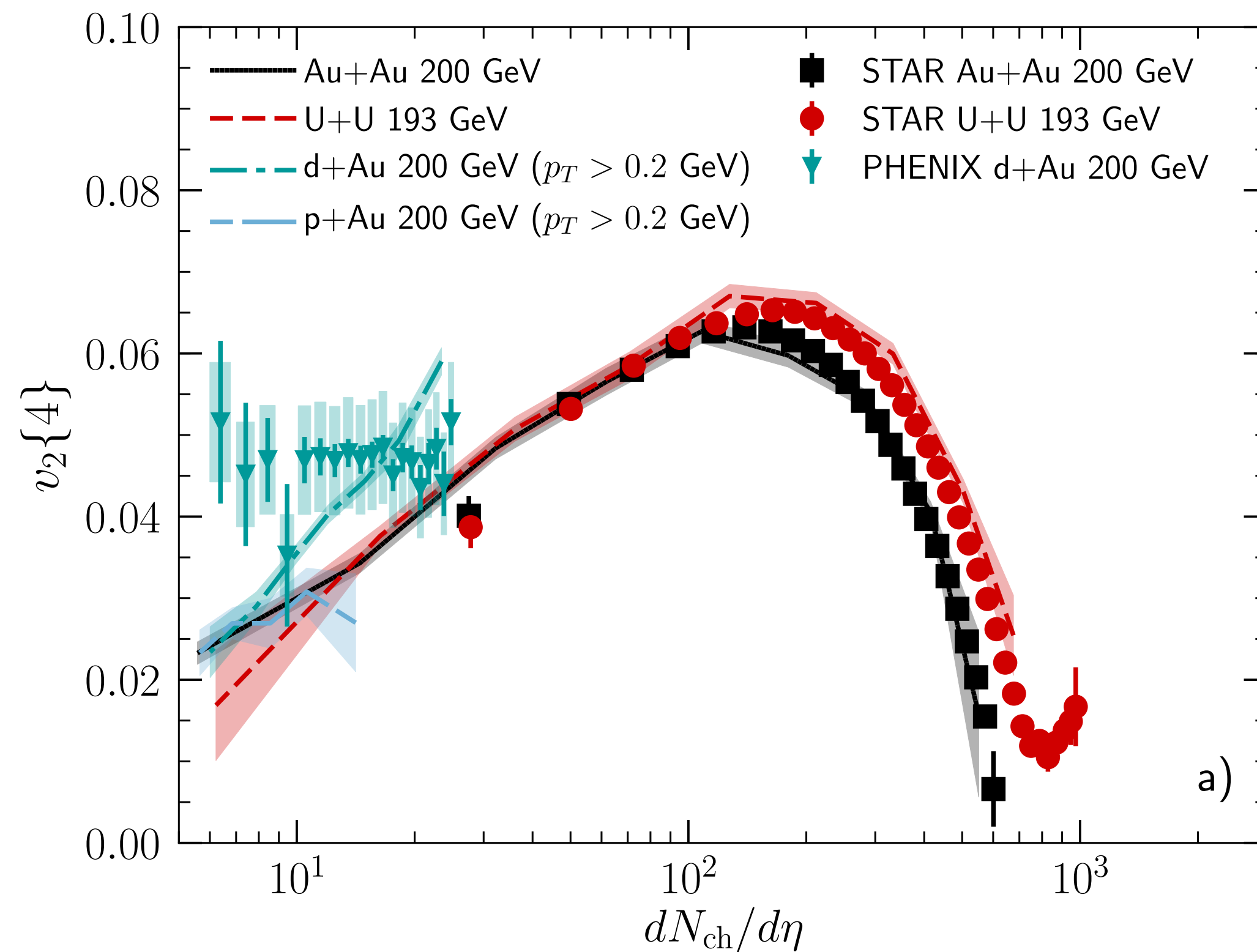
BACKUP: Model validation

B. Schenke, C. Shen, P. Tribedy, Phys. Rev. C 102 (2020) 4, 044905



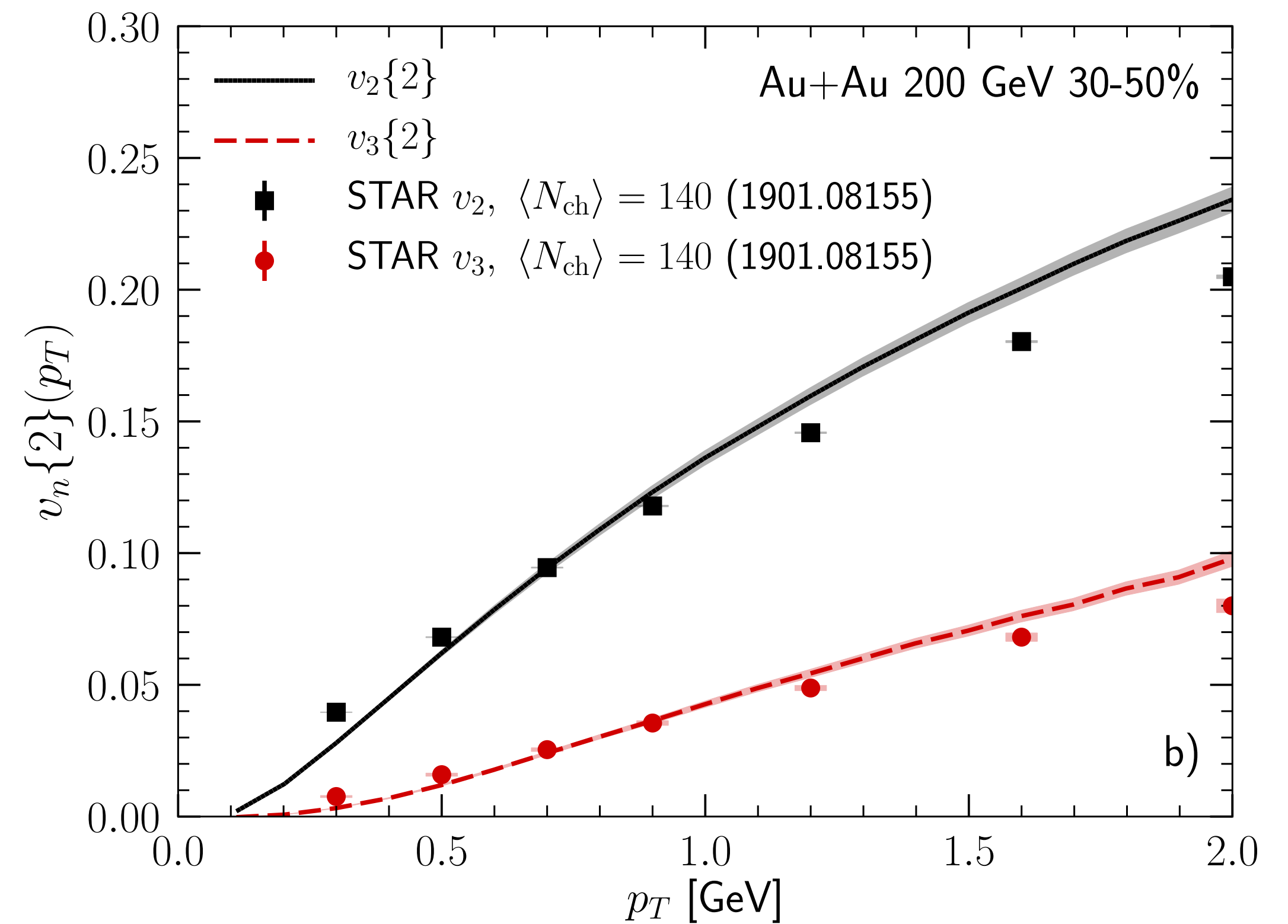
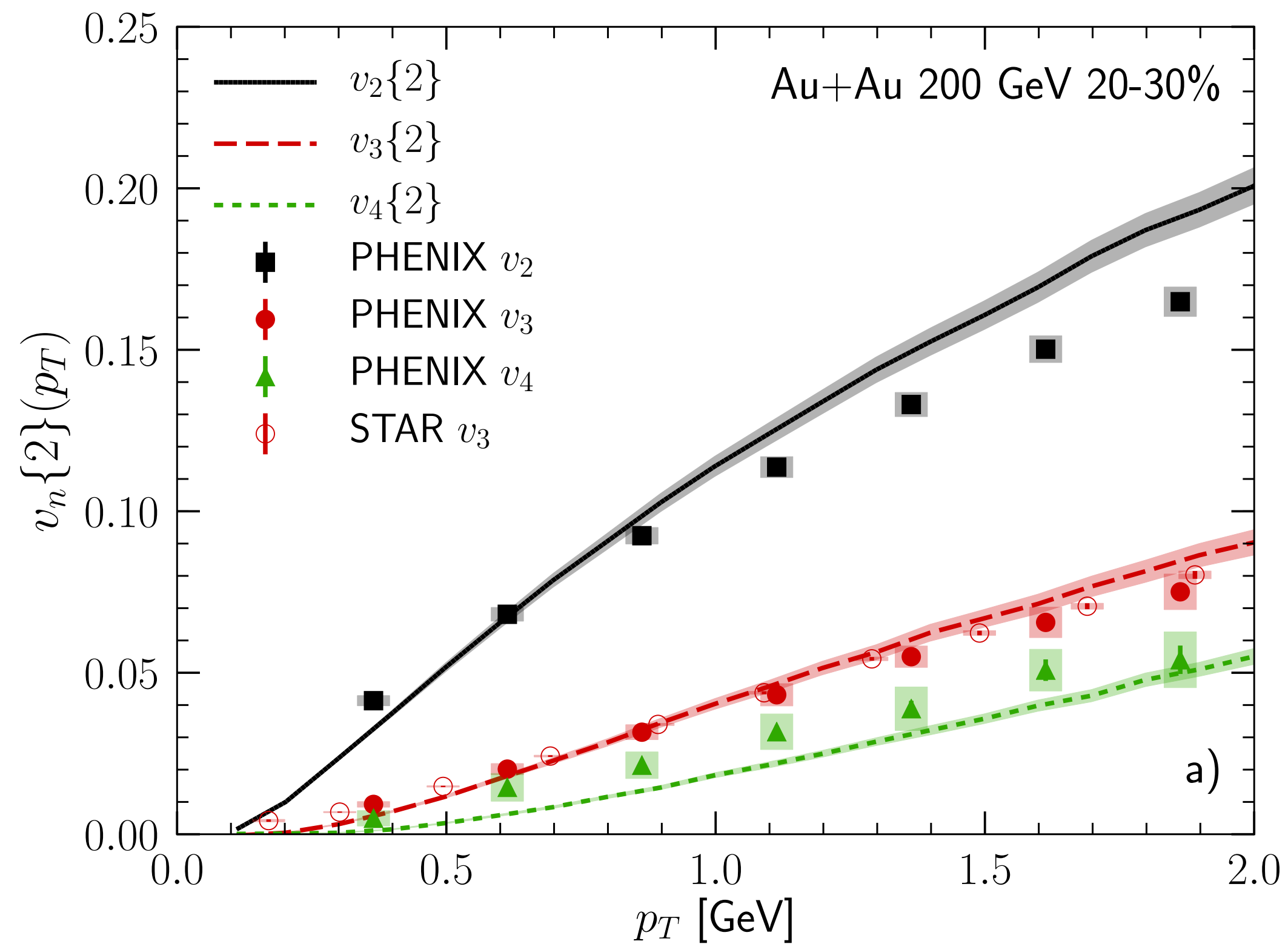
BACKUP: Model validation

B. Schenke, C. Shen, P. Tribedy, Phys. Rev. C 102 (2020) 4, 044905



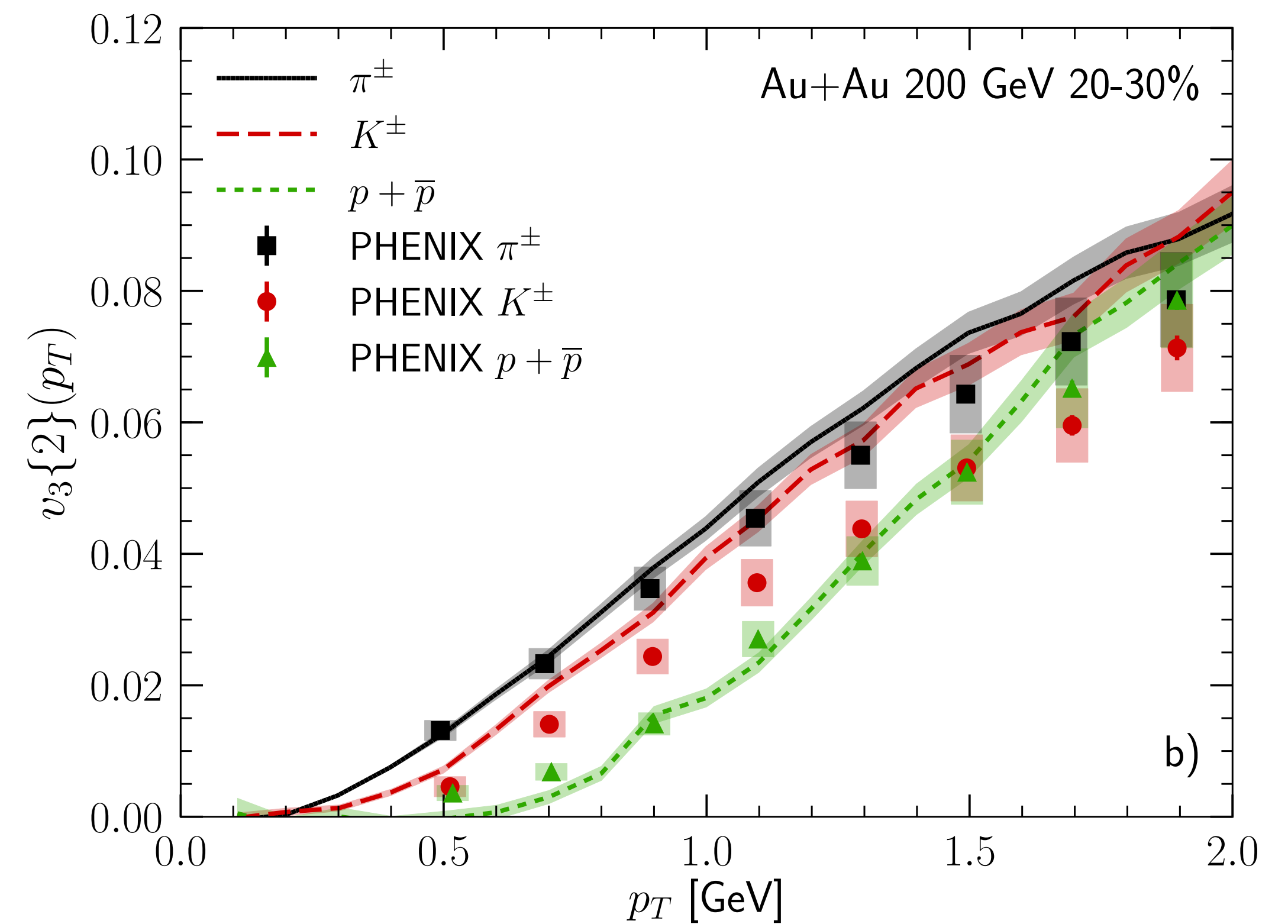
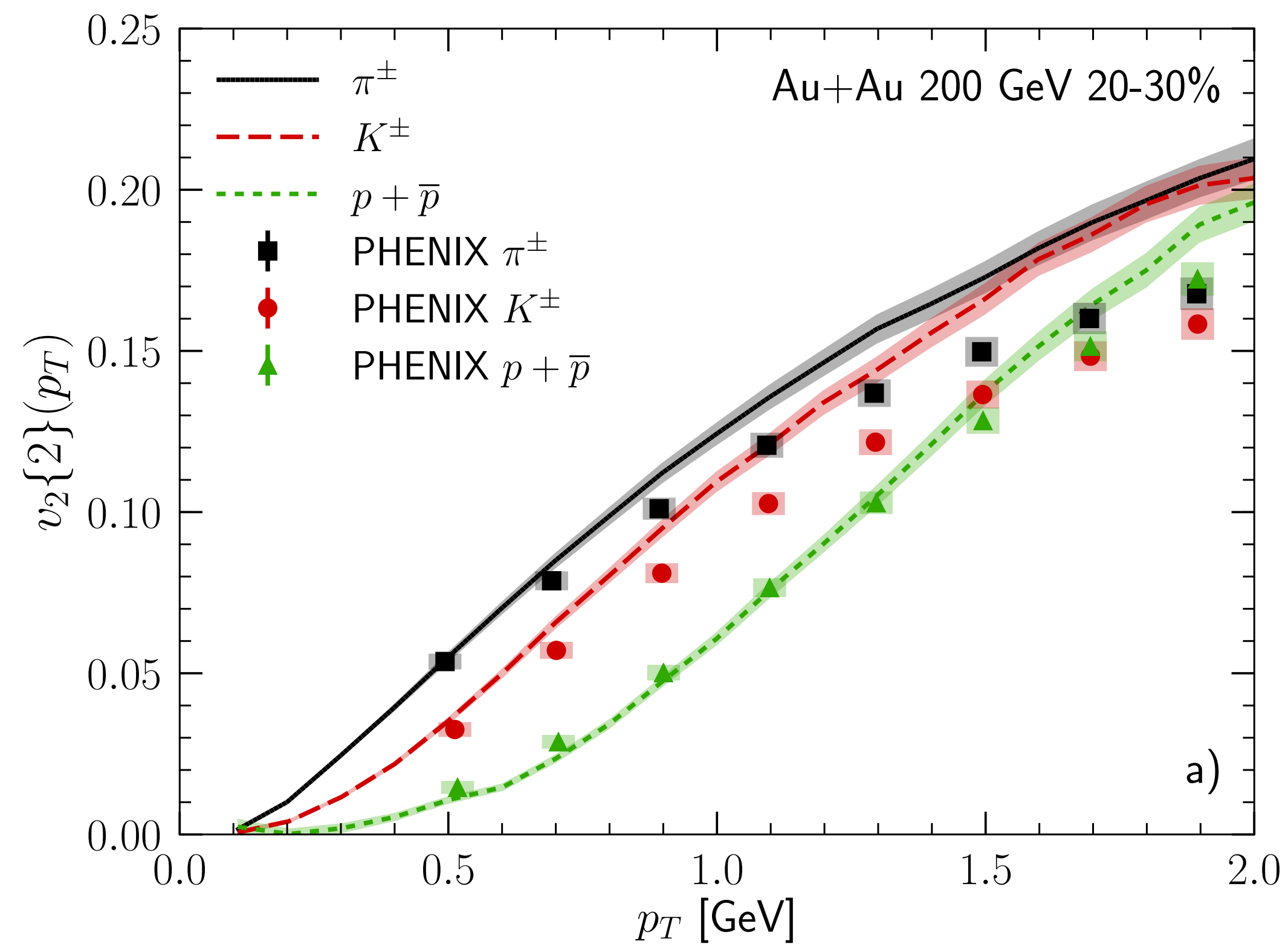
BACKUP: Model validation

B. Schenke, C. Shen, P. Tribedy, Phys. Rev. C 102 (2020) 4, 044905



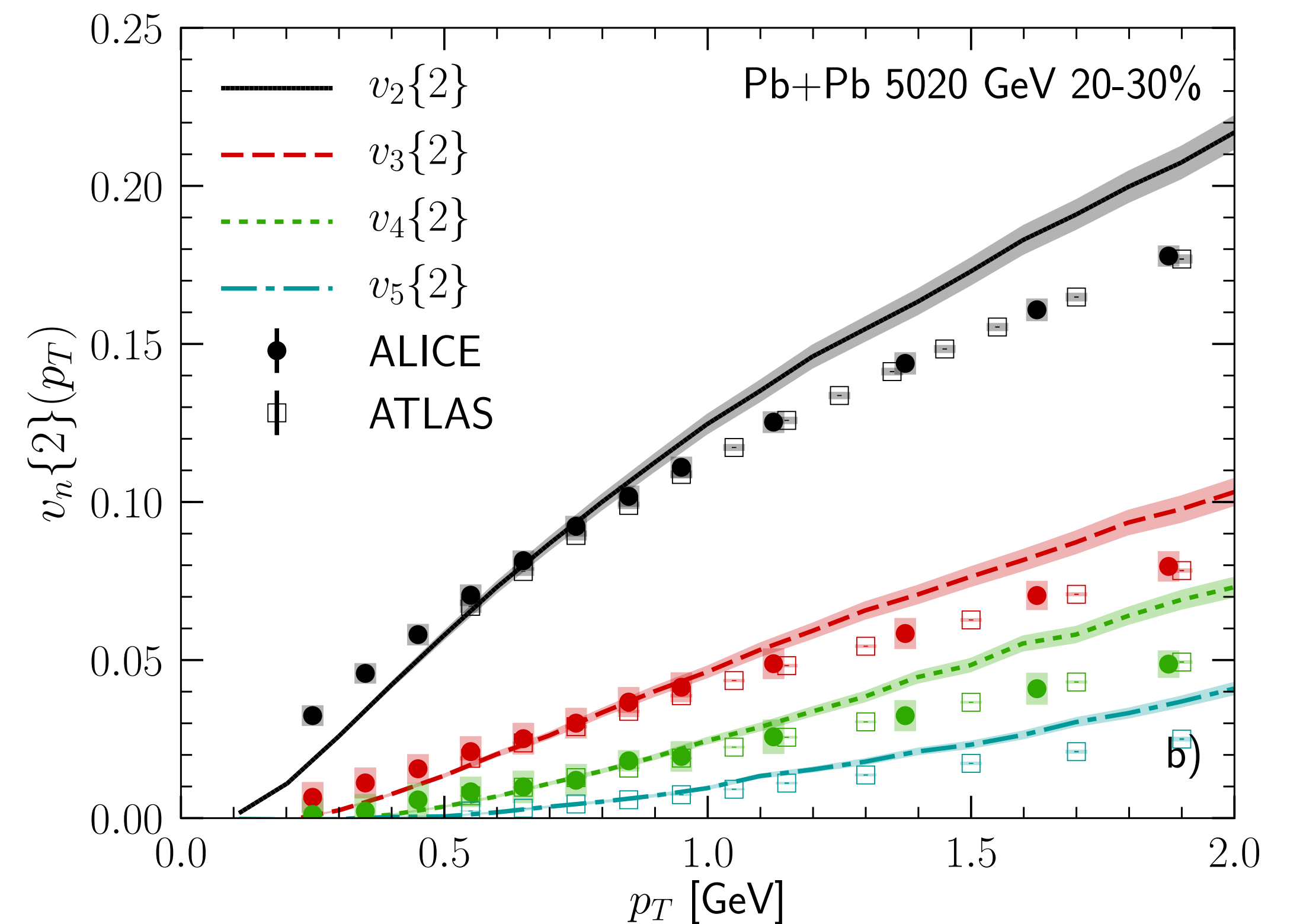
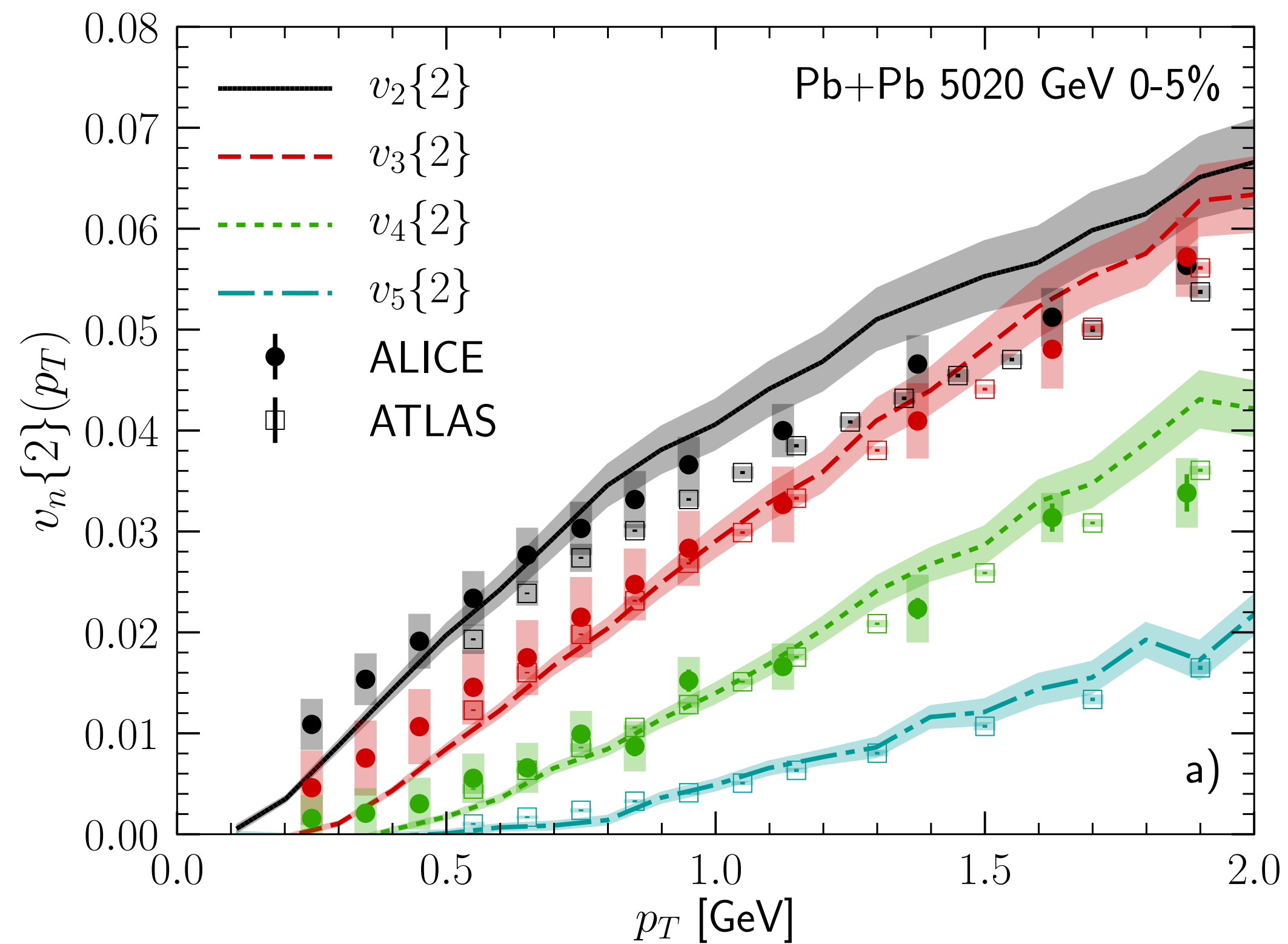
BACKUP: Model validation

B. Schenke, C. Shen, P. Tribedy, Phys. Rev. C 102 (2020) 4, 044905



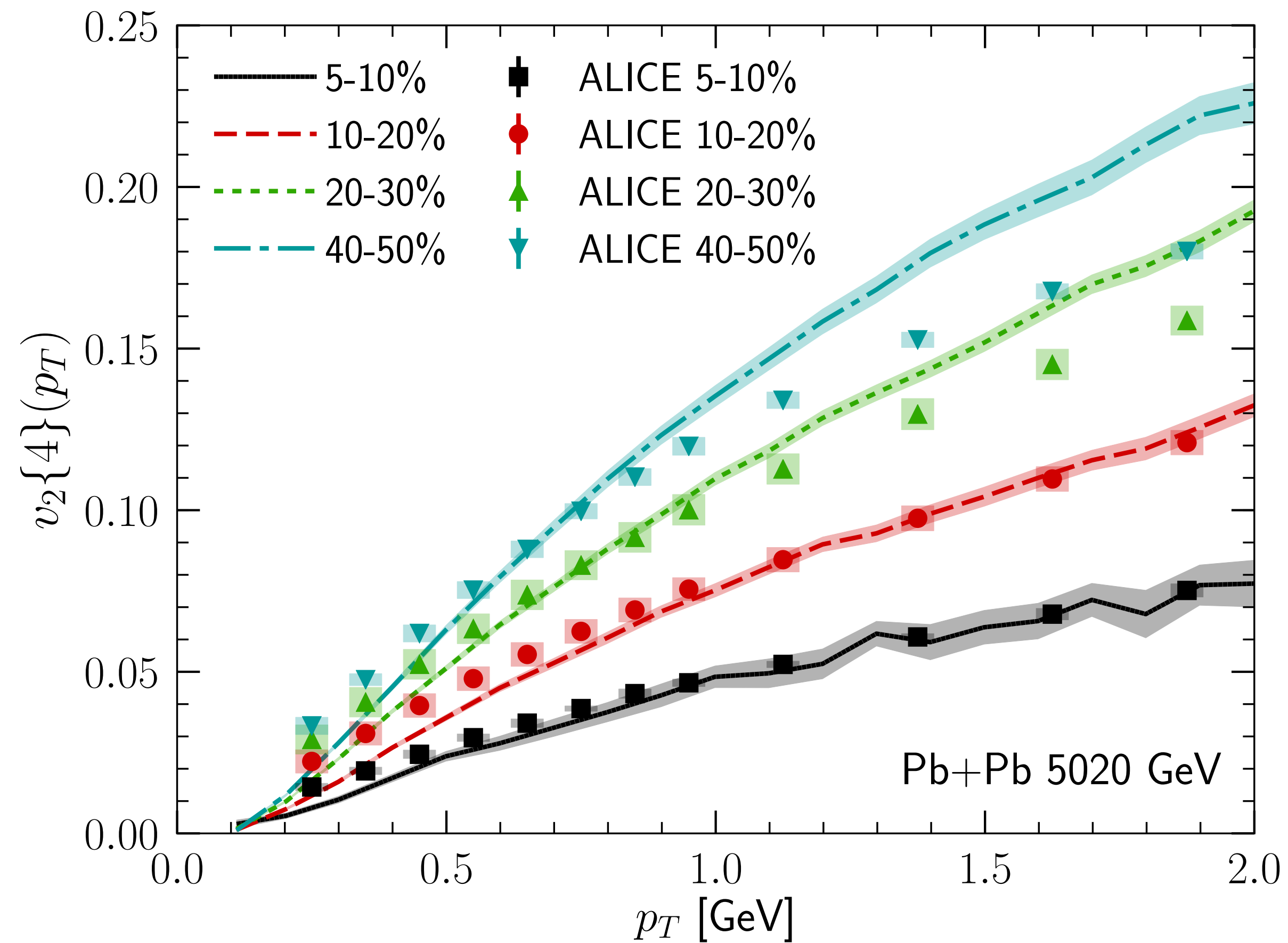
BACKUP: Model validation

B. Schenke, C. Shen, P. Tribedy, Phys. Rev. C 102 (2020) 4, 044905



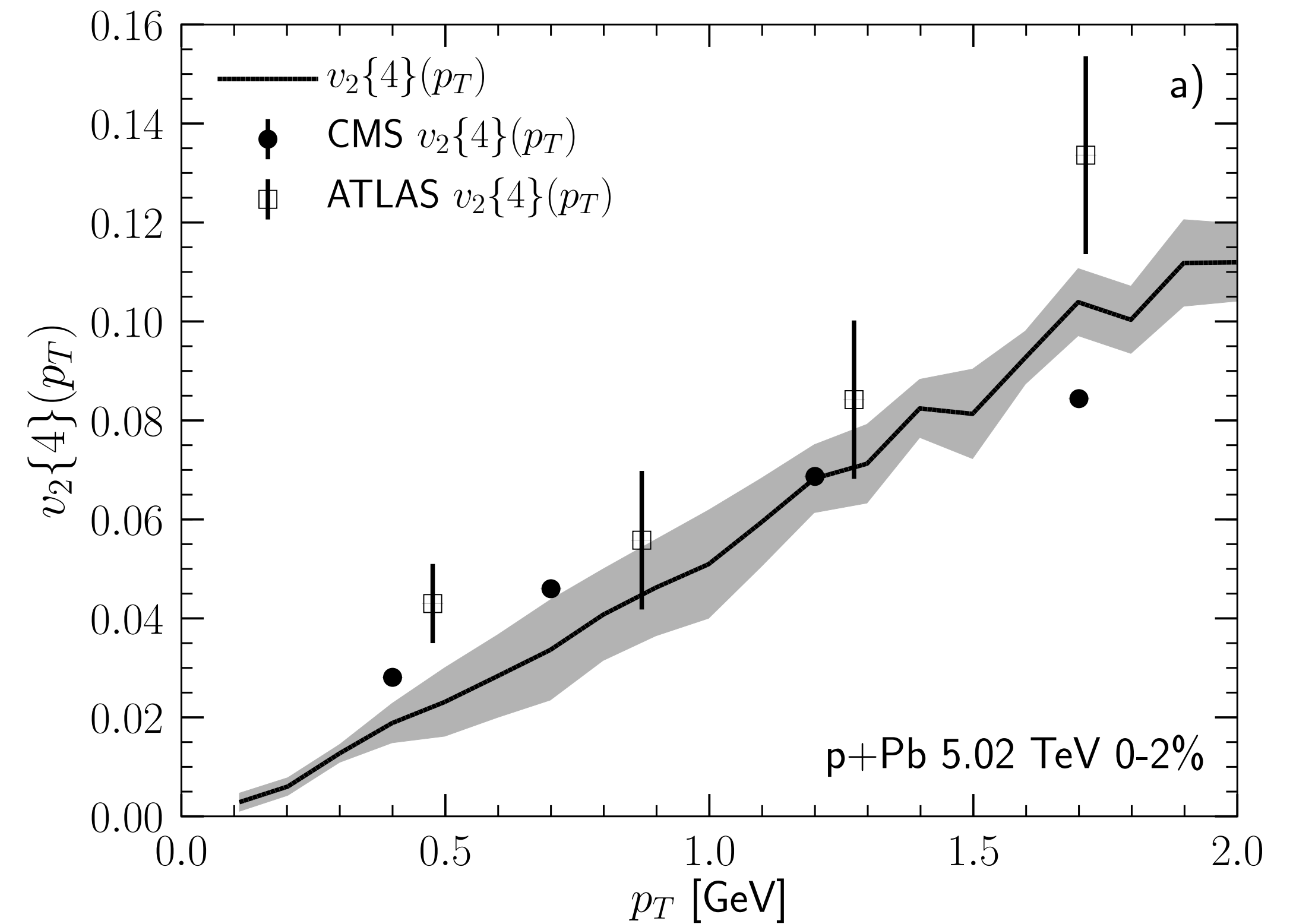
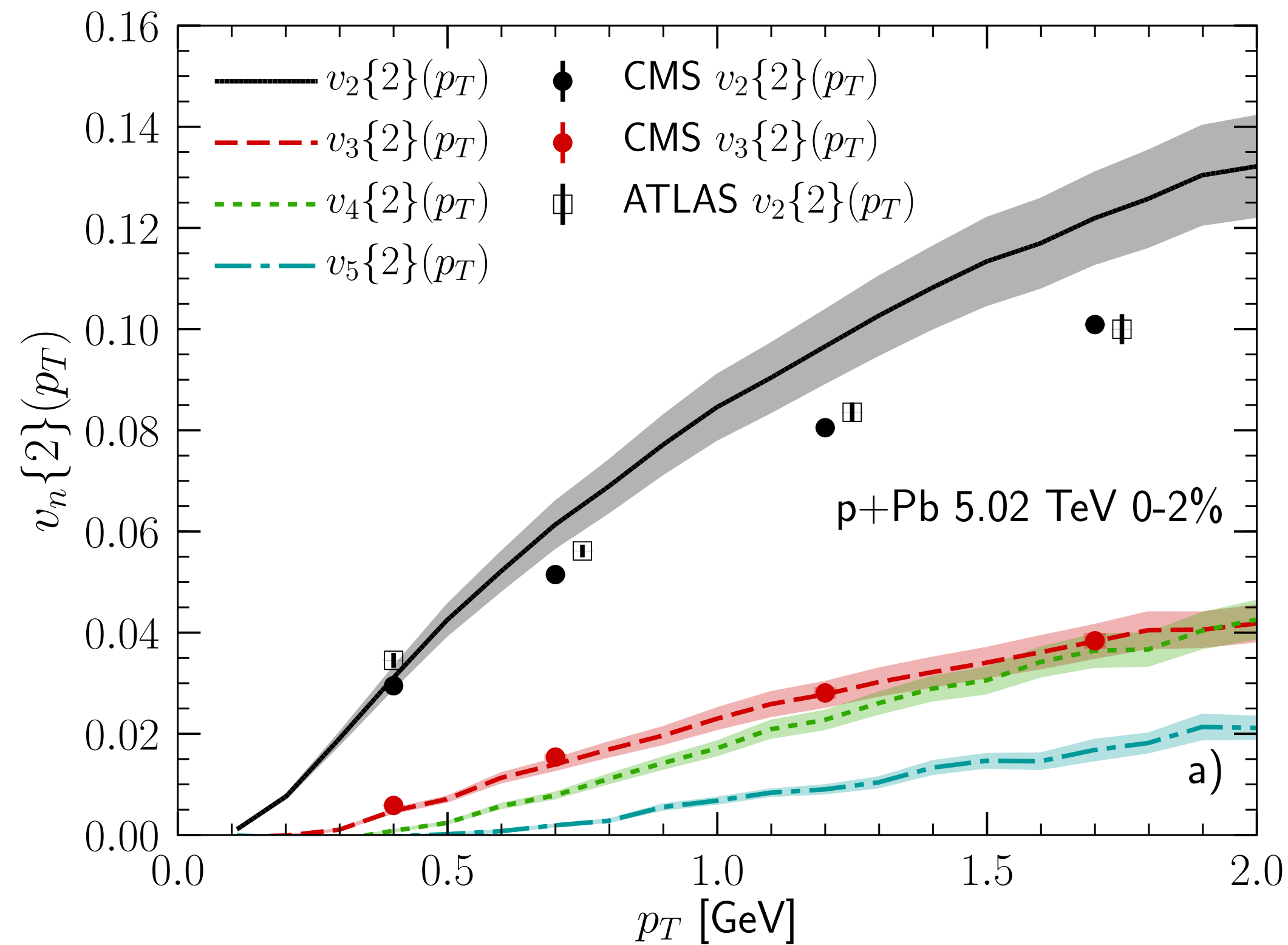
BACKUP: Model validation

B. Schenke, C. Shen, P. Tribedy, Phys. Rev. C 102 (2020) 4, 044905



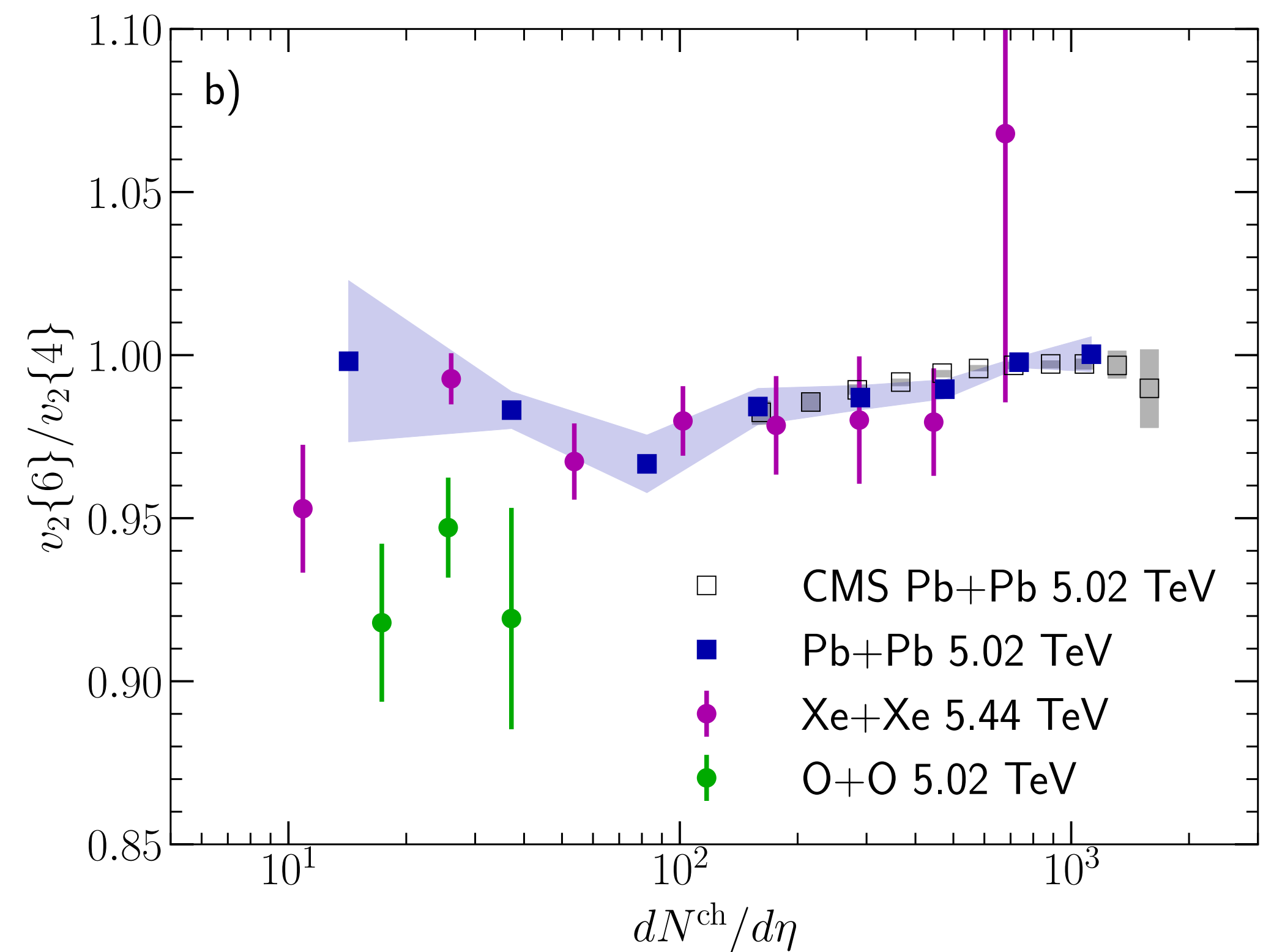
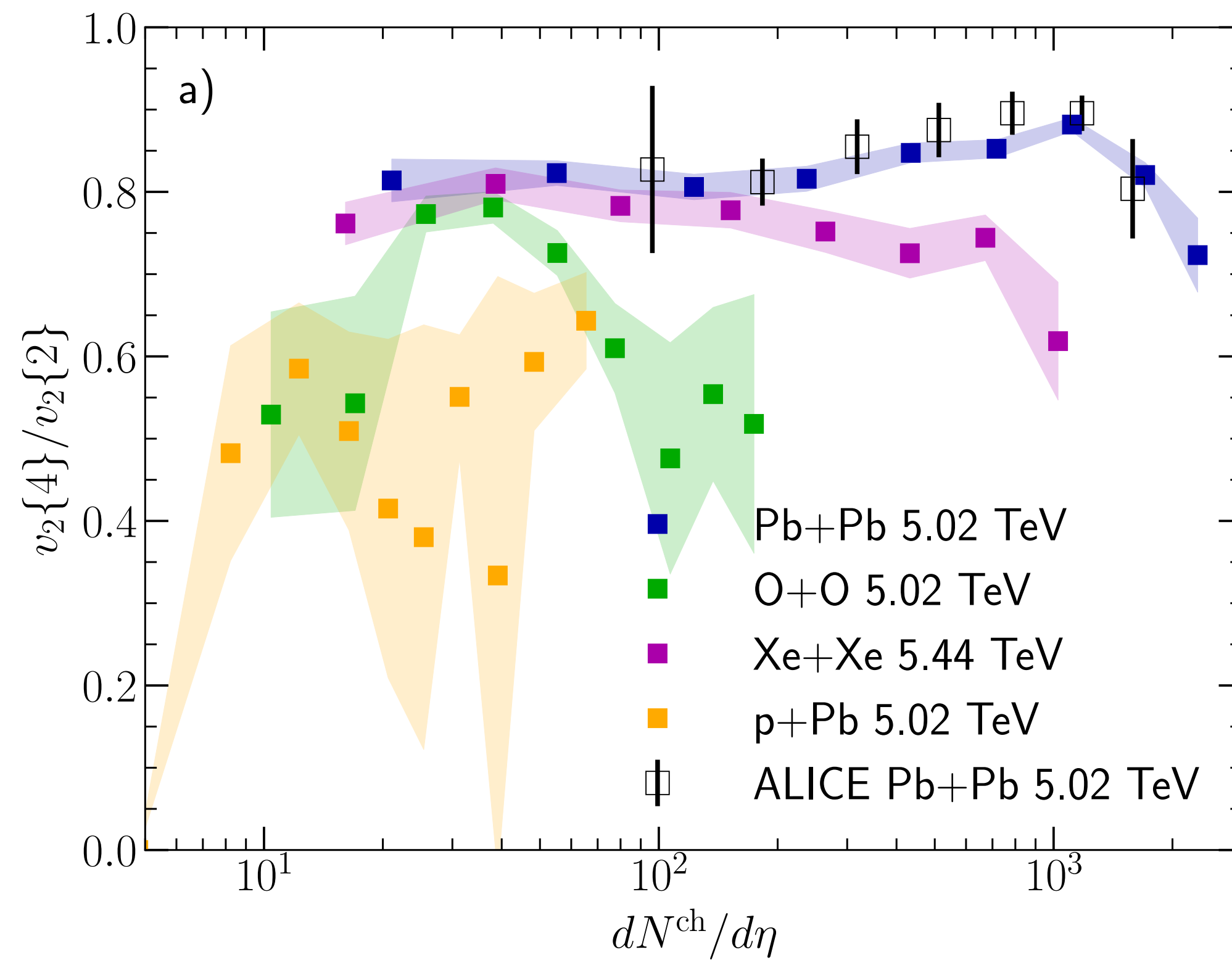
BACKUP: Model validation

B. Schenke, C. Shen, P. Tribedy, Phys. Rev. C 102 (2020) 4, 044905



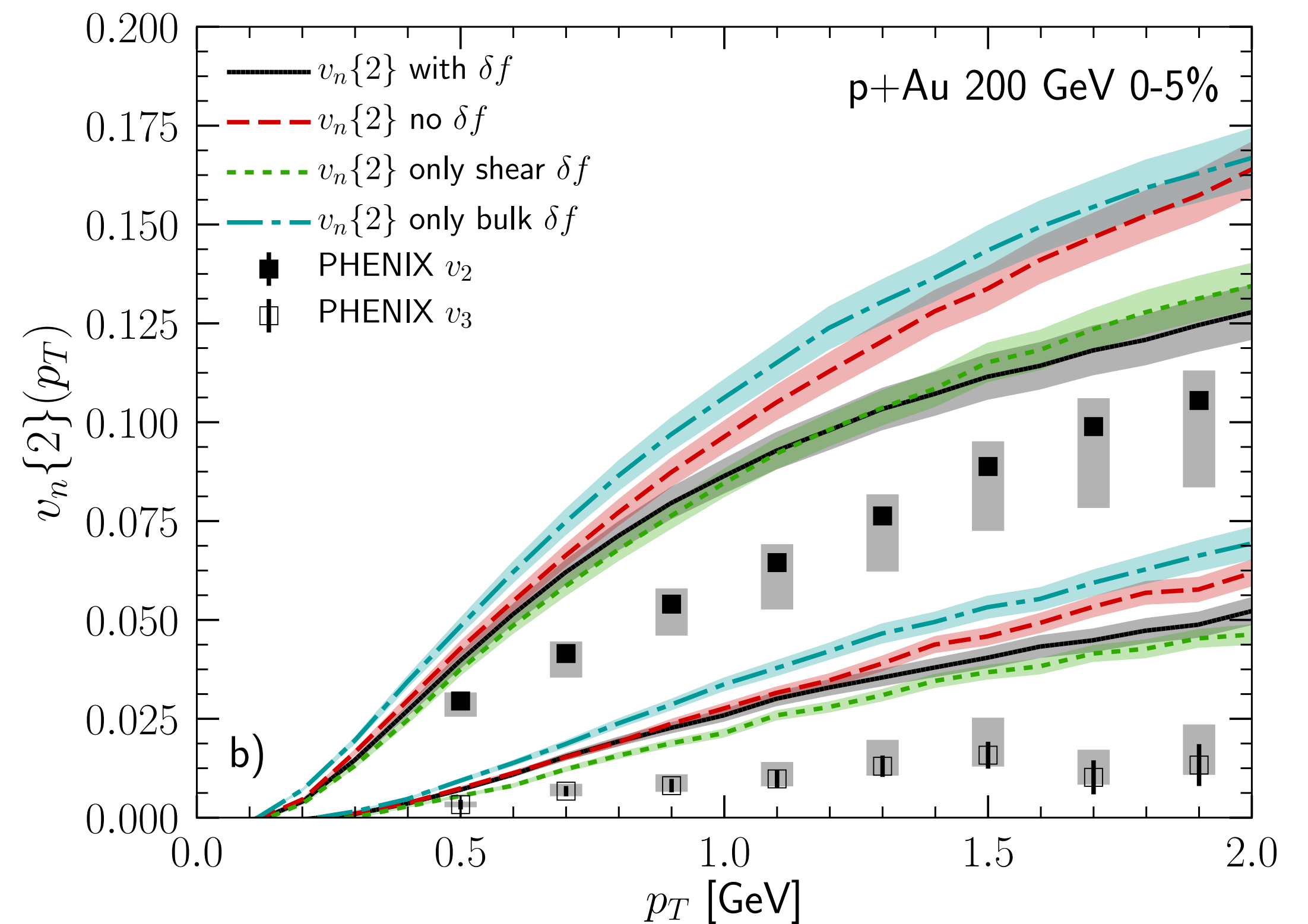
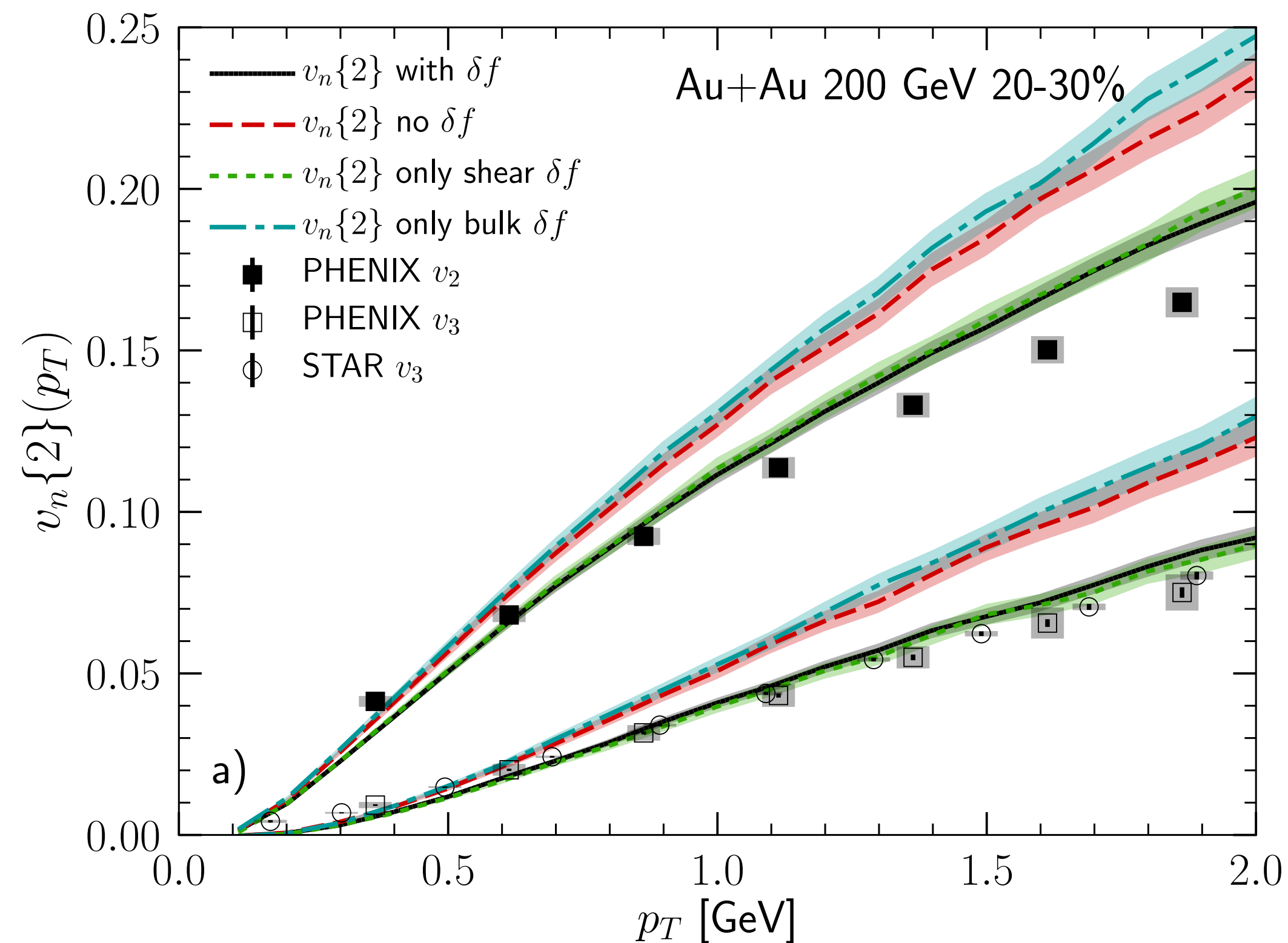
BACKUP: Model validation

B. Schenke, C. Shen, P. Tribedy, Phys. Rev. C 102 (2020) 4, 044905



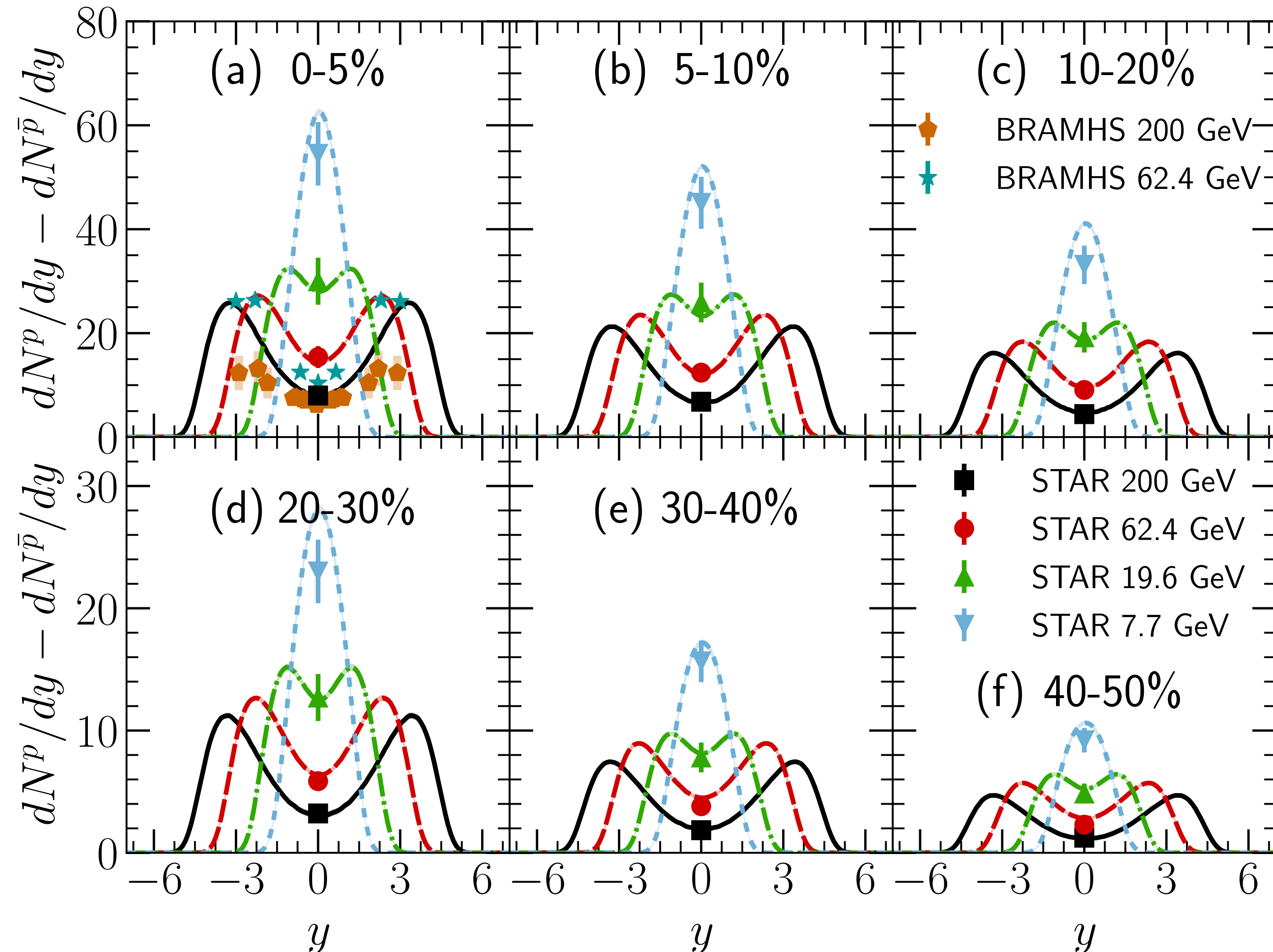
BACKUP: Effects of δf

B. Schenke, C. Shen, P. Tribedy, Phys. Rev. C 102 (2020) 4, 044905



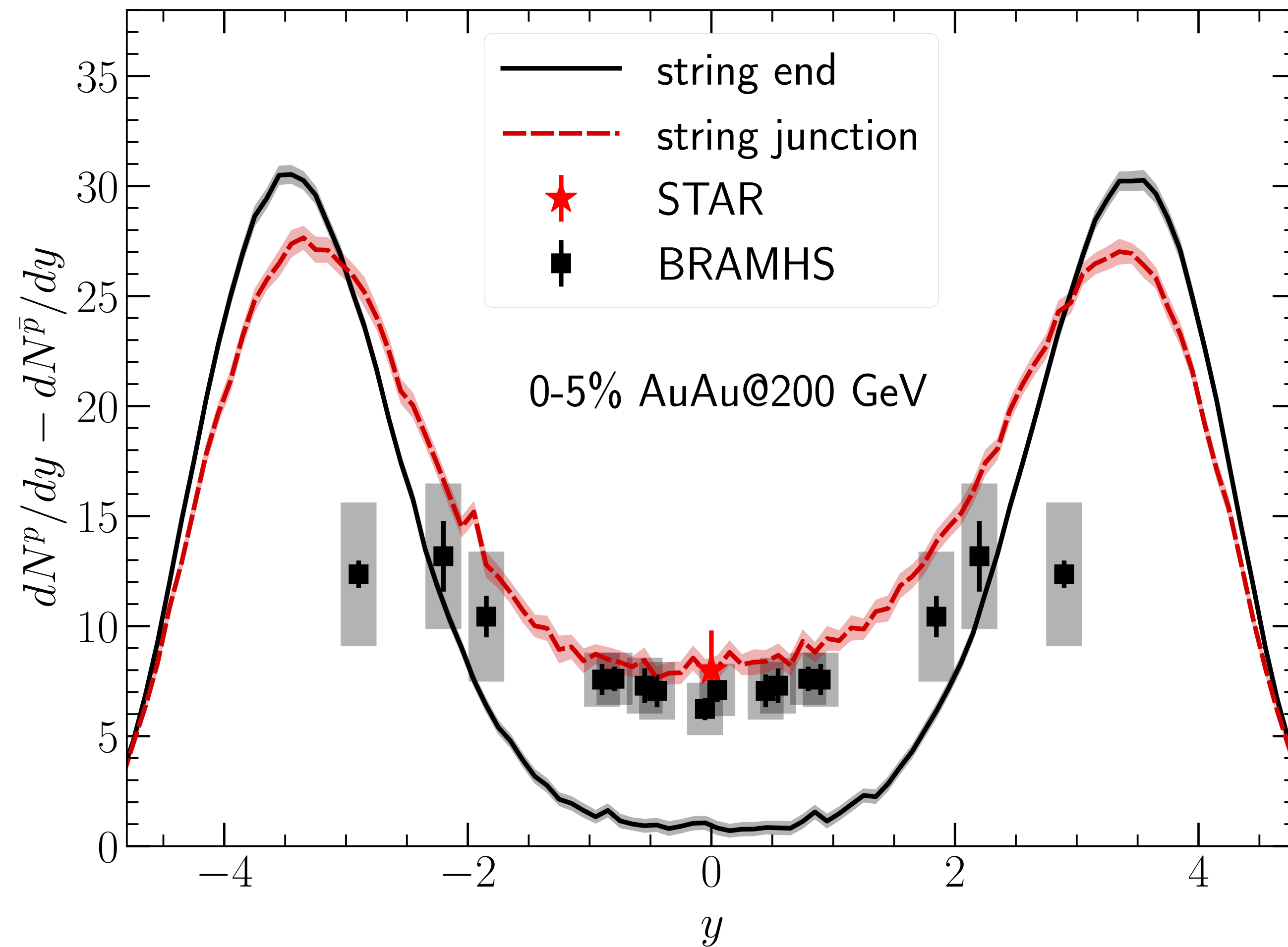
NET-BARYON DISTRIBUTIONS

C. Shen and B. Schenke, in preparation



NET-BARYON DISTRIBUTIONS

C. Shen and B. Schenke, in preparation



Effect of baryon junctions

